Temporal Variability of Arsenic Transport into the Upper Mystic Lake

by

Hank Boyd Seemann

B.A., Religious Studies
B.S., Civil Engineering
Stanford University, Stanford, CA, 1994

Submitted to the Department of Civil and Environmental Engineering
in partial fulfillment of the requirements for the degree of

Master of Science in Civil and Environmental Engineering

at the

MASSACHUSETTS INSTITUTE OF TECHNOLOGY

August 16, 1996
[September 1996]

Author .....
Department of Civil and Environmental Engineering
August 16, 1996

Certified by .....
Heidi M. Nepf
Professor of Civil and Environmental Engineering
Thesis Supervisor

Accepted by .....
Joseph M. Sussman
Chairman, Departmental Committee on Graduate Studies

Temporal Variability of Arsenic Transport into the Upper Mystic Lake

by

Hank Boyd Seemann

Submitted to the Department of Civil and Environmental Engineering on August 16, 1996, in partial fulfillment of the requirements for the degree of Master of Science in Civil and Environmental Engineering

Abstract

The Mystic Lake Upper Forebay (surface area 10.3 hectares, average depth 1.5 m) forms part of the intersection between the Aberjona River and the Upper Mystic Lake in eastern Massachusetts. The forebay's role in regulating the delivery of arsenic loads from the river to the main lake basin was investigated. Under extremely low-flow conditions in the summer internal loading from the sediments is significant for downstream concentrations, but during storms external loading from the river is dominant. The storm-induced arsenic load entering from the river is composed of two distinct pulses arriving ½ - 1 day apart. The first pulse is associated with surface runoff and re-suspended channel sediment and comes primarily in the particulate form, while the second pulse appears to be associated with release from a small contaminated lake (Halls Brook Storage Area) in the northern part of the watershed and has comparable portions of dissolved and particulate species. The forebay is able to retain at least half of the first pulse due to deposition but can allow much of the second pulse through to the main basin, depending on the momentum of the flow and the amount of vegetation present. The forebay thus affects the degree to which lake concentrations are event-driven and the timing of peak concentrations in the lake. During storms the peak concentration in the lake may be reduced 25-50% from the peak river concentration, and the peak lake concentration may occur 1-2 days after the rainfall has ended. Comparison with sediment cores suggests that the storms occurring during times when vegetation enhances retention are not representative of the storms that have the largest net effect on arsenic transport in this system.

Thesis Supervisor: Heidi M. Nepf

Title: Professor of Civil and Environmental Engineering

Acknowledgments

Thanks go first and foremost to Professor Heidi Nepf for giving me the opportunity to work on the Mystic Lake project and for her continued enthusiasm and support for this study. I appreciate the help of UROP students Laura Depaoli and Adel Rophaiel, who spent long hours on the lake during the summer and provided valuable assistance with the laboratory analysis. Thanks also go to Helena Solo-Gabriele for offering advice, even from long distance, and directing me to key parts of her research; Phil Trowbridge for training me to use the arsenic analyzer; Suzie Wetzel for accompanying me during fieldwork, often when it was cold, windy, and raining, and providing counsel during difficult times; Tom Ravens for discussions about transport issues and being willing to jump into the lake in October for a sediment core; Sara Zion for help with laboratory techniques and keeping the arsenic analyzer on-line; Peter Zeeb for advice on equipment and help in the shop; Professor Harry Hemond for the use of his laboratory facilities and allowing me to discuss my work at his group meetings; Sheila Frankel for good UROP recommendations and the use of her laboratory equipment; Brigette Burnell for assistance with sampling and labwork; Chin Wu for encouragement and humor; Tom Shepard for cheerfully delivering USGS data; and Bob Lautzenheizer for his commitment to providing meteorological data to small customers.

Table of Contents

List of Figures

List of Tables

Chapter 1

1.1 Introduction

The Aberjona watershed (Figure 1-1) in eastern Massachusetts was a major center of industrial activity around the beginning of the century, and although this activity has largely subsided the environmental impacts remain a serious concern (Durant *et al*, 1990, Aurilio *et al*, 1994). Wastes from tanning, leather finishing, and chemical manufacturing in the northern part of the watershed were commonly discharged to nearby water bodies and buried in pits, including an estimated 200 to 900 tons of arsenic released at Industriplex, a site that has been on the Superfund National Priorities List since 1981 (Aurilio *et al*, 1994). Recent studies indicate that the Aberjona River has carried large amounts of contaminants throughout the watershed since these releases began (Knox, 1991; Spliethoff and Hemond, 1996) and that this transport continues through the present (Solo-Gabriele, 1995). The present study looks at the transport of arsenic through the Mystic Lake Upper Forebay, the first of two shallow, vegetated bodies of water that join the Aberjona River with the Upper Mystic Lake (Figure 1-2). The purpose of the study is to understand the role of the forebays in regulating the delivery of arsenic loads from the river to the main lake basin.

1.2 Site Description

The Aberjona River collects drainage from a 65 km^2 watershed and flows approximately 14.5 km before arriving at the Mystic Lakes. The watershed is largely developed with residential, commercial, and industrial land-use. The river flows through two small forebays (Upper and Lower Forebays) before entering the first of two main basins (Upper and Lower Mystic Lakes). A dam separates the two basins, and the Lower Mystic Lake discharges into the Mystic River which leads to Boston Harbor. The forebays were created when the dam was built in 1864, which raised the water

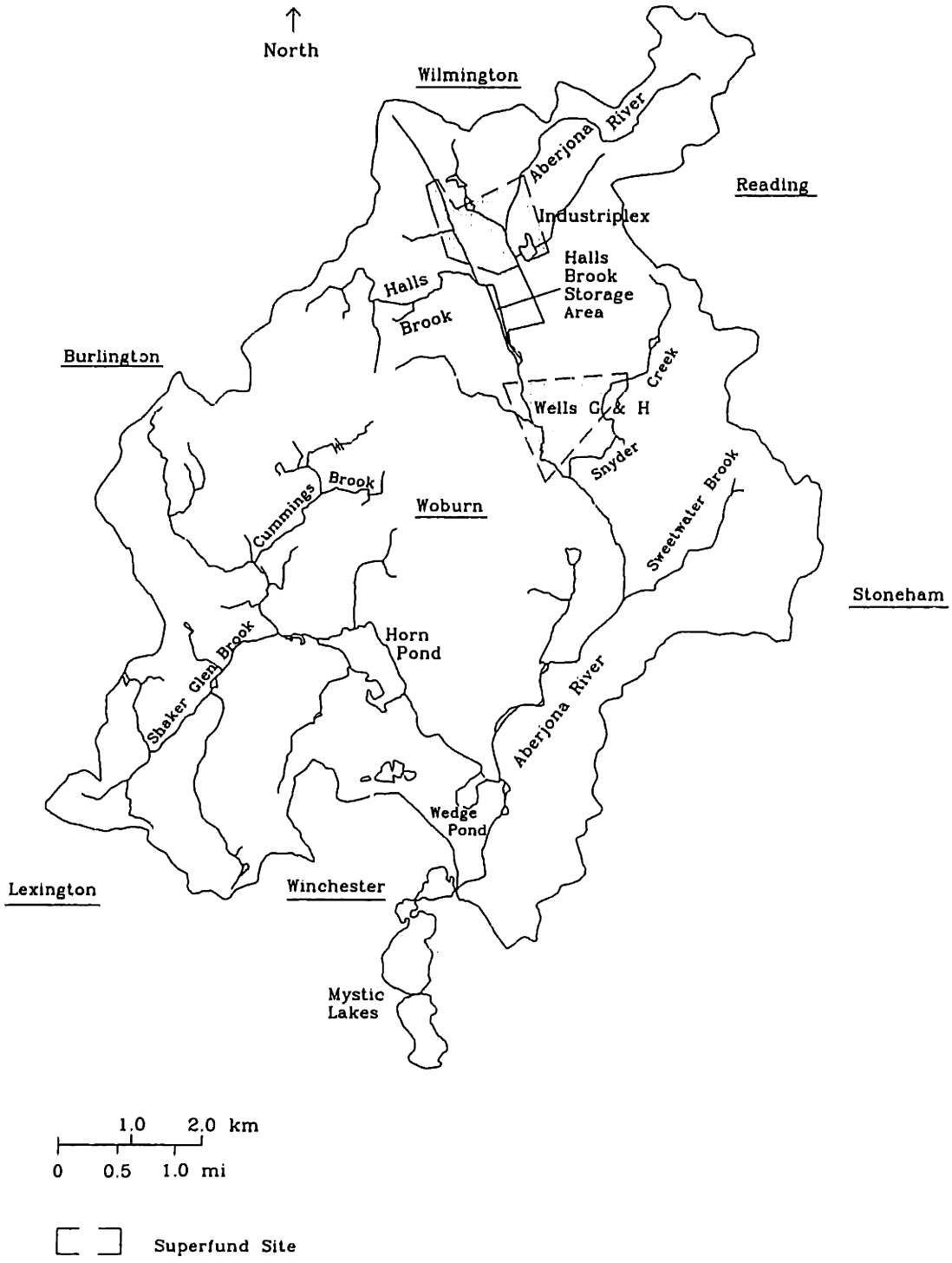

Figure 1-1: Aberjona Watershed

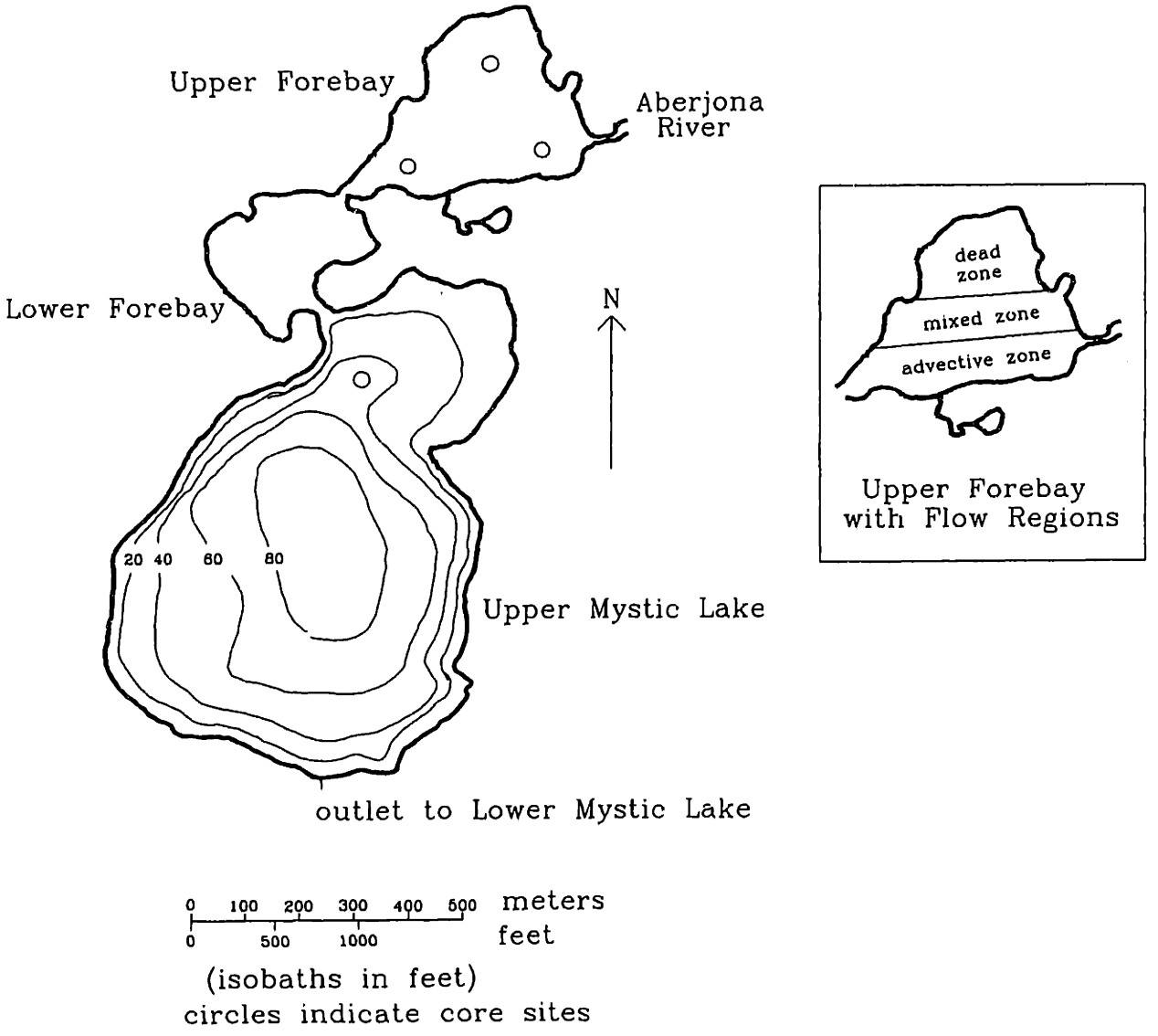

Figure 1-2: Upper Mystic Lake and Forebays

level and flooded the low-lying meadows through which the river had previously passed. Extensive boating and fishing take place throughout the lake system and there is a public beach for swimming on the north end of the Upper Mystic Lake.

Streamflow in the Aberjona River has been measured by the U.S. Geological Survey since 1939 with a water stage recorder at a site 800 meters upstream of the entrance to the Upper Forebay. The average streamflow over 54 years (1939-1993) is 0.82 m^3/s, and hourly flowrates have ranged from < 0.03 m^3/s to 37.7 m^3 /s. Peak flows have increased in recent years due to urbanization, with eight of the top 10 daily average discharges occurring after 1979 and 19 of the top 28 daily average discharges occurring after 1978 (Solo-Gabriele, 1995). The Upper Forebay has a surface area of 10.3 hectares, and while depths may reach 3 meters in some sections the average depth during normal flow conditions is 1.5 meters (Table 1.1). The Lower Forebay has approximately the same mean depth but is slightly smaller with a surface area of 7.7 hectares, while the Upper Mystic Lake has a mean depth of 13 meters, maximum depth of 25 meters, and surface area of 35 hectares. The northern and western sides of the Upper Forebay are residential areas and rock walls form part of the shore, while the southern side includes a meadow and forested hill and has a natural shore. Winds are typically aligned along the north-south axis, with the prominent direction varying with season (see Appendix A.2). During the winter the surface freezes, although there is often an opening in the ice that follows the path of the incoming river flow. During the summer the forebay water is generally 3-4 °C warmer than the river and there is diurnal stratification, with the vertical temperature gradients that develop during the day largely mixing overnight (Figure 1-4).

Table 1.1: Upper Forebay Characteristics

surface area (A)	10.3 hectares	distance from inlet to outlet (L)	520 m
average depth (z_{avg})	1.5 m	inlet cross-sectional area	16.1 m^2
Osgood Index ($z_{avg}/A^{.5}$)	4.7	outlet cross-sectional area	24.0 m^2
maximum depth (z_{max})	3 m	maximum fetch	~300 m

Note: 1 hectare = 10,000 m^2 = 2.47 acres

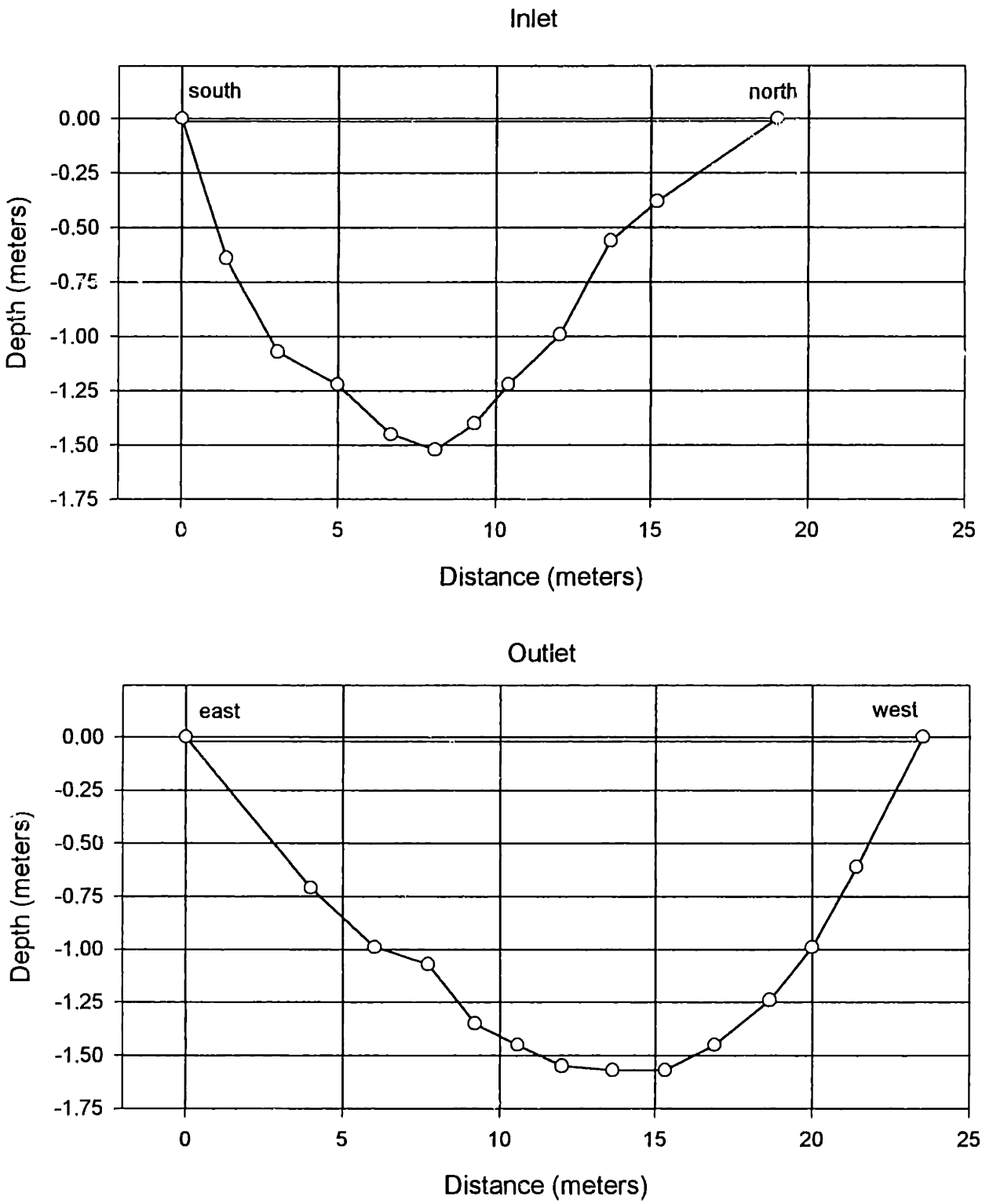

Figure 1-3: Cross-sections of Upper Forebay Inlet and Outlet

Note: areas were measured when water level was 65 cm above lowest summer level (lowest summer level was 82.5 cm below top of cement buttress at bridge)

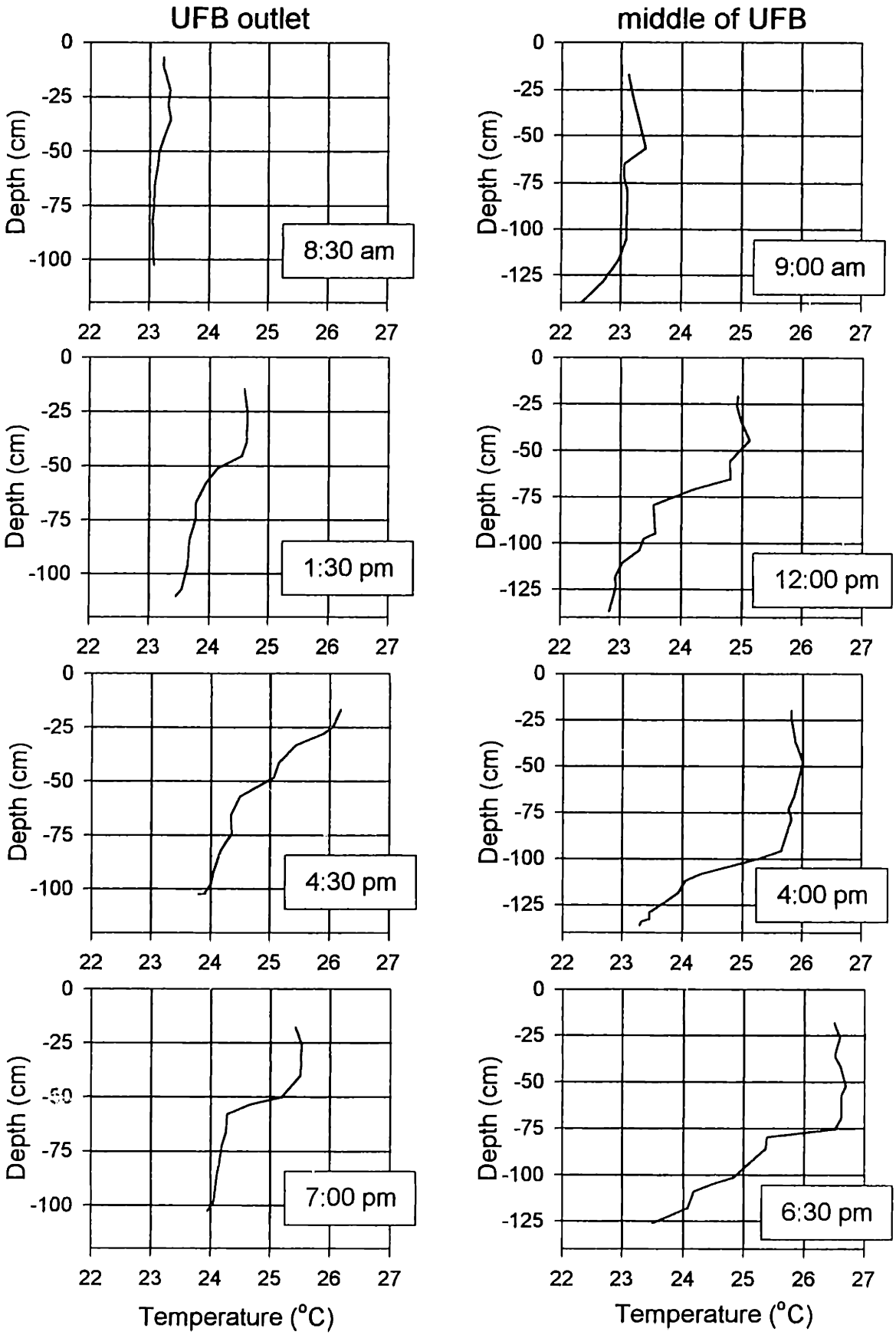

Figure 1-4: Temperature Profiles on July 19

The average nominal detention time (the time for the incoming water volume to equal the volume of the forebay) is approximately 2-3 days, but because of the morphometry of the forebay (Figure 1-2) the incoming water can have a wide range of residence times. The momentum of the river inflow carries it essentially in a direct line toward the forebay outlet, and this can result in a short-circuiting effect in which some of the inflow spends very little time in the forebay before being carried out. This means, in turn, that there may be regions of the forebay that have limited interaction with the inflowing water, and thus water can stay in these more remote regions for extended periods of time. In view of these conditions it may be helpful to distinguish three zones in the Upper Forebay (Thackston *et al*, 1987): an advective zone, where the velocity is uni-directional between the inlet and outlet; a mixed zone, where there is some exchange between the inflowing water and the existing forebay water; and a dead zone, which has little direct contact with the advective zone and interacts primarily with the mixed zone. The borders between such zones are not distinct, but these categories help to characterize the flow field and illustrate how there may be a wide distribution of residence times within the forebay. The extent of these zones will vary depending on the size of inflow as well as internal mixing processes. Large inflows may have enough initial momentum to continue through the forebay as a distinct flow region (i.e., the advective zone persists from inlet to outlet), whereas small inflows may be easily arrested before reaching the outlet (i.e., the advective zone essentially disappears before reaching the outlet). The inflow can create shear-induced mixing between the advective zone and mixed zone, while circulation generated by wind and differential heating/cooling will affect exchange between all three zones.

The forebays have a number of features that make them conducive for the growth of aquatic plants and algae. They are shallow enough so that the photic zone reaches much of the sediments, their large surface areas enhance heating by sunlight which leads to higher water temperatures, and substantial nutrient loads are delivered from the surrounding residential area. Spraying programs have been conducted on and off over the years to limit vegetation growth, depending on available funding,

and were re-continued in 1994. Following the summer of 1993 it was estimated that 100% of the bottom had been covered with submersed macrophytes, predominantly coontail (Ceratophyllum) and elodea (Elodea), and 40% of the surface water had been populated by waterlilies (Nymphaea and Nuphar) (ACT, 1994). During the summer of 1994 approximately 75% of the Upper Forebay was treated with herbicides, with 25% near the river inlet left untreated in an attempt to preserve fish habitat and reduce part of the incoming nutrient load. Herbicides that were used include Aquathol-K (coontail), Diquat (elodea), Rodeo (water lilies), and Cutrine-Plus and copper sulfate (algae). During the summer of 1995, when fieldwork for this study began, coontail and elodea grew back at moderate levels but were not expected to reach the surface by the end of the summer and thus were not targeted for spraying (ACT, 1995). Curly pondweed (Potamogeton crispus) was prevalent during May and June but died back before spraying was deemed necessary. Productivity of algae was high throughout the summer and spraying was conducted on June 22 and August 17. Water lily coverage was estimated as 30-50% over the non-treatment area and 5-10% over the treatment area, which was sprayed on August 17 and September 11. Spraying was again conducted periodically during the summer of 1996 but there was still considerable growth of water lilies and coontail.

The forebays are a fairly unique river/lake intersection and do not fit easily into conventional categories of aquatic systems. The U.S. Fish and Wildlife Service classification schema (Mitsch and Gosselink, 1993) subdivides lacustrine systems into littoral and limnetic areas, which are terms that describe a continuum of environments and do not have precise boundaries. Littoral areas extend from shoreline to a depth of approximately 2 meters and are commonly associated with the surrounding border of a lake, while the deepwater zones of the lake are the limnetic areas. The forebays could be regarded as extended littoral areas of the Upper Mystic Lake main basin, although they are nearly deep enough that they could also be viewed as small lakes with their own limnetic and littoral areas. Littoral areas are usually considered to be forms of wetlands, and although the forebays show the general wetland characteristics of shallow water, flooded soils, and extensive growth of aquatic plants, this is

not their regulatory classification (Paul DiPietro, personal communication). This is primarily due to the fact that the forebays are populated with floating-leaved and submerged vegetation but very little emergent vegetation, and these particular submerged plants tend to thrive in disturbed areas at the expense of other species. Nevertheless, it is helpful to make reference to the wetland literature for comparison with similar systems, in particular to deep marshes that undergo substantial exchange with their surroundings through streamflow.

1.3 Literature Review

Wetlands are generally considered to be beneficial to downstream water quality by reducing and/or modifying the incoming load of nutrients, sediment, and contaminants before it is carried out. This can occur in the littoral zone around a lake (lacustrine wetlands) and in marshes along stream channels (riverine wetlands). With the ability to reduce their input load, natural wetlands have been considered as resources by watershed managers to mitigate non-point pollution (Baker, 1992; Mitsch, 1992; Mitsch, 1995), and engineers have utilized constructed wetlands as components for wastewater treatment (Kadlec and Tilton, 1979). An important sink mechanism is deposition, which will be enhanced by the decrease in velocity that occurs when flow that is confined to a channel enters a large volume of standing water and mixes. Reduced velocity generally results in a reduction of the turbulence that keeps particles in suspension, and some fraction of these particles will be large enough that they will settle before arriving at the outlet. Another sink mechanism is adsorption by the bottom sediments, which may involve iron and aluminum oxides and particulate organic material. And there can be removal associated with vegetation. Both freshwater (Simpson *et al*, 1983) and saltwater (Gallagher *et al*, 1980) plants have been observed to accumulate metals during the growing season, and Orson *et al* (1992) have proposed that the litter during fall diedown acts as a sponge, absorbing metals and holding them until they are buried by deposited sediment.

The effect that wetlands have on the transport of nutrients and metals is often a function of season, and retention may be neither continuous nor permanent. Not only are the processes associated with vegetation seasonal activities, but elevated flows from rain storms or snowmelt may bypass sink mechanisms or flush out previously deposited material. Klopatek (1978) observed more than a 50% reduction of total and inorganic phosphorus in a Wisconsin cattail marsh during the time in which there was active aquatic plant growth, but a large portion of this was released in the spring. Another cattail marsh was found to retain 83% of the applied phosphorus load during the summer but only 8% during the spring, for a net annual reduction of 10% (Loucks, 1990). Pevery (1982) monitored nutrient fluxes through a riverine wetland for two years and found a net retention of nitrogen and phosphorus during one year and a net export during the other year when the yearly averaged flow was twice as large. The hydrodynamics in the wetland will determine whether such flushing will occur during floods and how much of the floodwater load will be deposited. Klarer and Millie (1989) monitored a freshwater estuary along Lake Erie during three storms (two in spring and one in autumn) and observed no flushing but rather 20-50% reductions in phosphorus concentrations and 40-50% reductions in metal concentrations. Mitsch and Reeder (1991) used model simulations of the same estuary to show that retention during storms depended on the water level in Lake Erie. When the water level was normal, stormwater passed quickly through the estuary with only 27% retention of the total phosphorus load. When the water level was high, the retention rate rose to 52% due to the longer residence time and increased deposition.

Along with retaining a portion of the input loads, wetlands can also provide a delay that is beneficial to downstream water quality. Lee *et al* (1975) noted that nutrient removal during the growing season may minimize summer algal blooms in downstream lakes. For wetlands with spring flushing the effectiveness of this removal will depend on the residence time of the downstream lake. Jones and Lee (1980) considered the role of wetlands in managing eutrophication in Lake Okeechobee and concluded that the residence time in this lake is so long (~ 1 year) that the large nutrient loads

flushed out of the wetlands in the spring would remain in the lake through the main algae growing period. Temporary storage also creates the opportunity for management practices such as harvesting vegetation if storage takes place in the plant tissue (Sloey *et al*, 1978). And by lowering peak concentrations during floods, wetlands can reduce downstream exposure to toxic substances and thus provide ecological and human health benefits.

1.4 Previous Work

Solo-Gabriele (1995) studied the transport of sediment, three metals (iron, chromium, copper), and one metalloid (arsenic, which will be referred to as a metal) along the Aberjona River. The watershed was divided into four sub-basins, each of which was modeled to estimate its contribution to the river load. Fluxes of metals and suspended sediment were sub-divided into components corresponding to the different streamflow components that are generated in each sub-basin (Figure 1-5). These components include a quick storm response (direct precipitation and runoff, water from storm sewers), a slow storm response (groundwater that arrives at the river prior to reaching the water table), and longterm baseflow (groundwater not affected by storms). Contributions of sediment and metals from the sub-basins were routed along two main channel reaches, where deposition or erosion could occur depending on the carrying capacity of the flow. The outlet of the watershed was approximated to be the USGS gauge station, 800 meters upstream from the inlet to the Mystic Lake Upper Forebay. The model was calibrated and verified with field samples which were collected on monthly intervals at five sample sites and hourly during three storms at the USGS station. Storm sampling began before the peak flowrate and continued for a duration of approximately 24 hours.

Table 1.2 shows the results of the model at the USGS station for arsenic and suspended sediment averaged over the three years the model was run. The long-term transport of arsenic is divided roughly equally between the dissolved and particulate phase, and storms contribute ~30% of

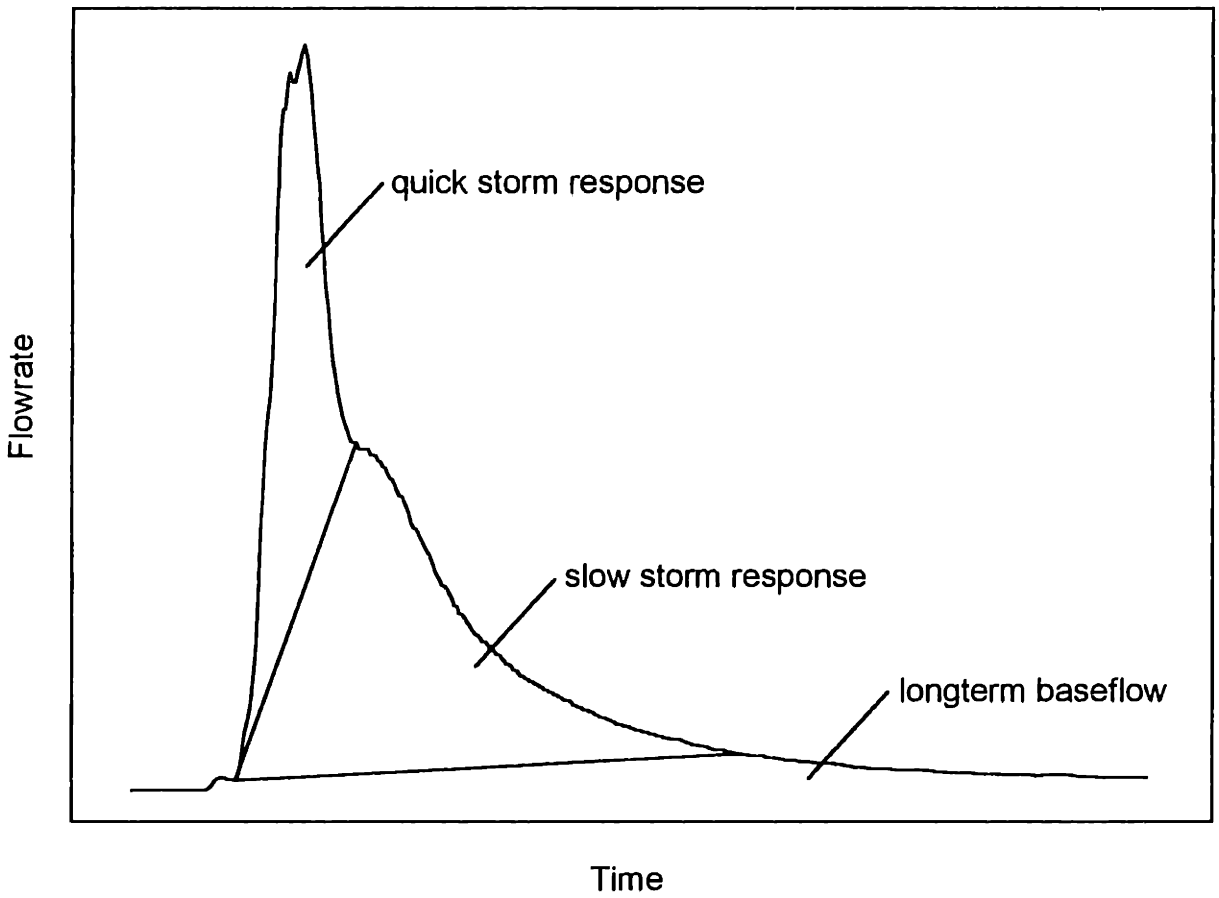

Figure 1-5: Aberjona River Hydrograph During September Storm Showing Streamflow Components

the total arsenic load. During storms more arsenic is transported in particulate form, whereas during the longterm baseflow the majority of arsenic is found in dissolved form. There is generally a large burst of sediment and particulate arsenic transport at the beginning of a storm event, due both to the quick-storm response and the mobilization of channel sediments (see Solo-Gabriele, Figure IV.4-64). Although fluxes (flowrate x concentration) of arsenic in both phases increase sharply during storms, concentrations may actually decrease at times (Solo-Gabriele, Figures IV.4-54 and IV.4-63). Concentrations of dissolved arsenic were found to drop down slightly below baseline values during peak flows due to the addition of large amounts of water that had little exposure to the contaminant. A dilution effect was also observed at peak flows for the average concentration of suspended particles (mg arsenic/kg total dry weight) due to the addition of relatively clean sediment, although the concentration of particulate arsenic in the water (nM or μg/L) increased due to the large sediment load. The mean particle size was measured throughout the largest of the three storms and once under low-flow conditions. The mean was found to range only from 7 to 12 μm and did not show significant variation between the different flow conditions.

Table 1.2: Arsenic Fluxes at USGS station on the Aberjona River (Solo-Gabriele, 1995)

	Average Distribution, 1991-1993 (%)				
	Quick Storm Response	Slow Storm Response	Longterm Baseflow	Channel Re-suspension	Range of Yearly Averaged Fluxes
Dissolved Arsenic	6	16	78	-	8-11 g/hr
Particulate Arsenic	17	1	66	14	7-9 g/hr
Suspended Sediment	57	11	18	15	32-66 kg/hr

Extensive sediment core analysis has been conducted to investigate the historical release of contaminants in the Aberjona watershed. Radionuclide dating indicates that deposition rates in the

deepest section of the Upper Mystic Lake main basin were ~0.6 cm/year during the early part of the century before increasing to ~1.0 cm/year in the last 30 years (Spliethoff and Hemond, 1996). One sediment core from the Upper Forebay has been dated with Pb-210 and indicates a rate of 0.42 - 0.60 cm/year (Knox, 1991), although the forebay sediments are quite heterogeneous and this rate may not be representative of all areas. Several cores were sampled but not analyzed, and some had sand layers at various points as well as the beginning of a peat layer at depths ranging from 30 to 50 cm (Knox, 1991). The main basin cores taken by Spliethoff and Hemond (1996) extended down 80-100 cm and provide a historical record of arsenic delivery to the lake, with well-pronounced peaks at 25-35 cm and 50-70 cm that correlate well with records of industrial activity and land-moving in the watershed. The Upper Forebay core that was analyzed extended down to 30 cm and has a distinct peak at a depth of 17 cm (180 mg arsenic/kg dry sediment), which may correspond to the first peak in the Upper Mystic Lake cores (600 mg/kg).

1.5 Overview

This study was conducted in order to understand how the Upper Forebay responds to different loading conditions and to identify the extent of reduction and delay in arsenic flux that occurs prior to the Upper Mystic Lake. Sediment cores were taken at four locations (Figure 1-2), and water samples were taken periodically under non-storm conditions and more frequently during five high-flow events at the inlet and outlet of the Upper Forebay (Figures 1-6 and 1-7; flowrate data was not yet available for some months). Collection for the first four of these events entailed taking daily samples 1-2 days before precipitation, 2-3 samples per day during peak flows, and daily samples for at least three days following peak flows. For the last high-flow event, samples were taken every 1-2 hours during the first two days of the storm and daily during the following days.

Fieldwork for this study was conducted from June, 1995, to July, 1996. During the summer of 1995 the weather was unusually dry, with near record-low rainfall in July and rainfall that matched the

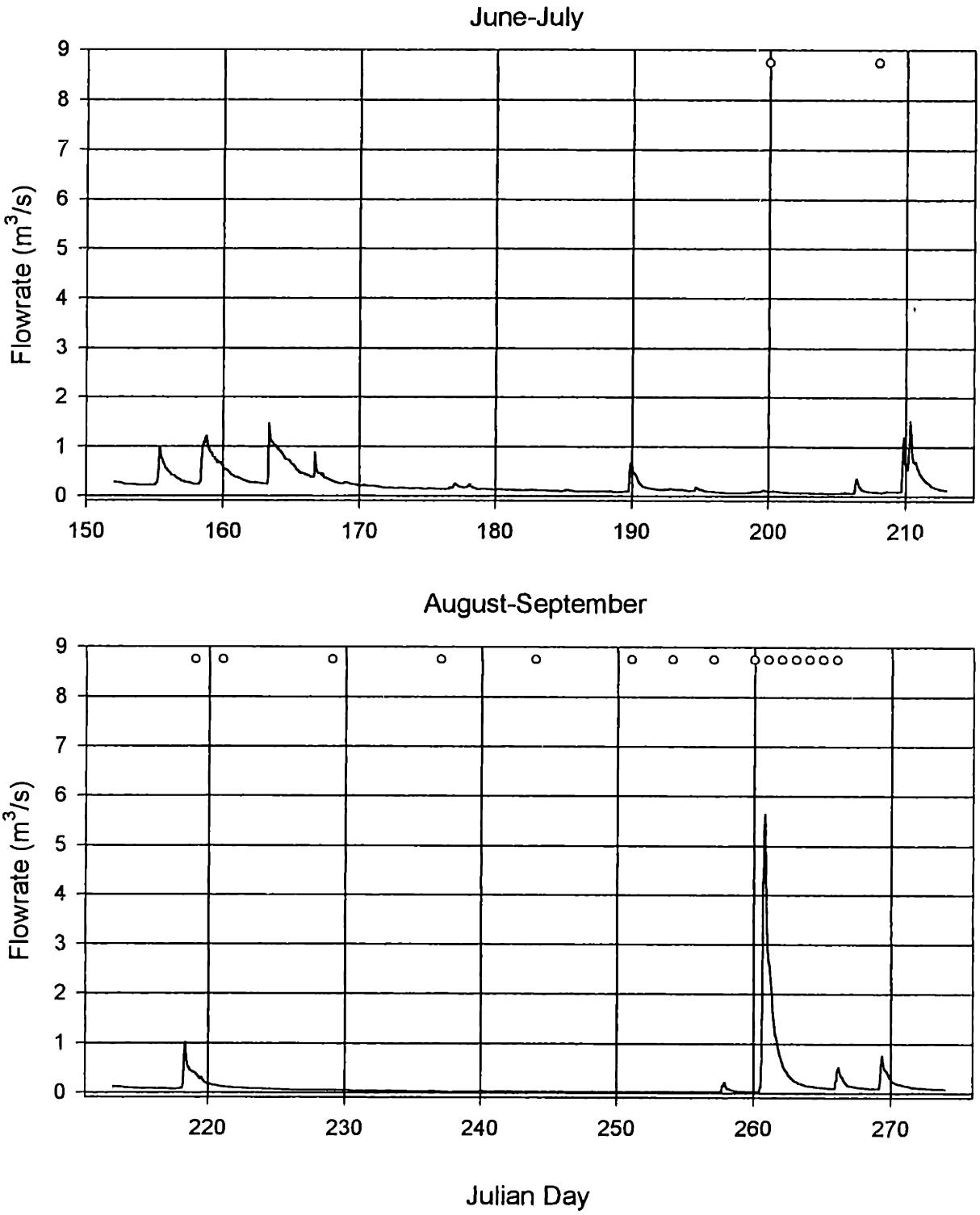

Figure 1-6: Aberjona River Hydrograph for June-September

Note: circles indicate days during which samples were taken

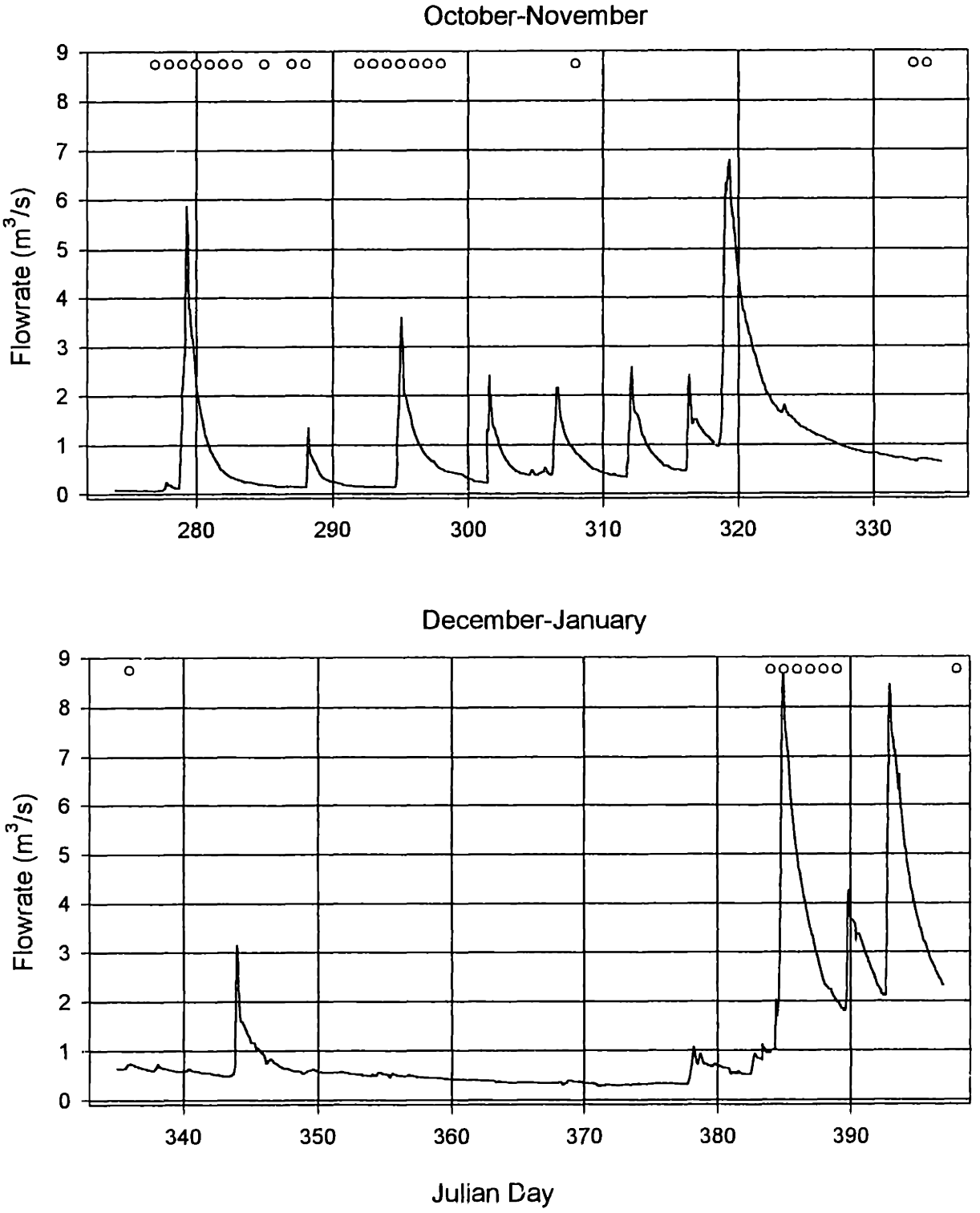

Figure 1-7: Aberjona River Hydrograph for October-January

record low in August (see Appendix A.2). Small rain events generally occurred every few weeks and caused modest increases in discharge (up to ~1 m^3/s), but there had not been a large storm (discharge > 5 m^3/s) since January 20, 1995. The first large storm during this study arrived on September 17, followed by storms on October 5-6 and October 21. Sampling was conducted for these three fall storms, a high-flow event starting January 19, 1996, caused by both moderate rainfall and large snowmelt, and a high-flow event starting July 13, 1996, caused by Tropical Storm Bertha.

Chapter 2

2.1 Methods

Samples were taken with HNO_3-washed polyethylene bottles near mid-stream, either by hand directly from a boat or from the shore with the bottle attached to the end of a long pole. Samples were regularly collected 20-30 centimeters below the water surface and also near the bed on occasion with a peristaltic pump. Arsenic concentrations were found by hydride-generation and atomic absorption spectrometry using a PSA Excalibur system. Samples were first acidified to pH 1 with hydrochloric acid and treated with potassium iodide/ascorbic acid to reduce As (V) to As (III). Then a much stronger reductant (sodium borohydride) was continuously mixed with the sample at a fixed rate to generate the hydride gas arsine (AsH_3), which was flushed into a hydrogen-air flame with argon gas and measured for absorbance. A switching valve alternated between the samples and a reagent blank to maintain a baseline fluorescence. The pre-reduction stage improved the accuracy of the analysis because only a fraction of As(V) is reduced to arsine by the sodium borohydride (Trowbridge, 1995). Ninety-five percent confidence intervals on these measurements were typically 1-3 nM (see Trowbridge (1995) regarding the method for calculating confidence intervals).

The dissolved arsenic fraction was separated using 0.45 μm Millipore membrane filters. Total and dissolved concentrations were measured directly and the particulate fraction was calculated as the difference between these measurements. The value of 0.45 μm is the conventional separation between particulate and dissolved phases but may result in the inclusion of colloids as well as true solutes in the dissolved fraction measurement.

Suspended sediment was determined gravimetrically using 0.45 μm filters and a Cahn electrobalance. A measured volume of sample was filtered through a pre-weighed filter, and the filter and sediment were dried at 85 °C for one hour before being re-weighed. Blanks were run to correct for incomplete drying, and replicate measurements for a number of samples with concentrations from 4 to

7 mg/L were consistent within 0.3 mg/L. This was a bulk measurement that included both mineral and organic particles. For the two days that sediment was measured for organic content samples were filtered with Whatman glassfiber filters, dried at 70 °C for 2 hours, weighed, ashed at 450° C for 24 hours, and re-weighed. Total dissolved carbon was measured with a Shimadzu TOC-5000 analyzer after filtering samples through 0.45 μm filters.

Sediment cores were obtained using a freeze corer developed by Spliethoff and Hemond (1996). Slabs of sediment 30-40 cm long (0.5-1.5 cm thick) were frozen onto the flat side of a hollow aluminum tube filled with dry ice and denatured ethanol, and the top 30 cm was subsectioned at 2 cm intervals for analysis. Each subsection was weighed, dried overnight at 80 °C, and re-weighed to determine water content. Following digestion with hot concentrated nitric acid and hydrogen peroxide, samples were filtered to remove any remaining solids and then diluted with hydrochloric acid. Arsenic analysis was performed on a Perkin Elmer 4100ZL graphite furnace atomic absorption spectrometer, with samples measured in duplicate at least and sometimes in triplicate. Note that this measurement does not distinguish between arsenic associated with particles and arsenic dissolved in the porewater.

Velocity measurements were taken with a Sontek acoustic doppler velocimeter mounted on a bottom-resting tripod. Mean velocities were found by taking three-minute records at 4-5 points in the water column and depth-averaging. Temperatures were taken with an Ocean Sensors Model OS200 CTD (conductivity/temperature/depth) profiler. Wind speed and direction were measured at 10 minute intervals with a cup anemometer on the top of a flag pole at the southern end of the Upper Mystic Lake and stored in a data logger. Hourly rainfall and daily minimum/maximum air temperature were measured by climatologist R. Lautzenheizer in Reading, a town on the northern edge of the Aberjona watershed.

2.2 Non-storm Conditions

2.2.1 Suspended Sediment

Observations

Concentrations and fluxes of suspended sediment during the summer are shown in Figure 2-1. Concentrations were higher at the outlet on all seven days of measurement prior to the September storm (Julian day 260), including two days in August that followed a small rain event (0.79 inches on Julian days 217-218). Average concentrations for this period were 8.5 ± 1.9 mg/L at the outlet and 3.6 ± 1.5 mg/L at the inlet. Flowrates at both the inlet and the outlet were taken to be the values measured at the USGS gauge station. The effect of evaporation on the water balance was examined by considering two empirical formulas but was found to be negligible (see Appendix A.3).

Figure 2-2 shows the results from separating the suspended sediment into two size classes using 8 μm filters. The concentration of particles less than 8 μm was essentially constant between the inlet and outlet on these four days, while the concentration of the larger size fraction increased by nearly a factor of three. Measurements of organic content were taken on September 14 (Figure 2-3) and are probably representative of the conditions in July and August because they occurred prior to the first storm. Samples were taken from the inlet, outlet, and at a location in the middle of the forebay and show an increase in organic content between the inlet and outlet. When organic content was measured again during the winter there was no significant difference between the inlet and outlet.

Figure 2-4 shows suspended sediment concentrations for samples taken under non-storm conditions when the rate of change in the hydrograph was relatively small (i.e., excluding the quick-storm response and the beginning of the slow-storm response, which will be discussed in the next section). The trend during the summer of having higher outlet concentrations than inlet concentrations can be seen for days prior to Julian day 260, and within two days after the September storm concentrations were again higher at the outlet and remained so for the five following days that were

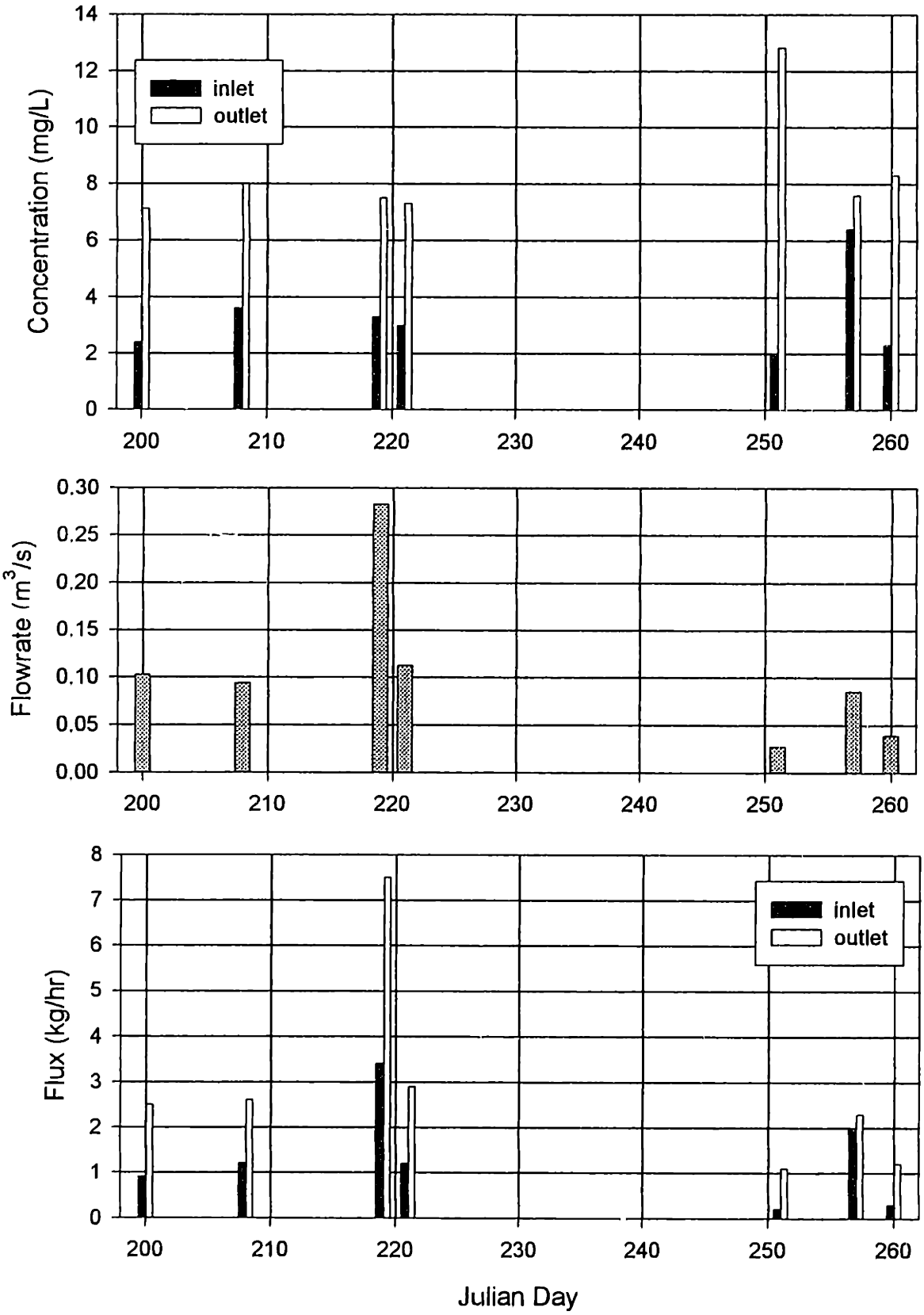

Figure 2-1: Suspended Sediment during Summer

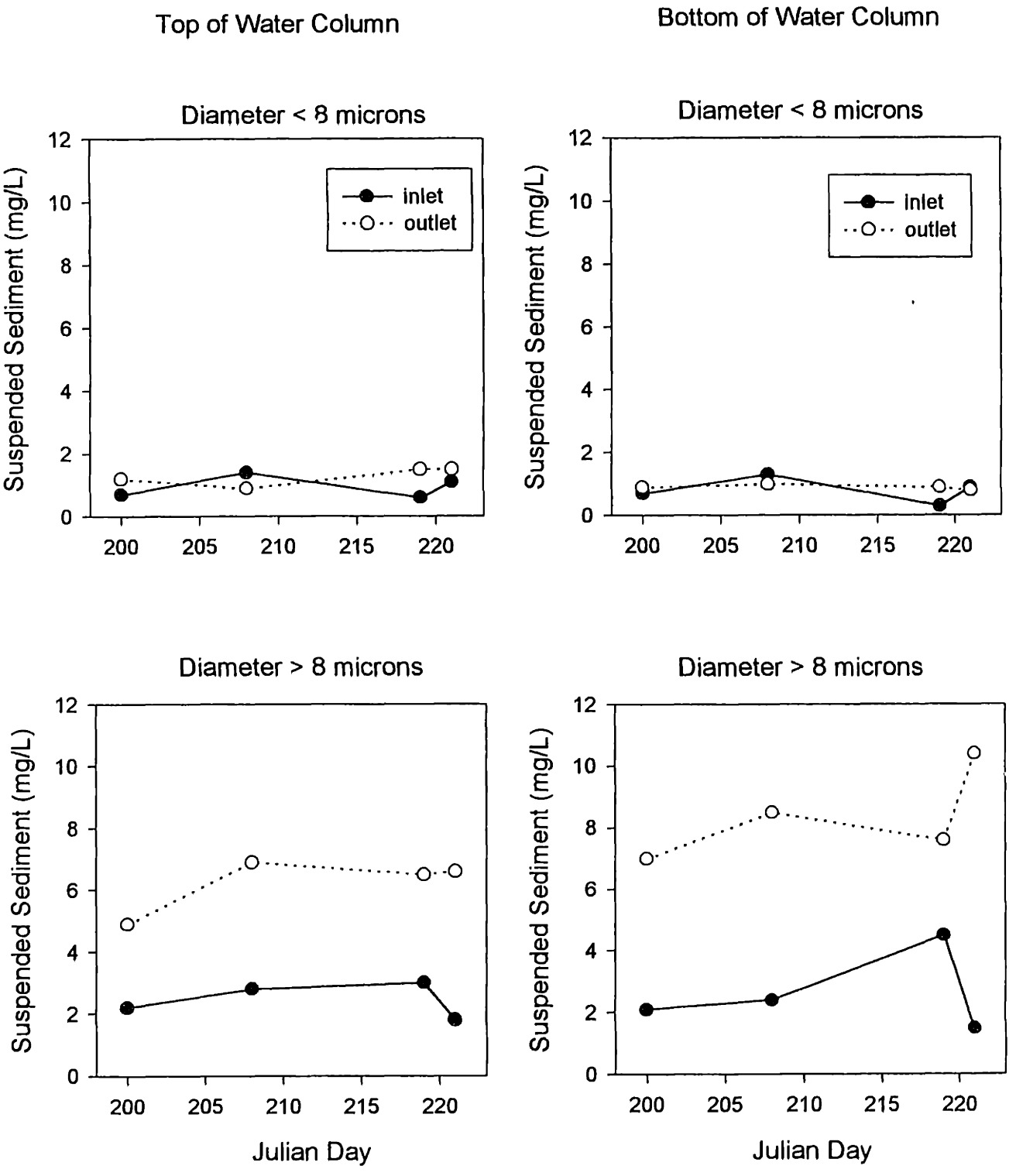

Figure 2-2: Size Fractionation of Suspended Sediment during Summer

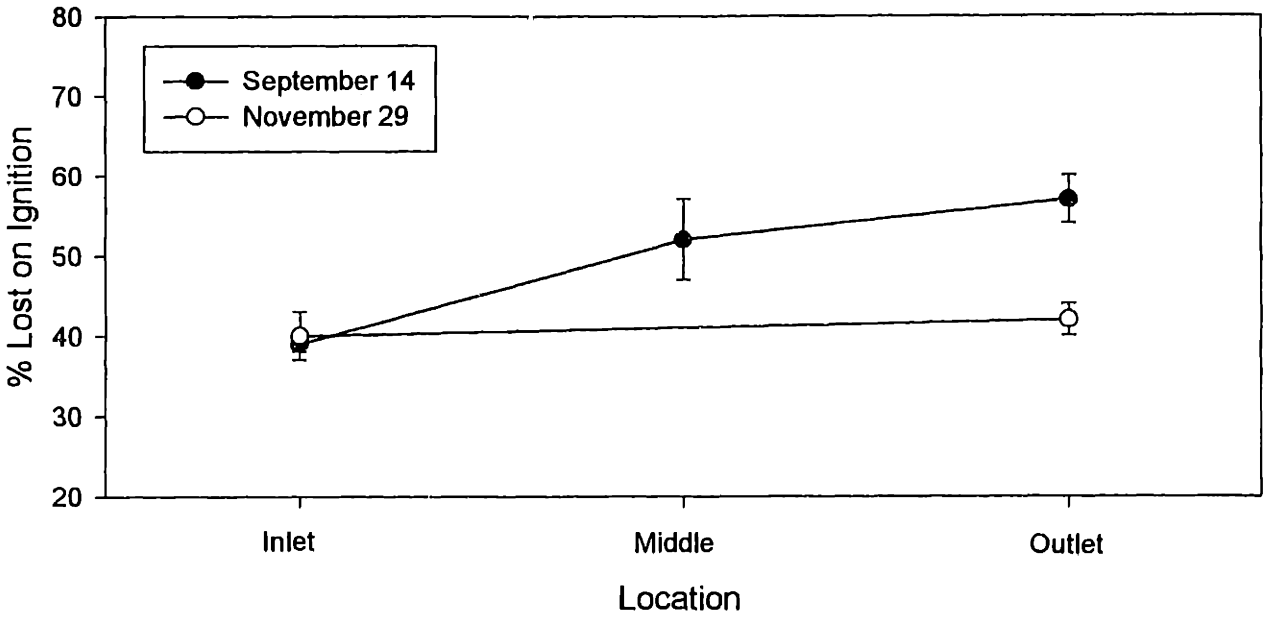

Figure 2-3: Organic Content of Suspended Sediment

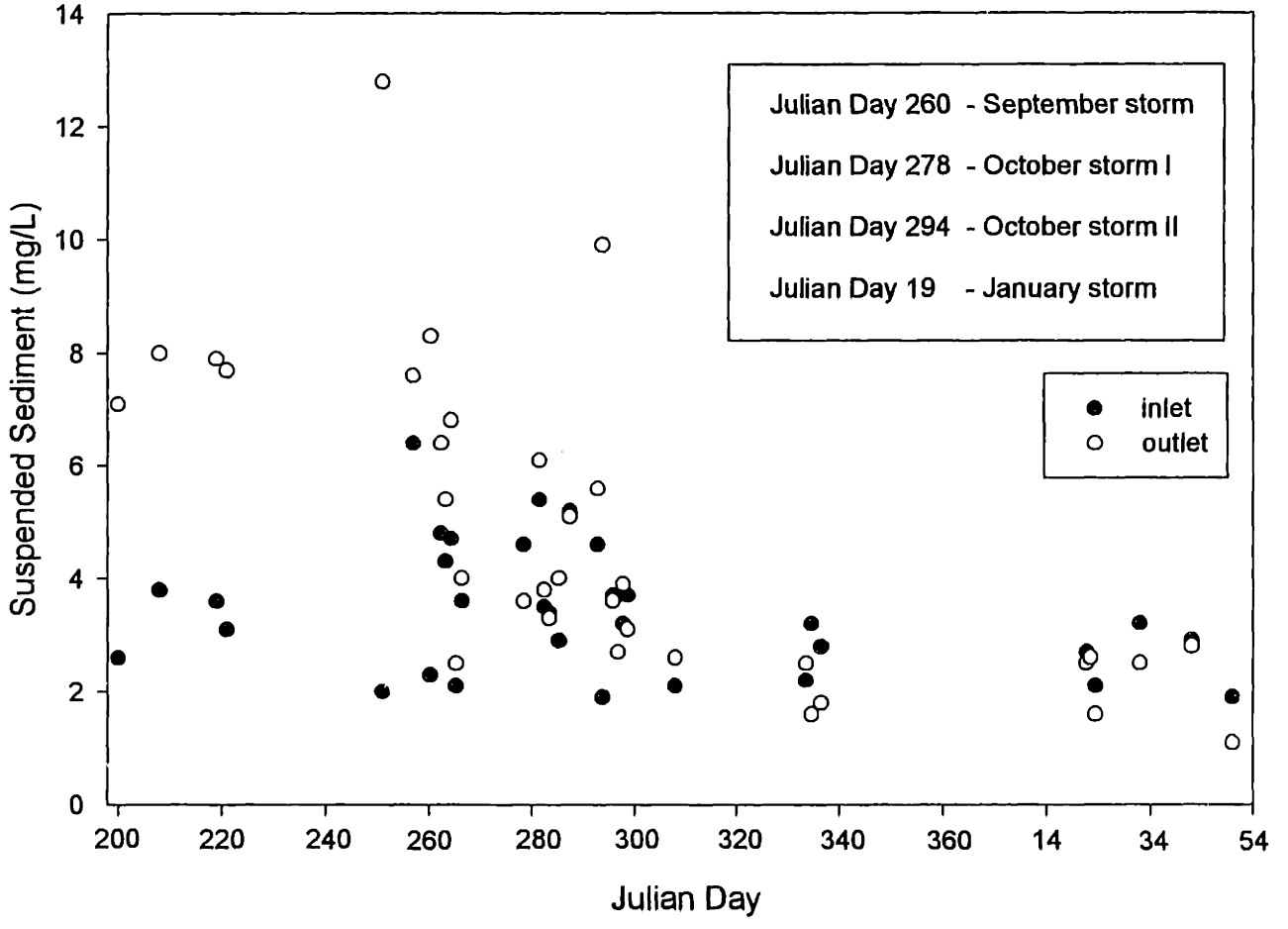

Figure 2-4: Suspended Sediment during Non-storm Conditions

sampled. The middle of October appears to be the transition point when the forebay stopped acting as a significant source of suspended solids. Measurements on six days between October storms I and II showed the outlet concentrations to be on average moderately higher, but for the four days after October storm II the concentrations were essentially the same. By the end of November, baseline concentrations were low (~ 2.5 mg/L) at both stations and inlet concentrations were slightly higher on two of three days. Following the January storm concentrations returned to ~ 2.5 mg/L at both stations and inlet concentrations were again slightly higher.

Discussion

Because of its eutrophic conditions the Upper Forebay appears to have acted as a source of suspended solids from at least the middle of July to the beginning of October. Although organic content of these solids was only measured on two days, this data shows an increase in organic content through the forebay during the summer but no change in the winter, supporting the hypothesis that a fraction of the primary production from the forebay was carried away by the flow. The source of these solids was not directly identified but could have been algae as well as plant detritus. Under normal conditions July and August would be early for the senescence, decay, and detritus production of most macrophytes, but given the spraying that occurred as well as the early decline of curly pondweed (Section 1.2) detritus was probably frequently available throughout the summer. Algae and detritus may be more mobile than mineral particles because of their lower densities (~1-1.5 g/cm^3 vs. 2.65 g/cm^3) and highly irregular shapes, qualities which contribute to lower settling velocities and thus a stronger tendency to remain in suspension. In addition, some planktonic algae have a number of mechanisms for enhancing flotation, including gas vacuoles for buoyancy regulation (Wetzel, 1983). This biological component to suspended solids transport may account for some of the variability in concentrations that do not appear related to increases in discharge. Some elevated concentrations at the

outlet (e.g., Julian day 293, Figure 2-17) may have been the result of fluctuations in the algal population or bursts of detritus production.

2.2.2 Arsenic

Observations

Figures 2-5 and 2-6 show that concentrations and fluxes of dissolved and particulate arsenic were generally higher at the outlet than the inlet prior to the September storm (Julian day 260), with the exception of two days in early August that followed a small rain event. Dissolved arsenic at the inlet was highest on the day immediately following the small rain event (Julian day 219) and had still not fallen to baseline values two days later (Julian day 221), while particulate arsenic was nearly the same on both days. There was no apparent change in concentrations at the outlet on these two days due to the small rain event. The last three samples before the September storm indicate a slight downward trend at the outlet for dissolved arsenic but not for particulate arsenic.

Size fractioning was conducted on four days, including the two days after the small summer rain event. Figure 2-7 shows that at both sampling sites the particles larger than 8 μm accounted for more arsenic than the particles smaller than 8 μm. In addition, the increase in total particulate arsenic concentrations between the inlet to the outlet was primarily due to the arsenic associated with the larger size class.

Aside from the two days after the small rain event, outlet concentrations were nearly two times higher than those at the inlet prior to the September storm (Table 2.1). The middle of October appears to be the time at which concentrations at the outlet were not regularly higher than at the inlet (Figure 2-8). On the two days (October 4 and 5) before October storm I concentrations were nearly equal, and on the two days (October 19 and 20) before October storm II concentrations at the inlet were slightly higher. For all following samples under non-storm conditions inlet concentrations were equal to or moderately higher than outlet concentrations.

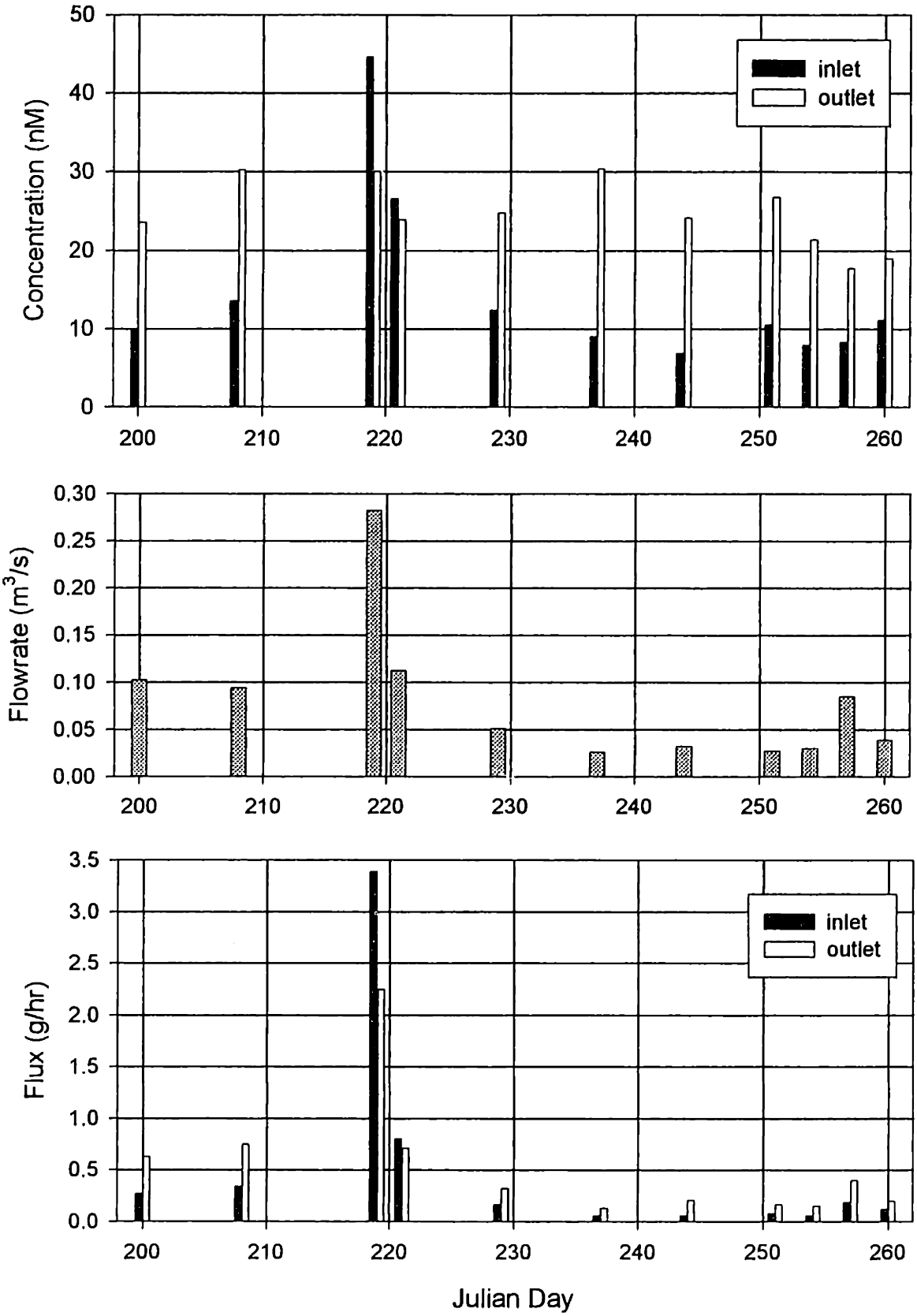

Figure 2-5: Dissolved Arsenic during Summer

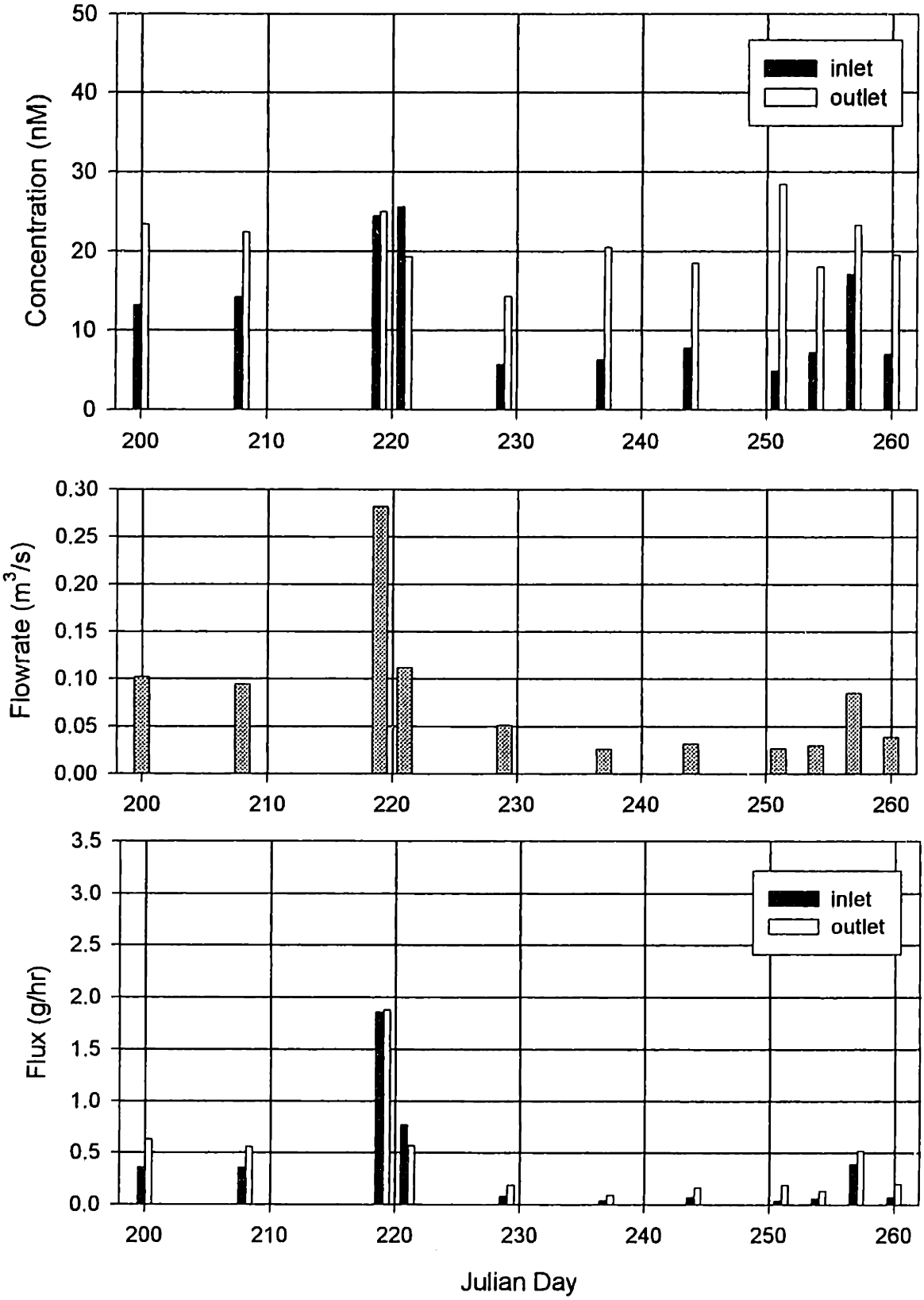

Figure 2-6: Particulate Arsenic during Summer

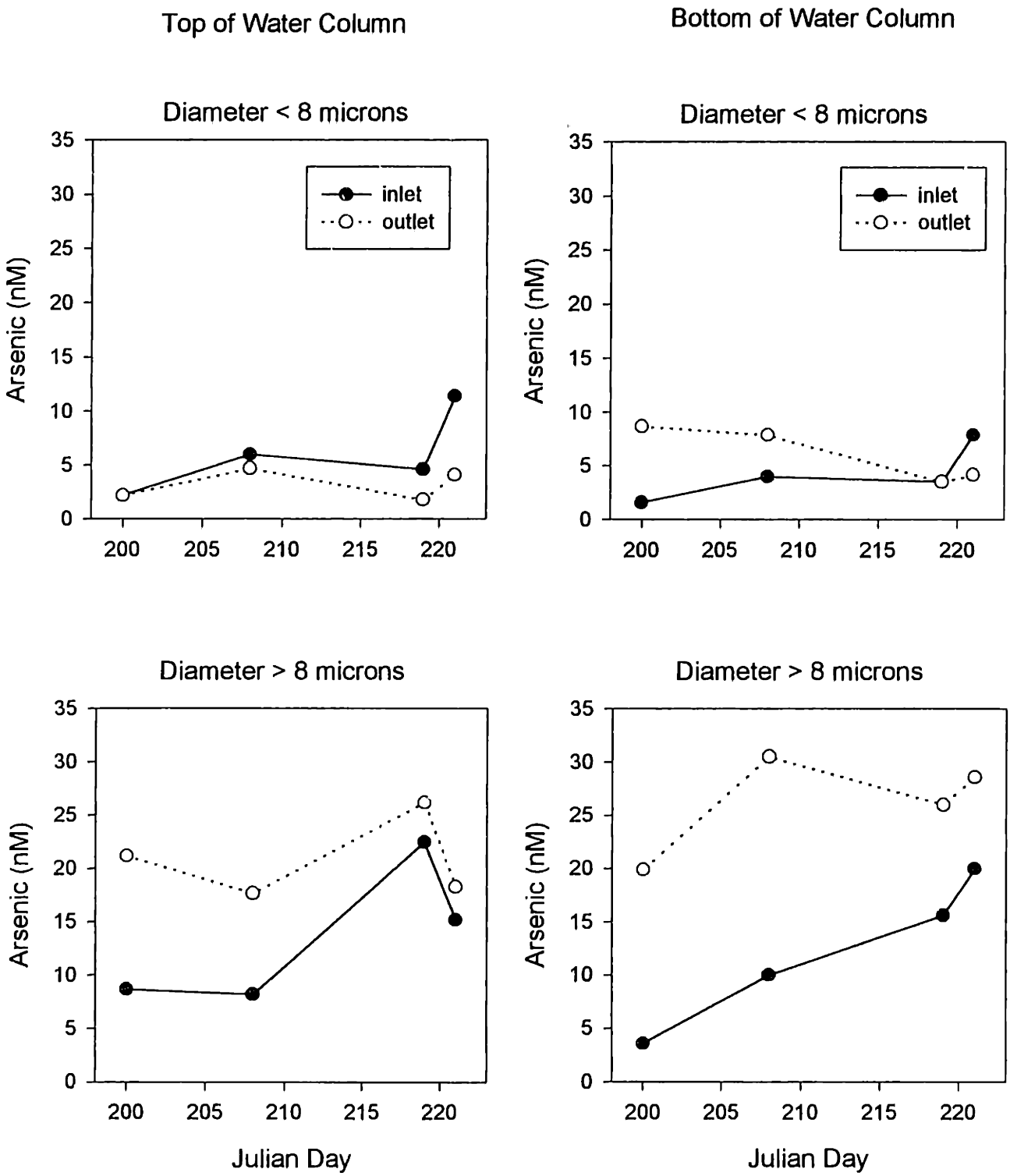

Figure 2-7: Size Fractionation of Particulate Arsenic during Summer

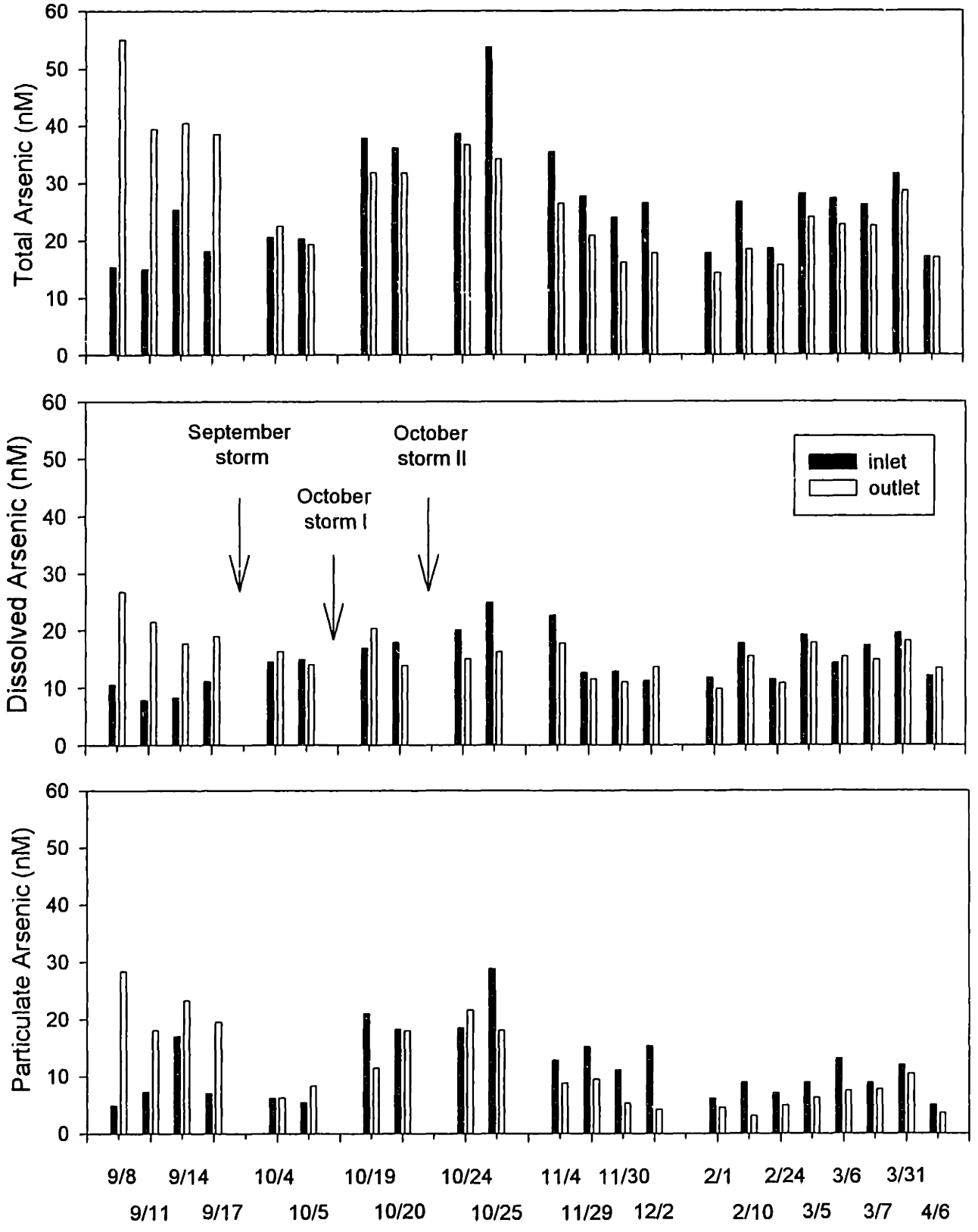

Figure 2-8: Arsenic during Non-storm Conditions, September-April

Table 2.1: Mean Summer Arsenic Concentrations, Excluding Julian Days 219, 221 (n=9)				
	Inlet		Outlet	
	Mean (nM)	Standard Deviation (nM)	Mean (nM)	Standard Deviation nM)
Dissolved	10.0	2.3	24.2	4.4
Particulate	9.2	4.4	20.9	4.0

Discussion

A distinguishing feature of the 1995 summer was the extremely low river flows, which affected the size of the input arsenic loads as well as the residence time of water in the forebay. As discussed in Section 1.2 there may be a range of residence times, with the shortest being the direct time-of-travel from inlet to outlet (T_{min} = L/U) and the longest being on the order of the nominal detention time (T_{nom} = V/Q), where

L = distance from inlet to outlet (m)
U = average inlet velocity (m/s)
V = volume of Upper Forebay (m^3)
Q = average flowrate (m^3/s)

For typical summer conditions U = 2.5 cm/s, Q = 0.05 m^3/s, V = 100,000 m^3 (assuming an average depth of 1 m due to the low water level), T_{min} ~ 6 hours, and T_{nom} ~ 20 days. For typical non-storm conditions in the winter U = 6.5 cm/s, Q = 0.65 m^3/s, V = 150,000 m^3, T_{min} ~ 2 hours, and T_{nom} ~ 3 days. Measurements under non-storm conditions on 12 days in late fall/winter show an average decrease between the inlet and outlet of 6% for dissolved arsenic and 36% for particulate arsenic (19% total arsenic), indicating that a portion of the incoming load is normally retained in the forebay (also observed by Spliethoff, 1995). During the summer residence times were longer and there was more time for settling, and thus we would expect to have seen at least as much reduction of the incoming load as seen in late fall/winter. Concentrations at the outlet were actually higher on most days, implying that there must have been particular circumstances during the summer influencing the arsenic balance in the forebay.

In addition to higher outlet concentrations, particles in the larger size class (diameter > 8 μm) accounted for more arsenic at the outlet than the inlet. Because the forebay was a source of organic solids during the summer, a large fraction of which was larger than 8 μm, one hypothesis is that arsenic was transported out of the forebay after becoming sorbed onto these organic solids. The association between arsenic and the organic solids probably occurred throughout the forebay but especially in the unsprayed area in front of the inlet, where a dense growth of macrophytes and algae flourished throughout the summer (including many spots where elodea nearly reached the surface).

One possible explanation for the consistently higher outlet concentrations is that the vegetation in the unsprayed area acted as a temporary filter, trapping the relatively large bursts of arsenic flux brought in following small rain events (e.g., Julian day 218) and then slowly releasing a portion of it over time. As the river flow entered the forebay and passed through this area, colloidal and particulate arsenic could have collected on the algae and plant tissue. Much of the free-floating algae would then have been distributed to other areas of the forebay before eventually reaching the outlet, while particles on the plants could have been released into the water column by agitation from wind waves or during the decay of the plant.

A mass balance was performed from Julian day 200 to Julian day 260 (the period during which data was collected prior to the September storm) in order to determine whether the relatively large arsenic fluxes that are carried in during small rain events could by themselves account for the consistently high concentrations at the outlet over a long period of time. Figure 1-6 shows that the last large input pulse of arsenic probably occurred at least 30 days prior to Julian day 200 (with a smaller pulse occurring 10 days prior to Julian day 200), and most of arsenic in these pulses should have settled to the sediments or been flushed out by this time. Figure 2-9 shows that concentration at the inlet increased linearly with flowrate until ~ 0.3 m^3/s and then appeared to level off for higher flowrates. (Data from September and October were included because availability conditions for arsenic during these months were most likely to be similar to summer conditions). A best-fit line was used to

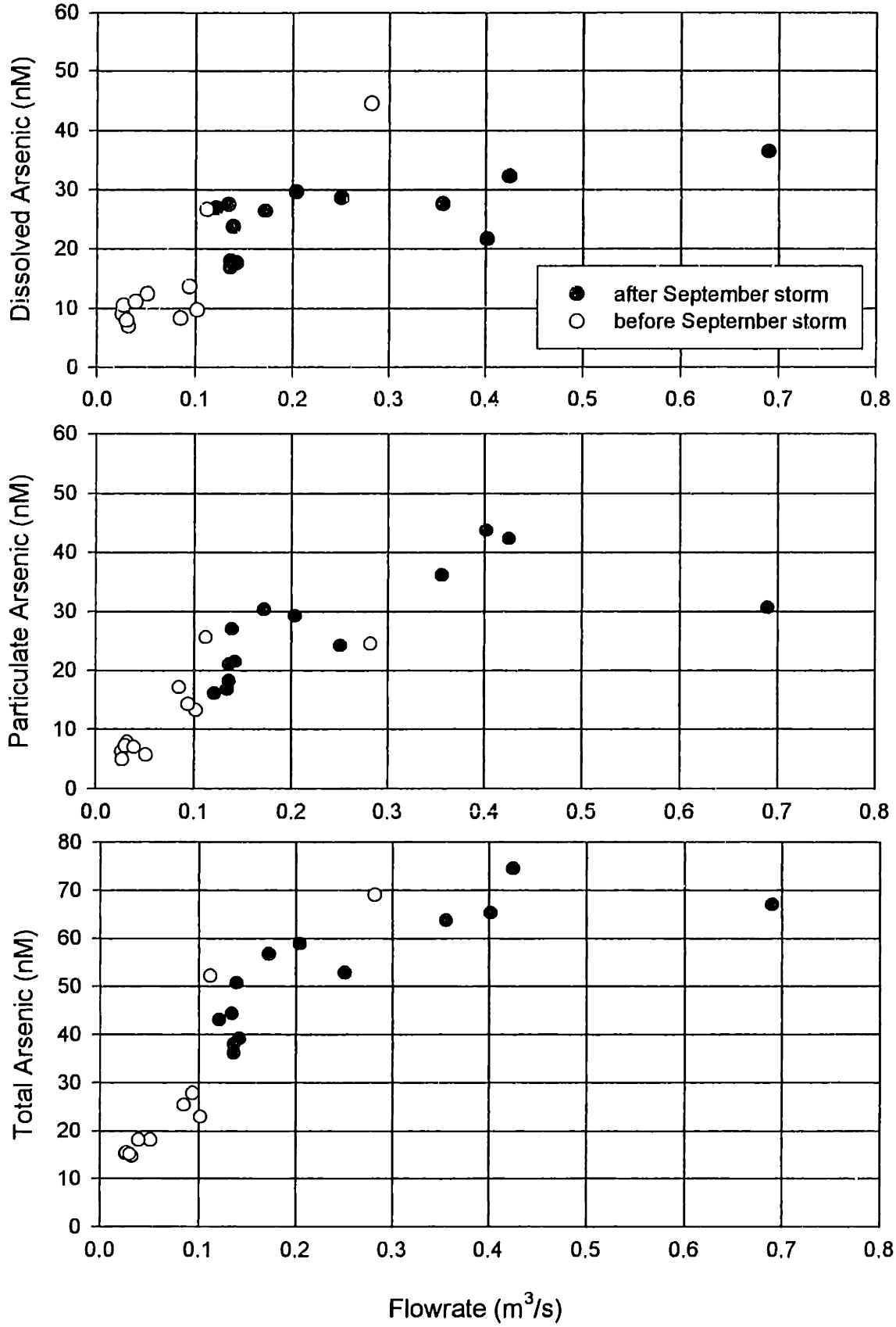

Figure 2-9: Arsenic vs. Flowrate for Summer Mass Balance

estimate total arsenic concentrations below 0.3 m^3/s, while concentrations for flows higher than 0.3 m^3/s were assumed to be constant (67.9 nM).

Because concentrations at the outlet during the summer were not significantly correlated with either inflow conditions or windspeed, the average value from all the samples (mean = 45.6 nM, sample variance = ± 6.3 nM) was used to estimate the concentration for days that were not sampled. During the study the largest changes in concentration were observed following high-flow events, as discussed in the following section, but the small rain events that occurred during the summer did not appear to affect outlet concentrations. Wind-driven sediment re-suspension was also not observed to be a major factor. Figure 2-10 shows that there was no direct correlation between wind and particulate arsenic at the outlet during the summer even though there was a fairly large range of wind speeds. Wind waves are often a cause of sediment re-suspension in shallow water environments, but this mechanism is limited in the Upper Forebay by the relatively small fetch (the open-water distance for wave development). Winds of over 10 m/s would be required before waves "feel" the bottom and begin to start generating shear stresses that could re-suspend sediment (see Appendix A.4).

The total arsenic loads entering and exiting the forebay were estimated as follows:

$$L_{in} = \int C_1 Q_1 dt + C_2 \int Q_2 dt$$

$$var(L_{in}) = (\int Q_1 dt)^2 \, var(C_1) + (\int Q_2 dt)^2 \, var(C_2)$$

$$L_{out} = C_{out} \int Q dt$$

$$var(L_{out}) = (\int Q dt)^2 \, var(C_{out})$$

$$SE = var^{1/2}$$

where

L = total arsenic load
Q = discharge
C_1 = arsenic concentration at inlet for Q < 0.3 m^3/s using best-fit line
C_2 = average arsenic concentration at inlet for Q > 0.3 m^3/s
C_{out} = average arsenic concentration at outlet
var = variance
SE = standard error

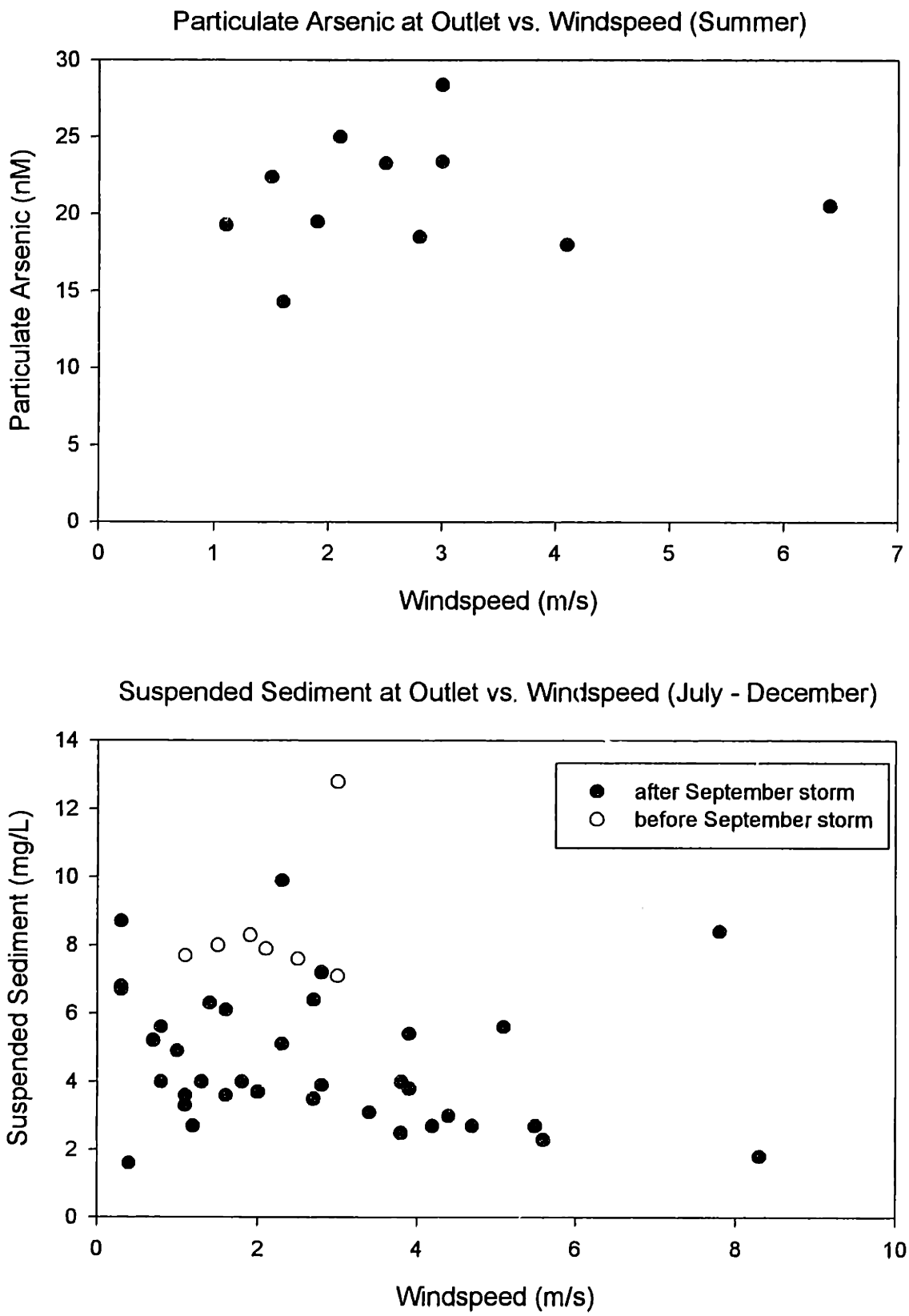

Figure 2-10: Comparison of Outlet Concentrations vs. Windspeed

Calculations using this approach show that 1.40 kg (SE = 0.17) of arsenic entered the forebay and 1.62 kg (SE = 0.22) exited during this sixty day period. Although the estimated load exiting the forebay is larger than the estimated load entering the forebay, they are not statistically different given the uncertainty of the calculation. It is probably unlikely that all of the entering load was filtered by the vegetation and then re-released with zero retention, and another possible explanation for the consistently higher outlet concentrations is that there was loading by an internal arsenic source. The existence of an internal source would also explain why outlet concentrations show little or no decline during the 30-40 day period in late August/early September when there were no rain event pulses. The magnitude of the fluxes during the summer may have been small enough such that internal loading, which would normally be overshadowed by the much larger river loading, became significant. The implied internal loading at the end of the summer (flux out - flux in) was at most ~0.25 g/hr, while during non-storm conditions in the winter there was a net loss to the forebay (flux in - flux out) of ~2-3 g/hr. Assuming that the internal loading did not increase considerably under the higher flow conditions, its existence would not be easily recognized.

Although wind-induced re-suspension was probably not a factor, three other possible sediment release mechanisms include anoxia, "pumping" by aquatic macrophytes, and groundwater seepage. When bottom waters become anoxic, the thin oxidized micro-layer at the sediment/water interface can erode and metal-rich water from the anaerobic sediments underneath can then be released into the water column. This was unlikely to have occurred in the forebay because dissolved oxygen in the bottom waters was high on the two mornings in September during which measurements were made (Table B.12; also observed at the beginning of the summer in ACT, 1995), and temperature profiles (Figure 1-4) show that the water column became isothermal overnight, which implies that oxygenated surface water was regularly mixed to the bottom. The second possible mechanism comes about because arsenic acts as a phosphorus analog for primary producers. Phosphorus is taken up from the sediments by rooted macrophytes for metabolism and then released through excretory or decay

processes (Barko and Smart, 1980). Because of the high sediment concentrations, arsenic may have been inadvertently taken up along with phosphorus by the roots and rhizomes and then subsequently released into the water column (Otte and Ernst, 1994). Finally, and perhaps most likely, groundwater seepage may have caused exfiltration of arsenic from the sediment porewater.

2.3 High-flow Events

Figures 2-11 and 2-12 show hydrographs and hyetographs for the first four high-flow events during which sampling was conducted (the hydrograph for the July storm was not yet available). After 41 days with only trace amounts of precipitation, 2.25 inches of rain fell in 13 hours on September 17, with 56% (1.27") falling in a 3-hour period. On October 5 and 6 (October storm I), 2.60 inches of rain fell in 21 hours, and on October 21 (October storm II), 1.64 inches of rain fell in 14 hours. For these three rain storms the peak flowrate occurred 3-4 hours after the hour with the highest rainfall and 5-6 hours after the center of mass of the rainfall. For the January high-flow event, flowrates started increasing before the moderate rain (0.62 inches in 6 hours) due to the rapid melting of snow that had accumulated over nearly four weeks. For the July storm, 3.65 inches of rain fell over the course of 20 hours (Figure 2-13).

The time for a kinematic wave to travel from the USGS station to the Upper Forebay inlet is approximately 7 minutes, which is small enough relative to the interval of discharge measurement (hourly) such that the inlet discharges were taken to be the discharges measured at the USGS station (see Appendix A.1). Discharges at the outlet were estimated according to conservation of mass:

$$Q_{out} = Q_{in} - \frac{dh}{dt} A$$

where

Q = discharge (m^3/s)
A = surface area (m^2), assumed constant
h = Upper Forebay water level (m)

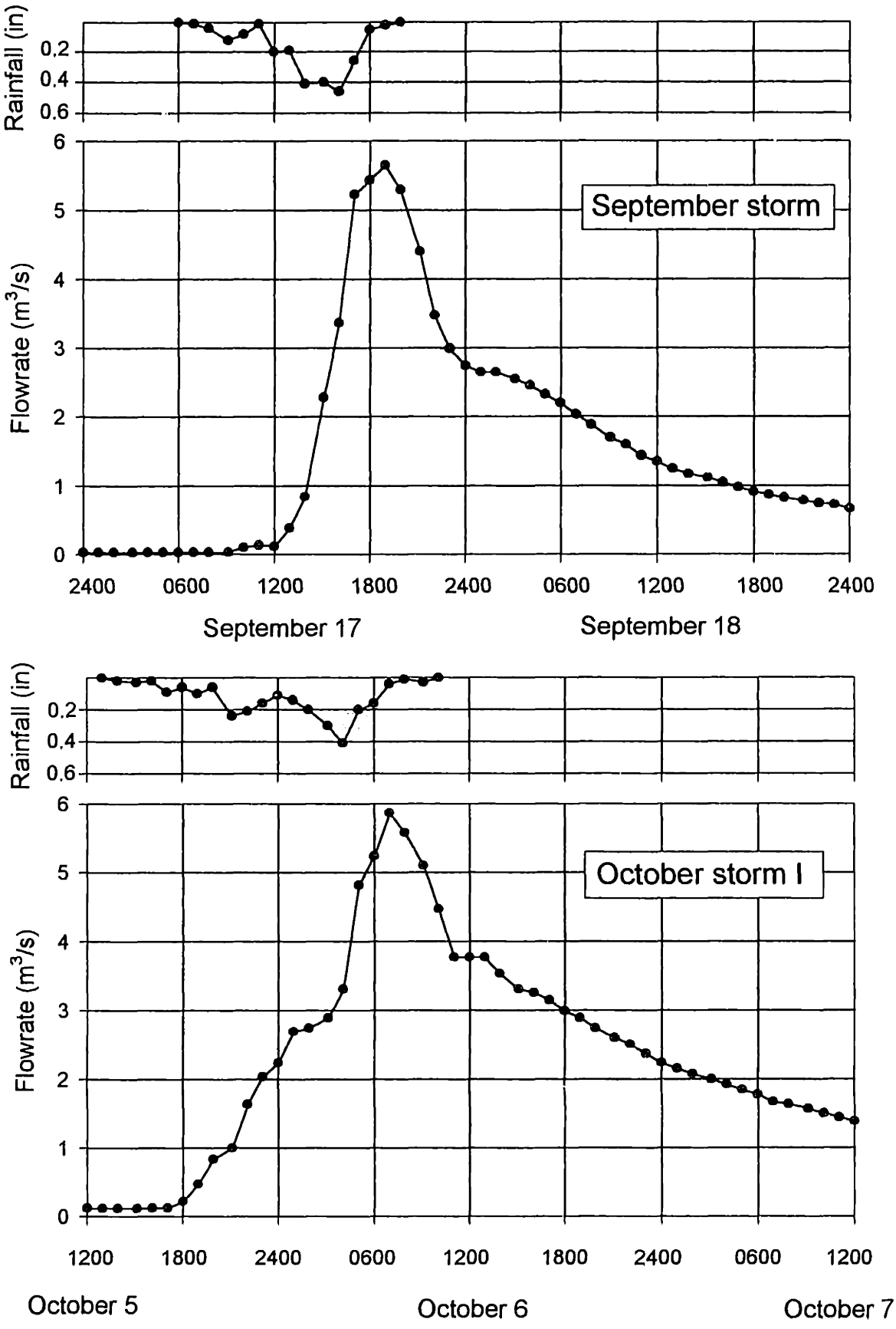

Figure 2-11: Hydrographs and Hyetographs for September Storm and October Storm I

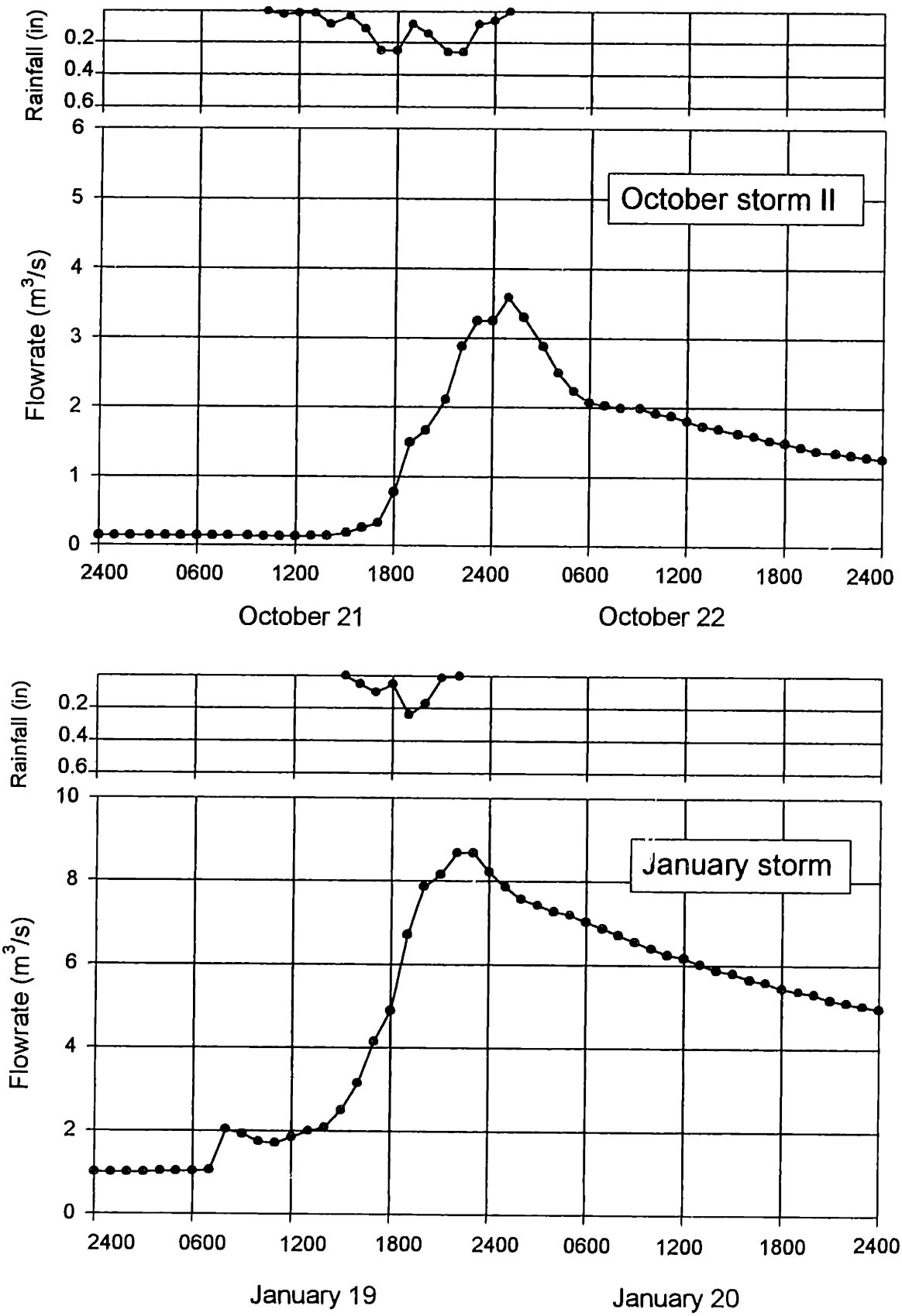

Figure 2-12: Hydrographs and Hyetographs for October Storm II and January Storm

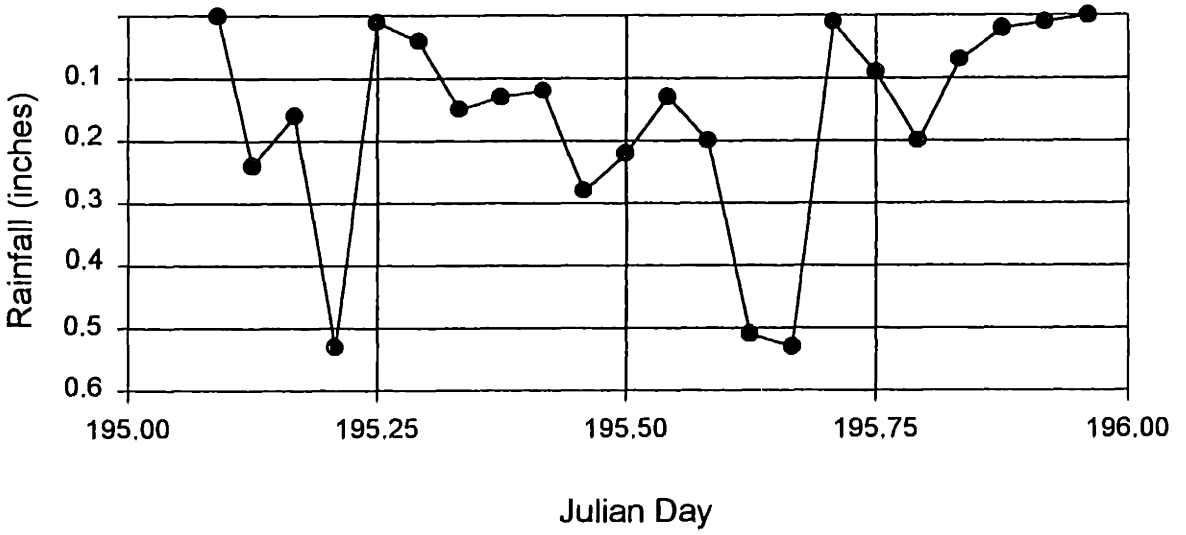

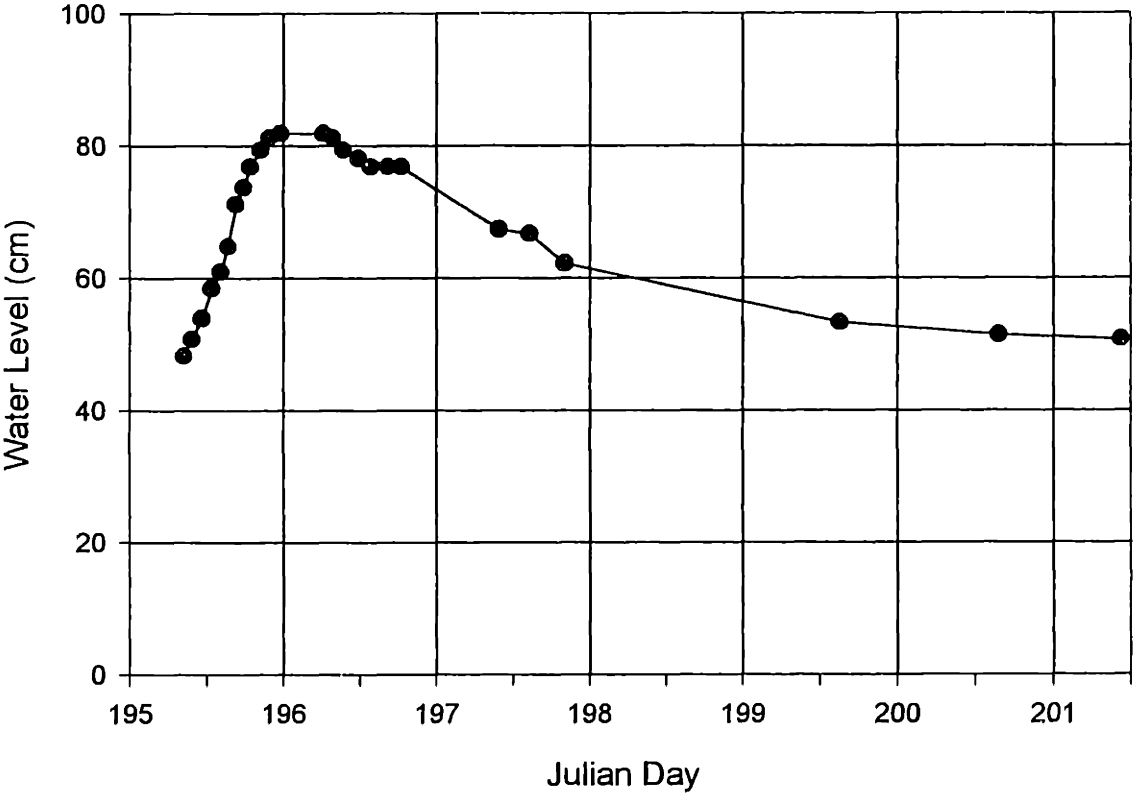

Figure 2-13: Rainfall and Water Level during July Storm

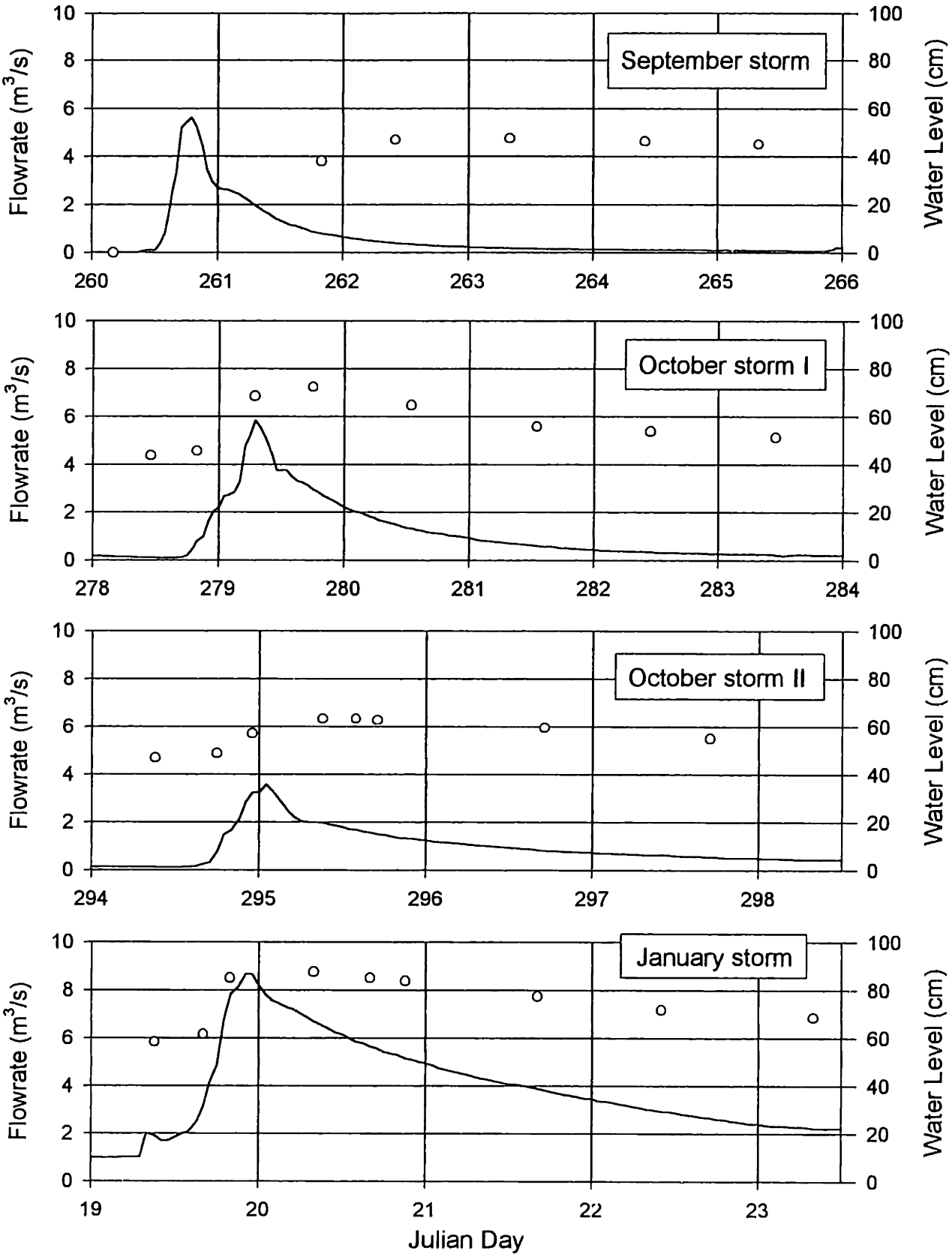

Figure 2-14: Water Level during September Storm, October Storm I, October Storm II, January Storm
(Line = Flowrate; Circle = Water Level)

Figures 2-13 and 2-14 show changes in water level in the Upper Forebay during the high-flow events relative to the lowest 1995 summer water level, and Figures 2-15 through 2-30 show concentrations and fluxes. Some graphs are shown twice but with different scales, and only Figure 2-23 includes 95% confidence intervals for the arsenic measurements (showing that the confidence intervals are nearly the size of the circles for most points). Although lines were drawn to connect the data points, linear interpolation may not be an accurate estimate of concentrations between points at times when there is a rapid rate of change, as will be discussed later.

2.3.1 Suspended Sediment

Observations

Suspended sediment at the inlet rose to 95.5 mg/L during the peak discharge of the September storm while there was no significant change at the outlet (Figure 2-15). When samples were taken nearly a day later the inlet concentration was still elevated (11.3 mg/L) but the outlet concentration remained at pre-storm levels (8.7 mg/L). By the next day inlet concentrations had dropped down to pre-storm values and the trend of having higher concentrations at the outlet continued for the next five days, although there was a modest decline in outlet concentrations following the storm. Suspended sediment reached 50.5 mg/L at the peak discharge of October storm I with a modest rise (7.2 mg/L) at the outlet (Figure 2-16), and October storm II saw a peak concentration at the inlet of 26.9 mg/L with no sign of a suspended sediment pulse at the outlet (Figure 2-17). The January storm had higher flowrates than the three previous storms that were sampled, and suspended sediment at the inlet reached 149.0 mg/L two hours before the peak flowrate (Figure 2-18). Two hours after the peak flowrate the concentration had dropped down to 73.3 mg/L, and the next sample taken eight hours later shows concentrations very near baseline values. Four hours after the peak concentration at the inlet suspended sediment at the outlet was 43.8 mg/L, but by the time of the next sample eight hours later it

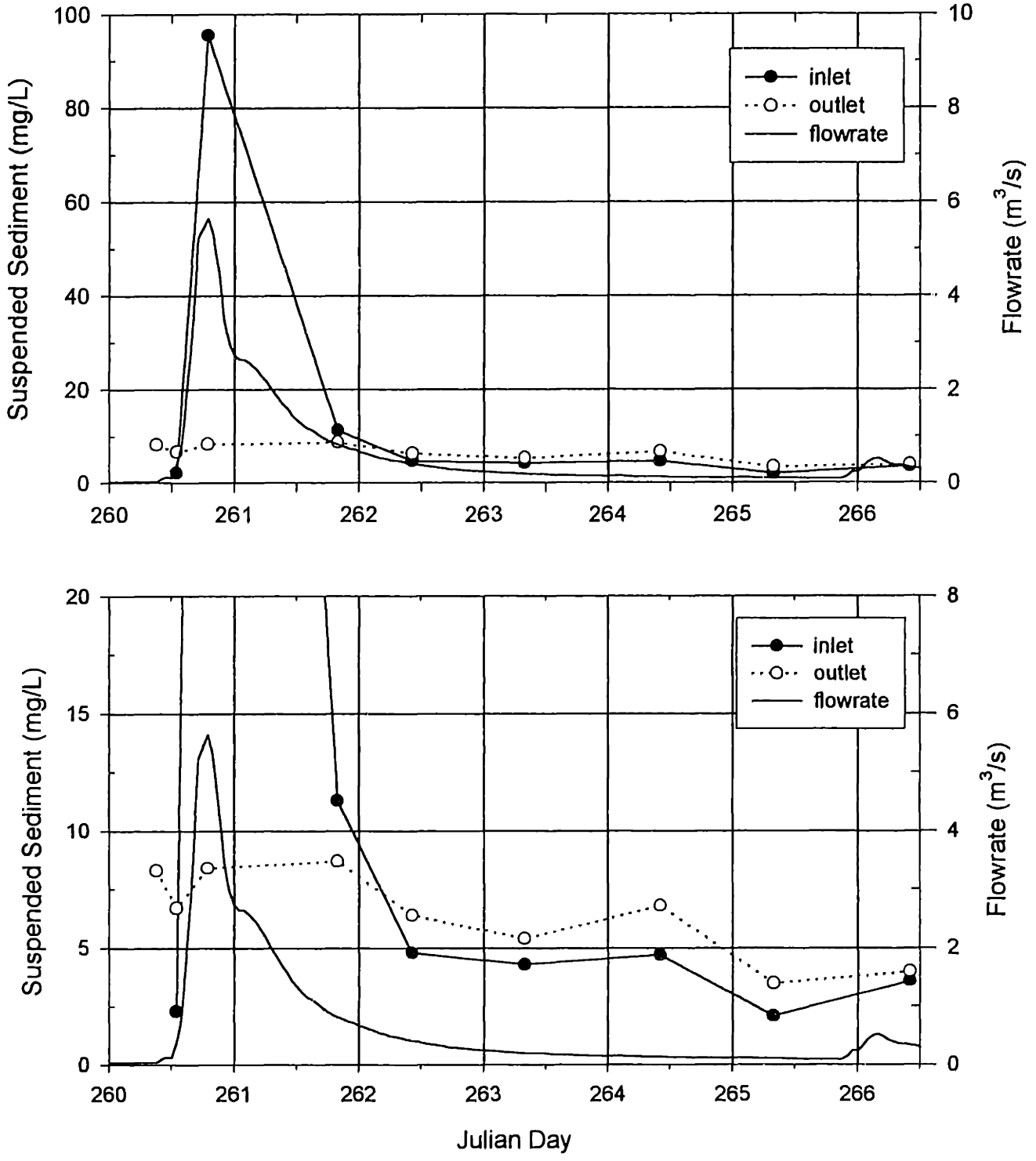

Figure 2-15: Suspended Sediment during September Storm

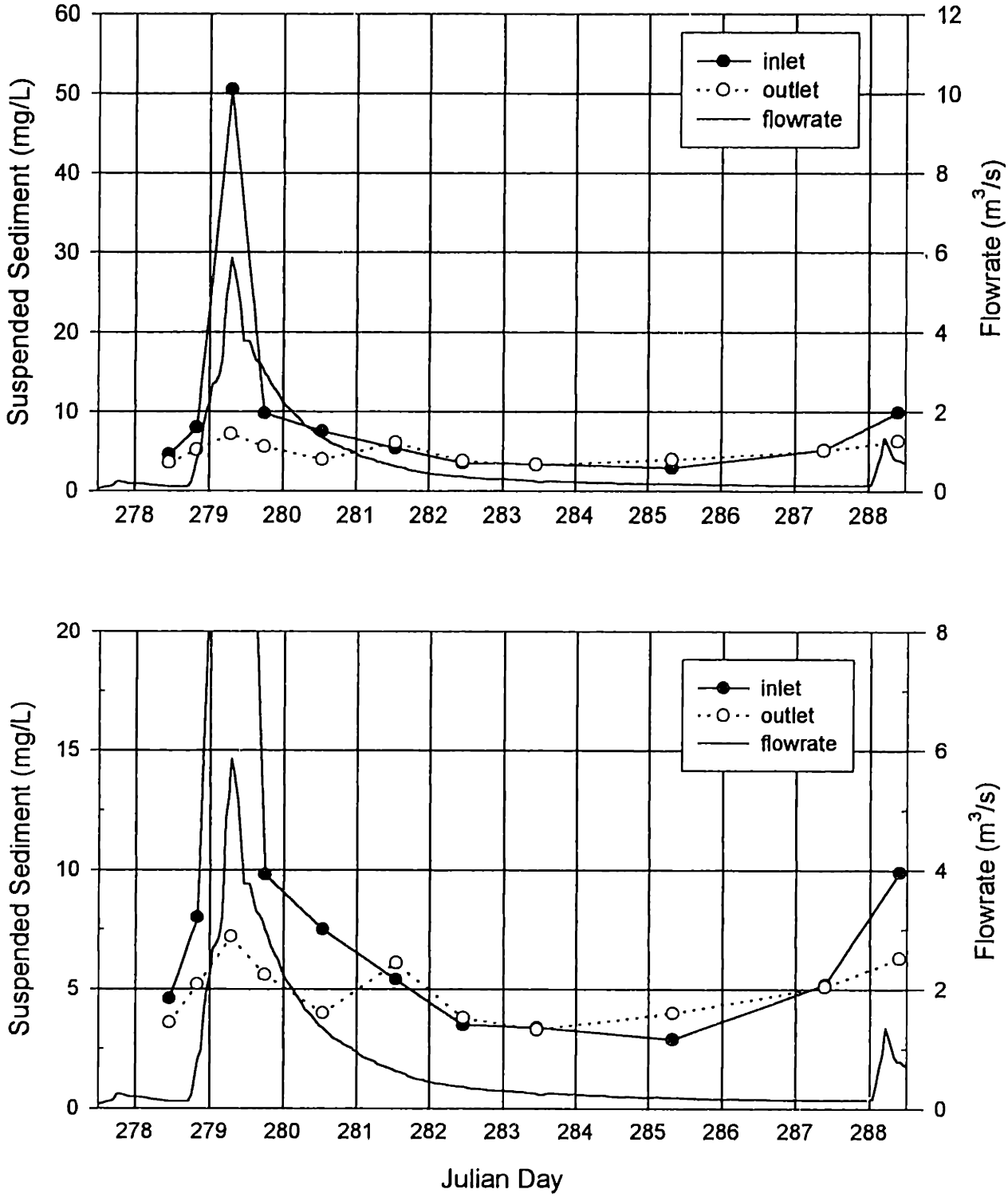

Figure 2-16: Suspended Sediment during October Storm I

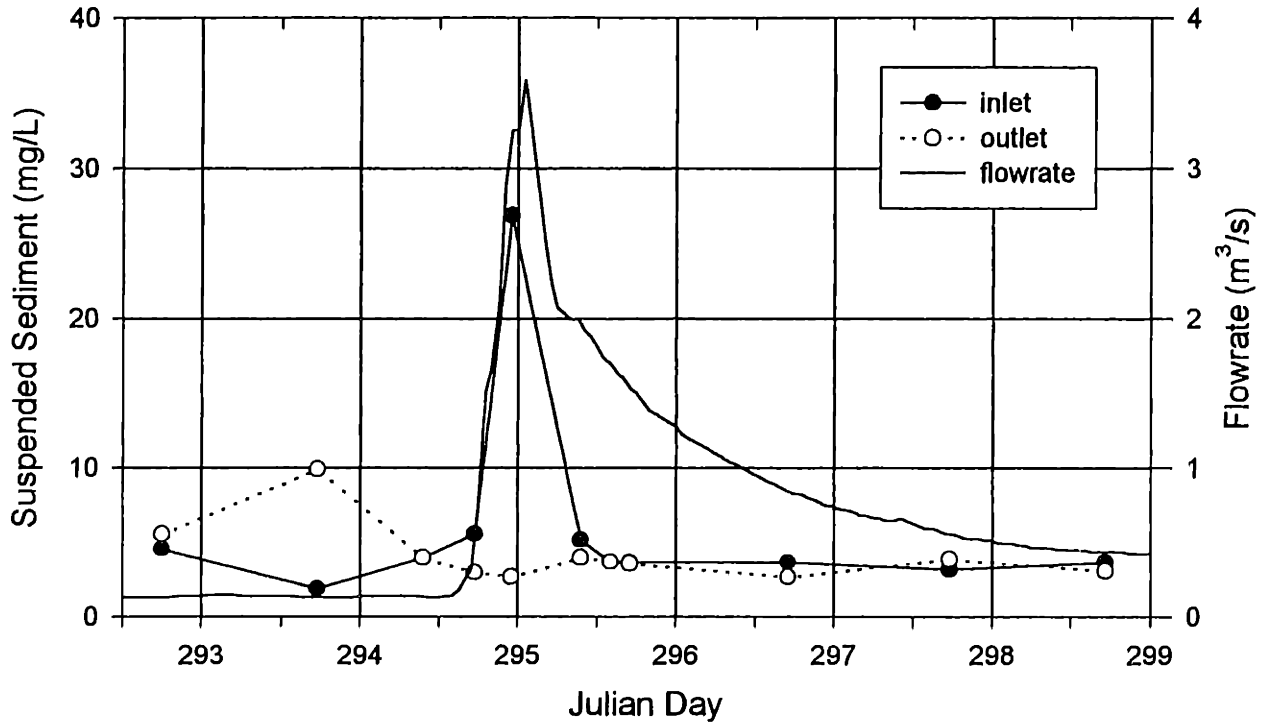

Figure 2-17: Suspended Sediment during October Storm II

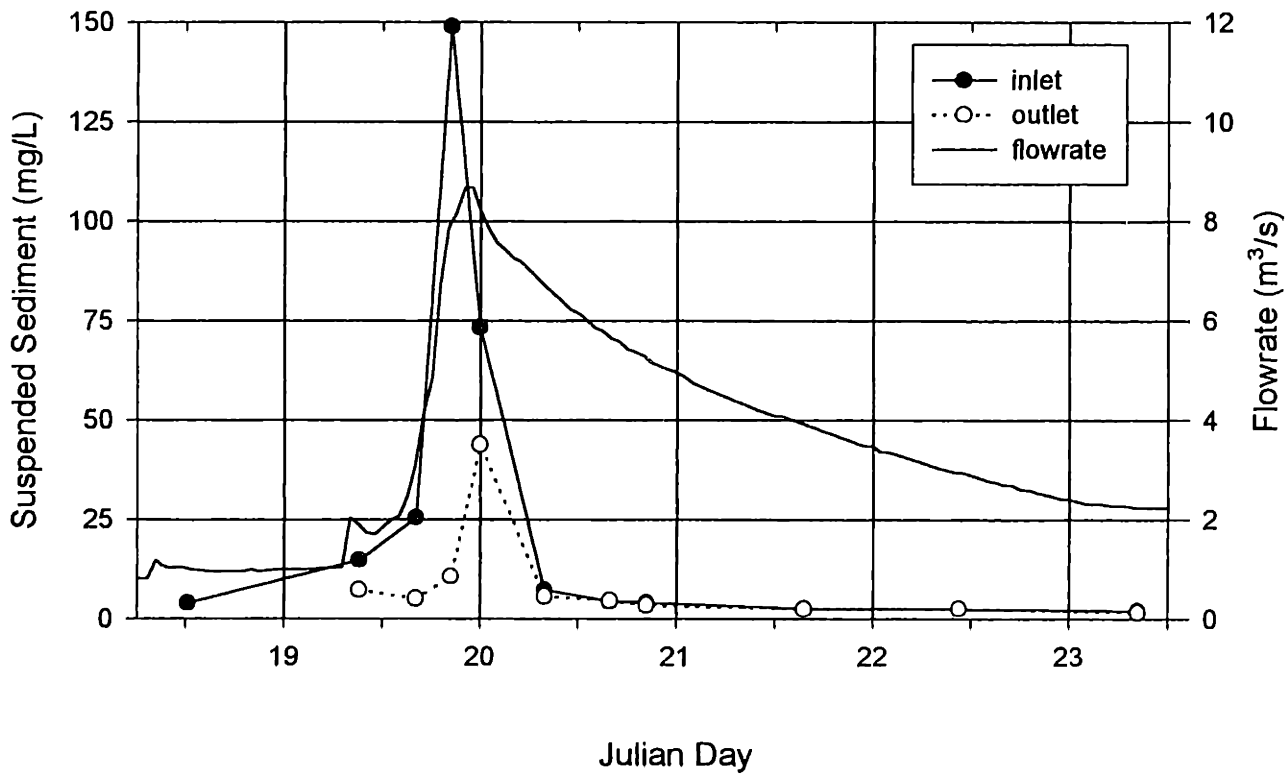

Figure 2-18: Suspended Sediment during January Storm

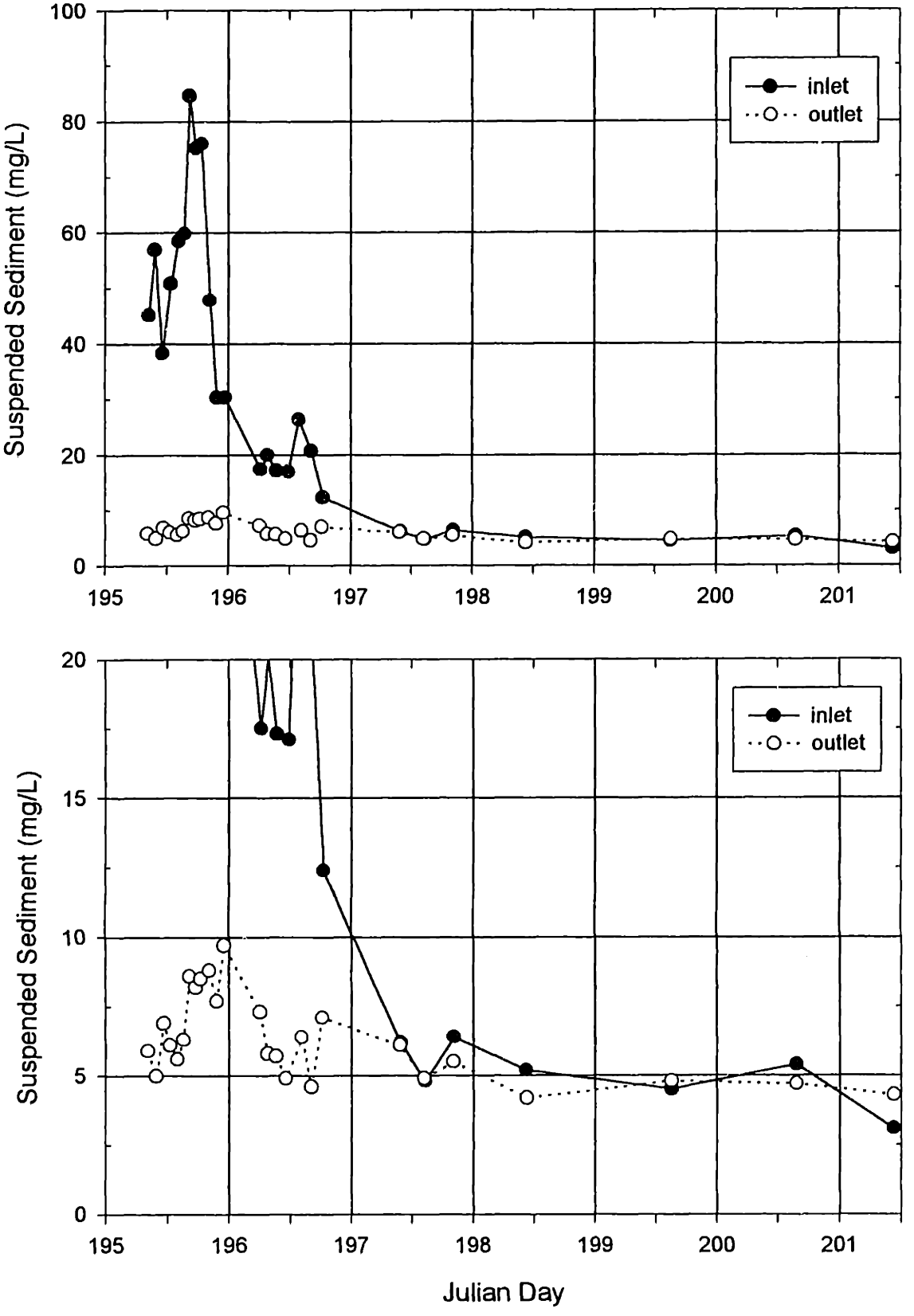

Figure 2-19: Suspended Sediment during July Storm

had dropped down to baseline values. For the July storm, the inlet concentration peaked at 84.7 mg/L while the outlet concentration reached only 9.7 mg/L (Figure 2-19).

Discussion

The observations of suspended sediment made during this study agree with the finding of Solo-Gabriele (1995) that suspended sediment transport in the Aberjona River during storms is limited by availability of sediment rather than by the carrying capacity of the flow. The peak discharge of October storm I was nearly the same as the peak discharge for the September storm, yet the concentration of suspended sediment at the inlet was only half as large, indicating that the September storm had flushed out much of the sediment that had accumulated since the previous high flows. For the January storm the sample on Julian day 20.33 showed near-baseline suspended sediment concentrations (7.3 mg/L) at the inlet even though the flowrate (6.7 m^3/s) was still larger than the peak flowrates of the other three storms, indicating that the high flows during the beginning of the storm had already flushed out much of the available sediment.

The concentration of suspended sediment remains elevated in the river for approximately 10-20 hours during the quick-storm response (Figure 2-19; see also Solo-Gabriele, Figures IV.3-12 through IV.3-14). With the interval of sampling used during the first four storms only 1-3 samples were collected during this time and thus the sampling record may not show all the important features of these increases (i.e., pulses of sediment may have slipped through the outlet between samples). Concentrations were elevated at the inlet during all of these storms, but only the results from the January storm indicate a large increase at the outlet (Figure 2-18). For the July storm the interval of sampling was increased considerably in order to catch any potential increases at the outlet (Figure 2-19). Concentrations at the outlet rose slightly at the end of Julian Day 195 but much of the suspended sediment was again observed to be retained in the forebay, most likely due to a filtering effect by the large mid-summer vegetation growth. Vegetation can cause direct blockage of the particles as well as providing drag on the flow and reducing the turbulence that keeps particles in suspension (Leonard *et*

al, 1995). This effect was probably highly significant during the September storm and at least partially significant during the October storms, but during the January storm vegetation was not a factor, although the sediment load was still subject to deposition due to partial mixing of water in the advective zone with the ambient forebay water.

The extent of deposition between the inlet and outlet for the January storm between Julian days 19.67 and 20.33 was estimated using a first-order settling model:

$$\frac{dC}{dt} = -k_s C$$

$$k_s = \frac{w_s}{h}$$

$$C = C_i e^{-k_s T}$$

where

C = concentration at outlet (mg/L)
C_i = concentration at inlet (mg/L)
k_s = time constant (hr^{-1})
w_s = settling rate (cm/hr)
h = depth (cm)
T = residence time (hr)

Concentrations at the inlet were linearly interpolated between sample points, and it was assumed that the suspended sediment could be represented by a single size class of spherical particles that exhibited Stokes settling rates and had specific gravity 2.0 (40% organic material). Residence times of $2xT_{min}$ and $4xT_{min}$ were considered (representing different amounts of exchange between the advective zone and mixed zone, where T_{min} = V/Q is the direct time-of-travel from inlet to outlet), with the actual residence time likely falling within this range. For each of these residence times the value of w_s was found that resulted in the best fit for the observed concentrations at the outlet using the above settling model. Concentrations during non-sampled times were then calculated and total loads were determined by integrating the flux curves (Table 2-2). The loads entering the forebay during this period were $2.97x10^4$ kg sediment and 2.27 kg particulate arsenic, and approximately 60% of the sediment and 70% of the particulate arsenic were retained in the forebay.

Table 2-2: Settling Estimates for January Storm (Julian days 19.67- 20.33)						
Residence Time (hrs)	Particle Diameter (μm)	Settling Rate (cm/hr)	Loads Exiting Forebay (kg)			
			Sediment	% Reduction	Particulate Arsenic	% Reduction
2 x Tmin	25	109	1.27×10^4	57	0.72	68
4 x Tmin	20	70	1.10×10^4	63	0.63	72
		Average:	1.19×10^4	60	0.68	70

2.3.2 Arsenic

Observations

For the September storm there was a large increase in both dissolved and particulate arsenic at the inlet during the peak discharge (Figure 2-20). Total arsenic at the inlet reached 222.2 nM (16.6 ppb), the highest concentration measured during the study and more than ten times higher than typical concentrations under low-flow conditions during the summer (20 nM, 1.5 ppb). Dissolved and particulate arsenic declined gradually over the next few days following the peak discharge, until particulate arsenic rose on Julian day 266 in response to a small rain event. Dissolved arsenic at the outlet rose to 30 nM a day after the peak discharge and remained at this level for three days before dropping slightly, while particulate arsenic showed no increase from pre-storm levels and may have dropped slightly over the course of the week.

October storm I had a similar hydrograph to the September storm but a number of differences in arsenic transport (Figure 2-21). Dissolved arsenic didn't rise at the inlet until the slow-storm response, and there appears to have been multiple peaks in particulate arsenic. Particulate arsenic (nM) increased in conjunction with the large suspended sediment load during the quick-storm response, but then dropped down at the start of the slow-storm response before rising again a day later in conjunction with the dissolved arsenic peak. Figure 2-25 shows that the second peak was composed of more concentrated particles (700-800 mg/kg) than the first peak (200 mg/kg). At the outlet small

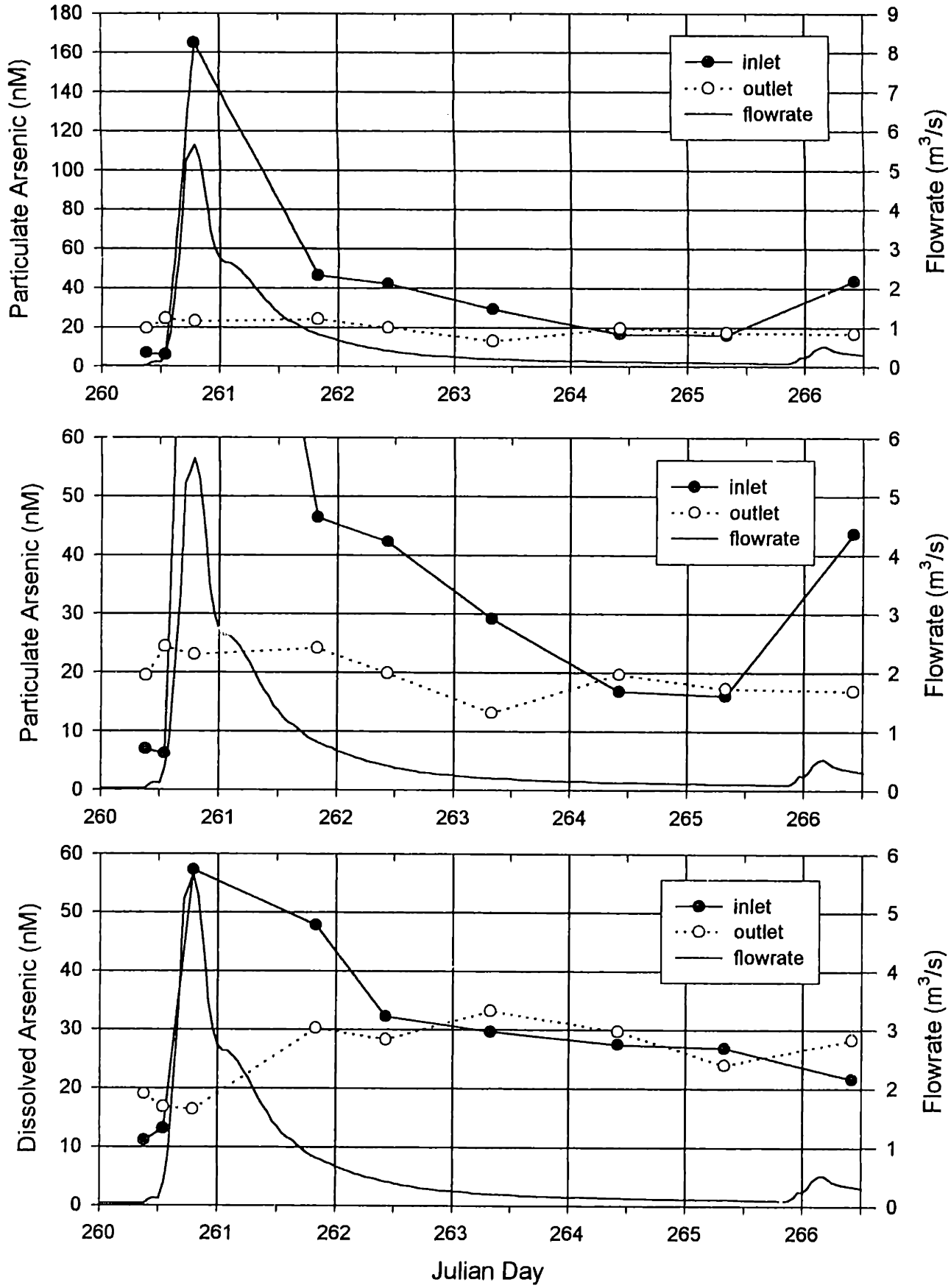

Figure 2-20: Particulate and Dissolved Arsenic during September Storm

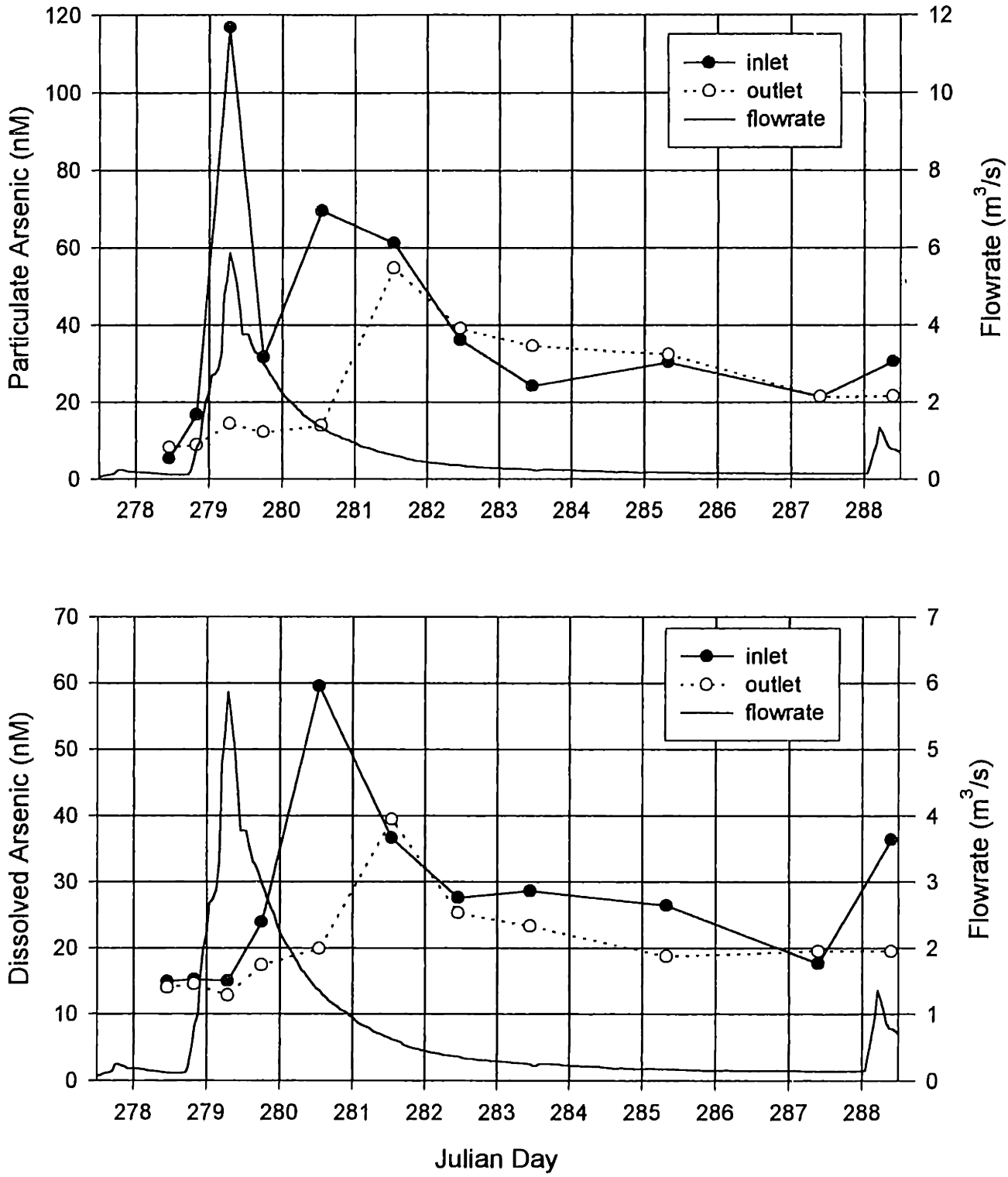

Figure 2-21: Particulate and Dissolved Arsenic during October storm I

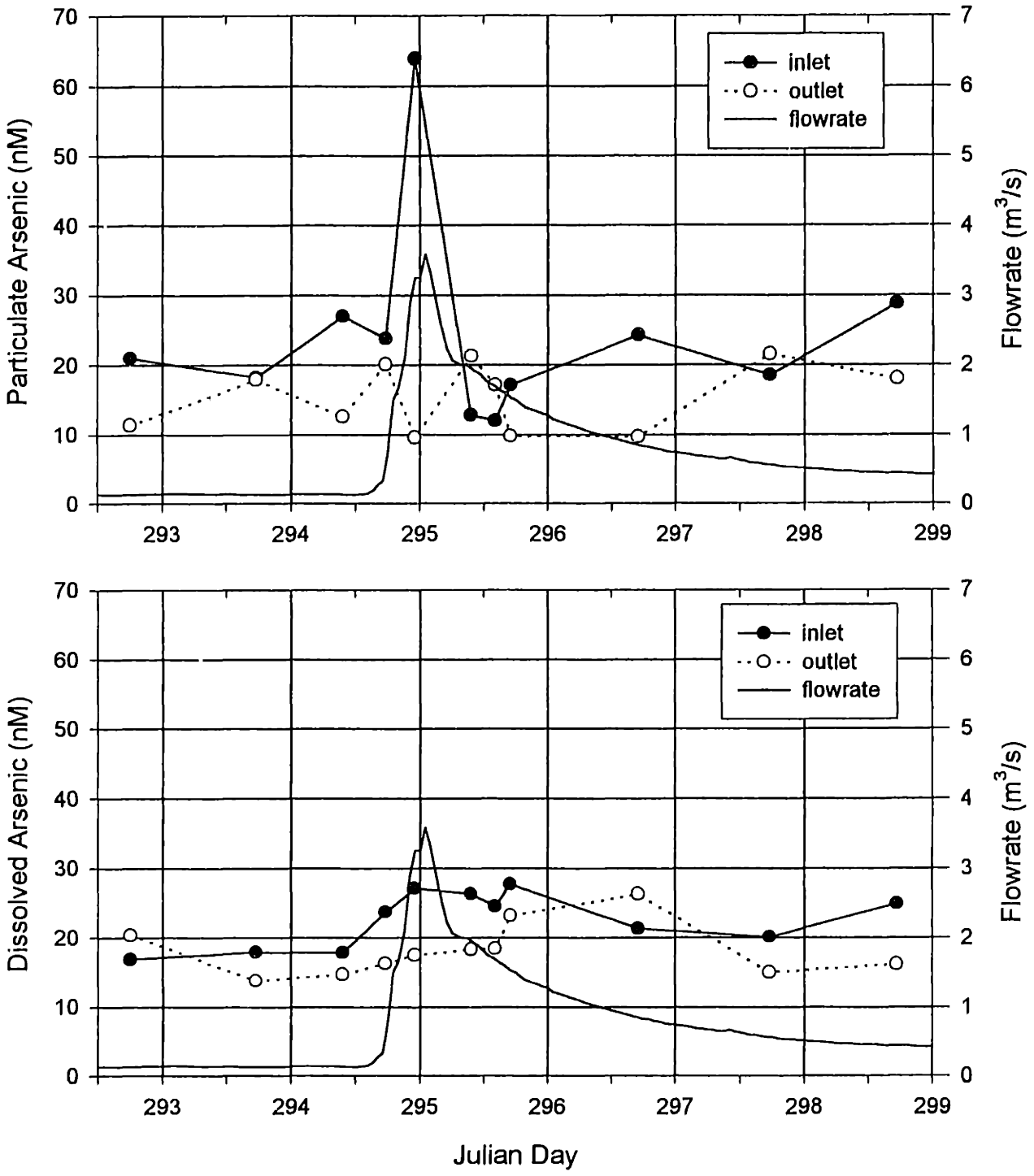

Figure 2-22: Particulate and Dissolved Arsenic during October Storm II

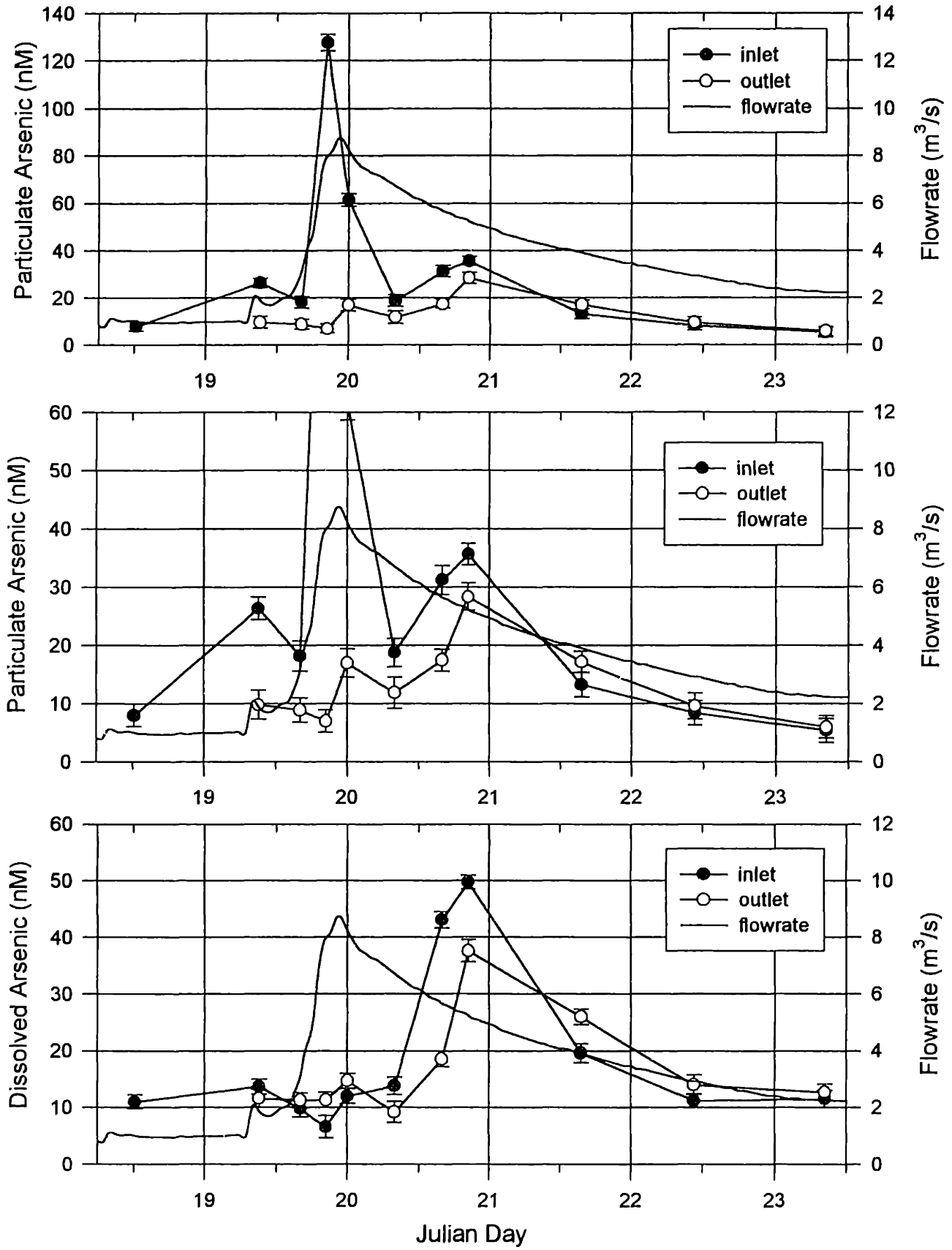

Figure 2-23: Particulate and Dissolved Arsenic during January Storm

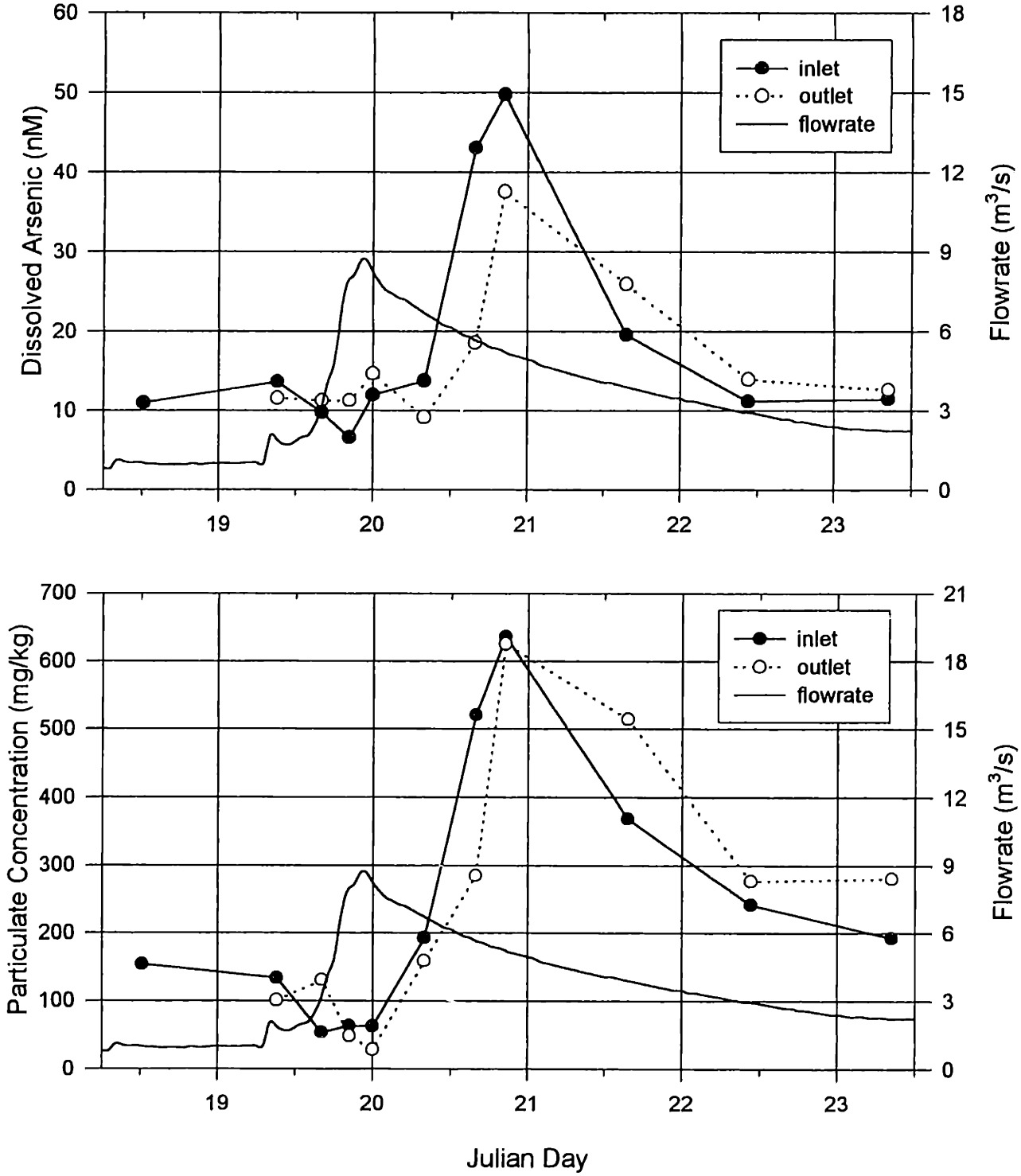

Figure 2-24: Dissolved Arsenic and Particulate Concentration during January Storm

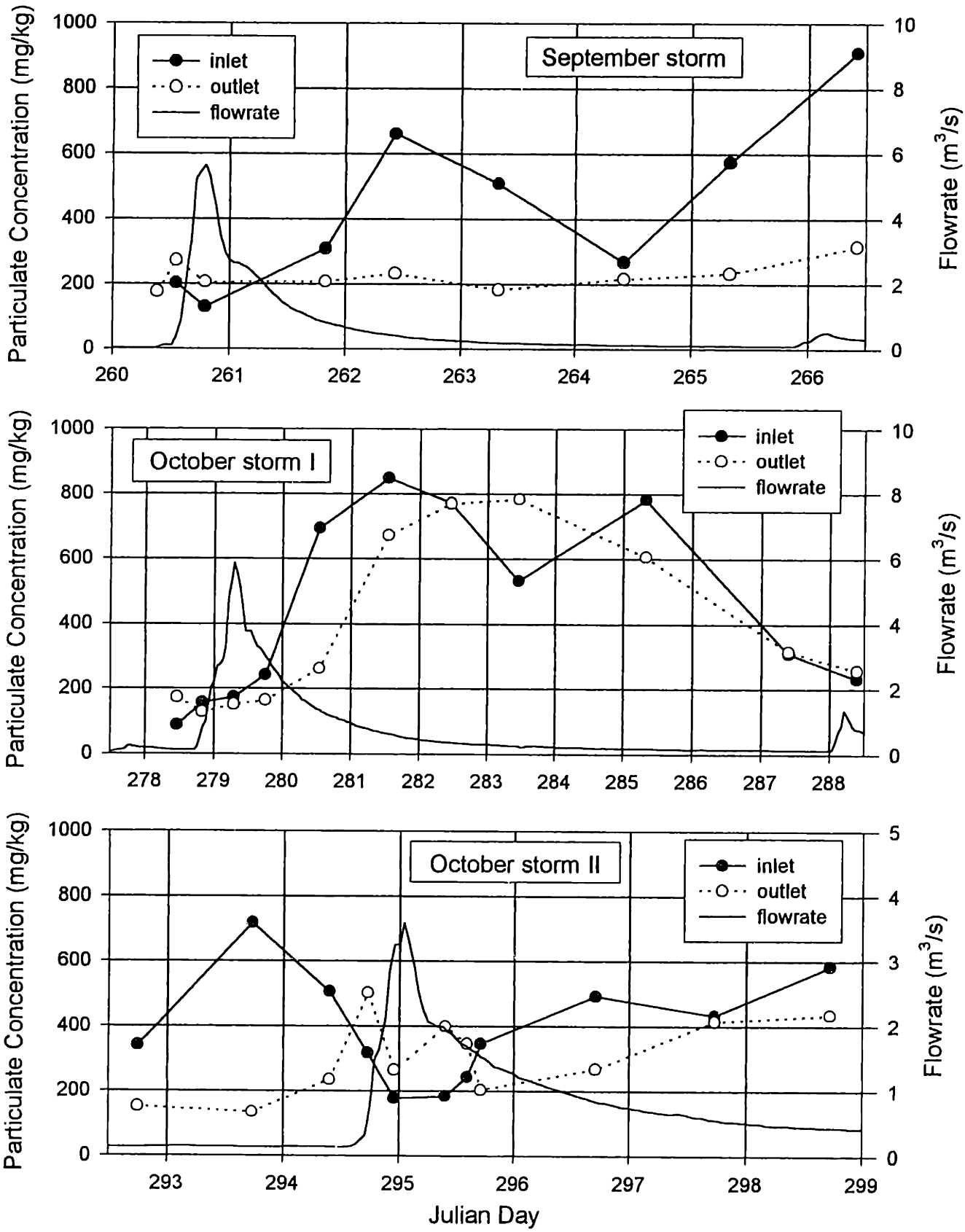

Figure 2-25: Particulate Concentration during September Storm, October Storm I, October Storm II

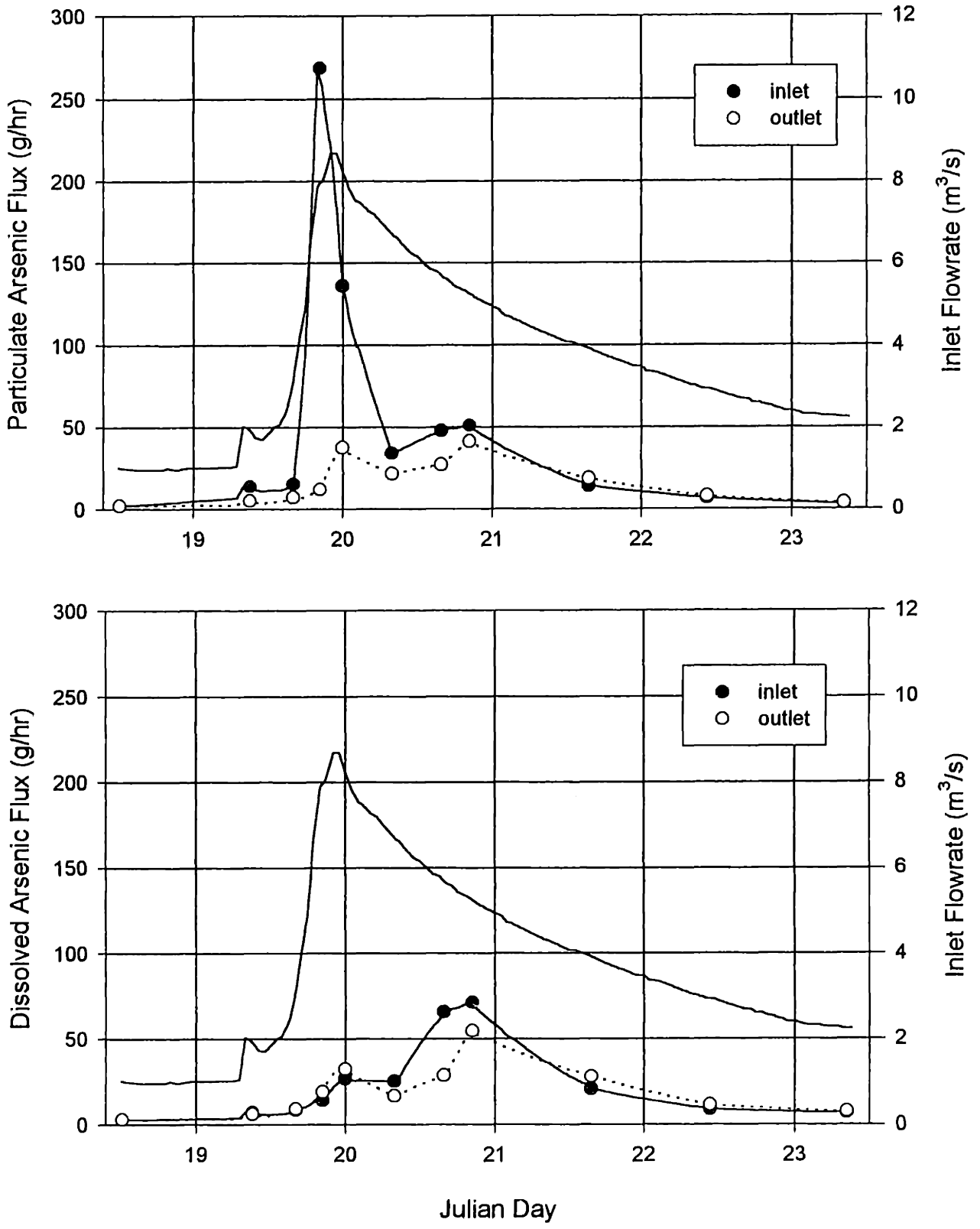

Figure 2-26: Particulate and Dissolved Arsenic Flux during January Storm

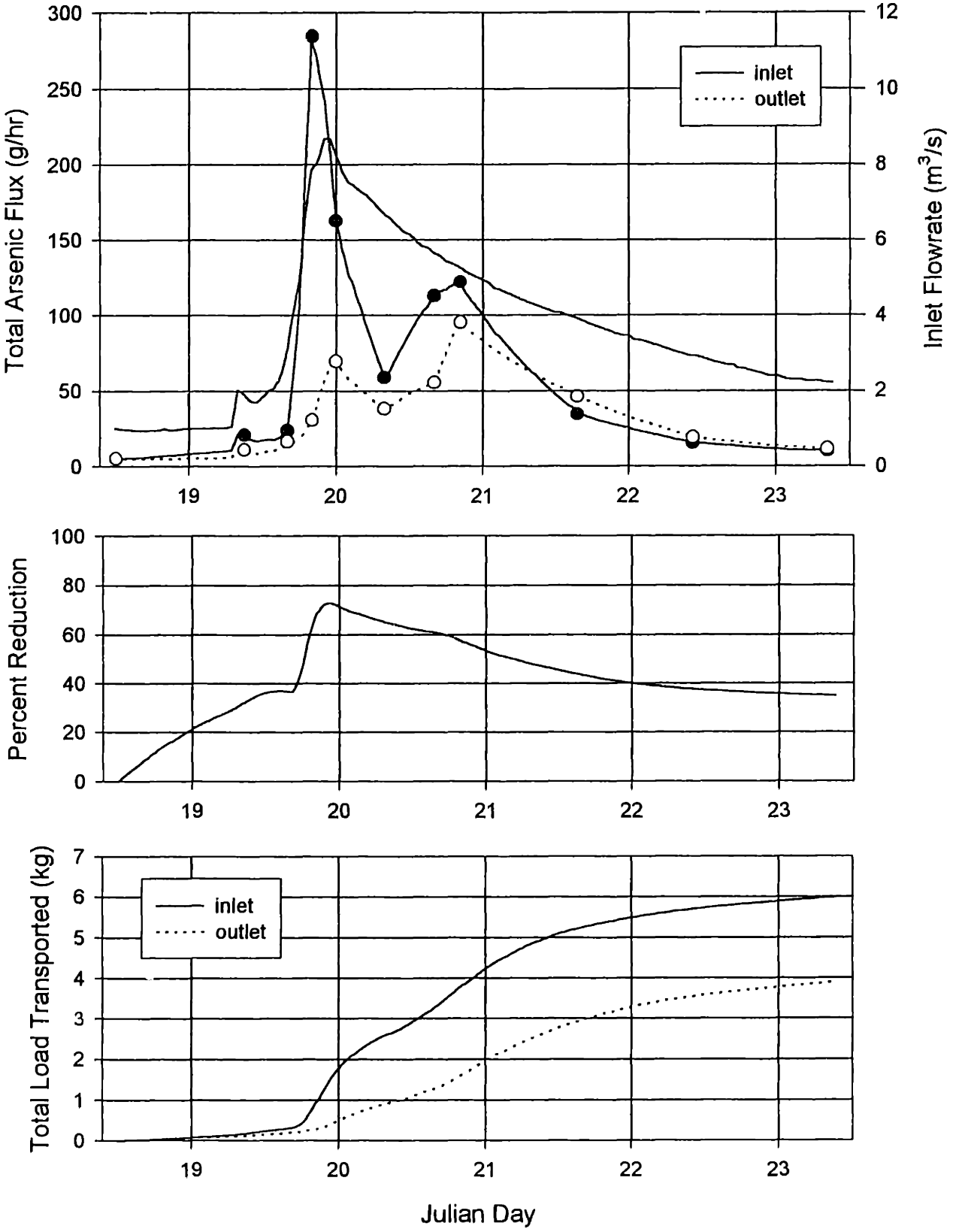

Figure 2-27: Total Arsenic Flux during January Storm

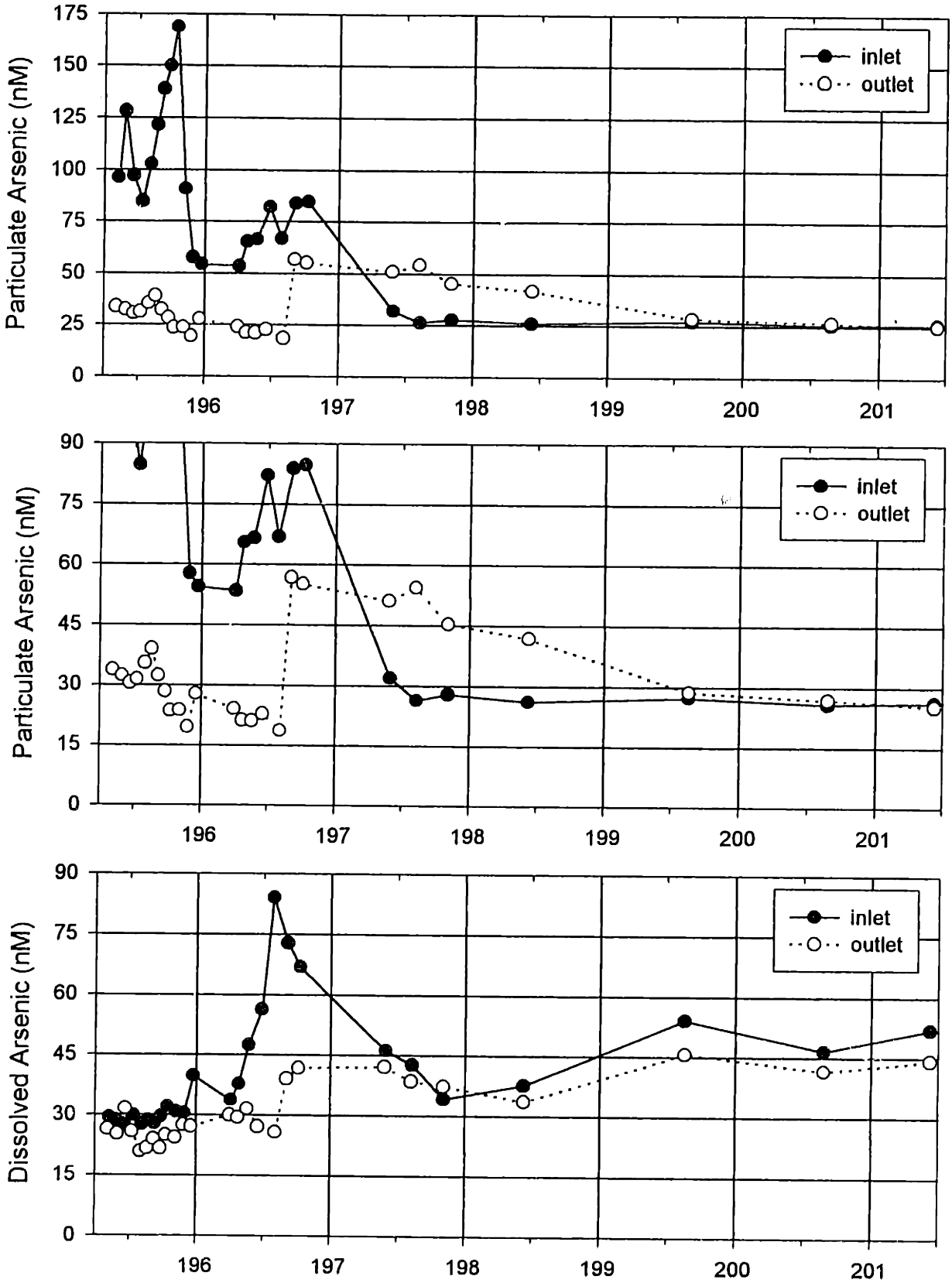

Figure 2-28: Particulate and Dissolved Arsenic during July Storm

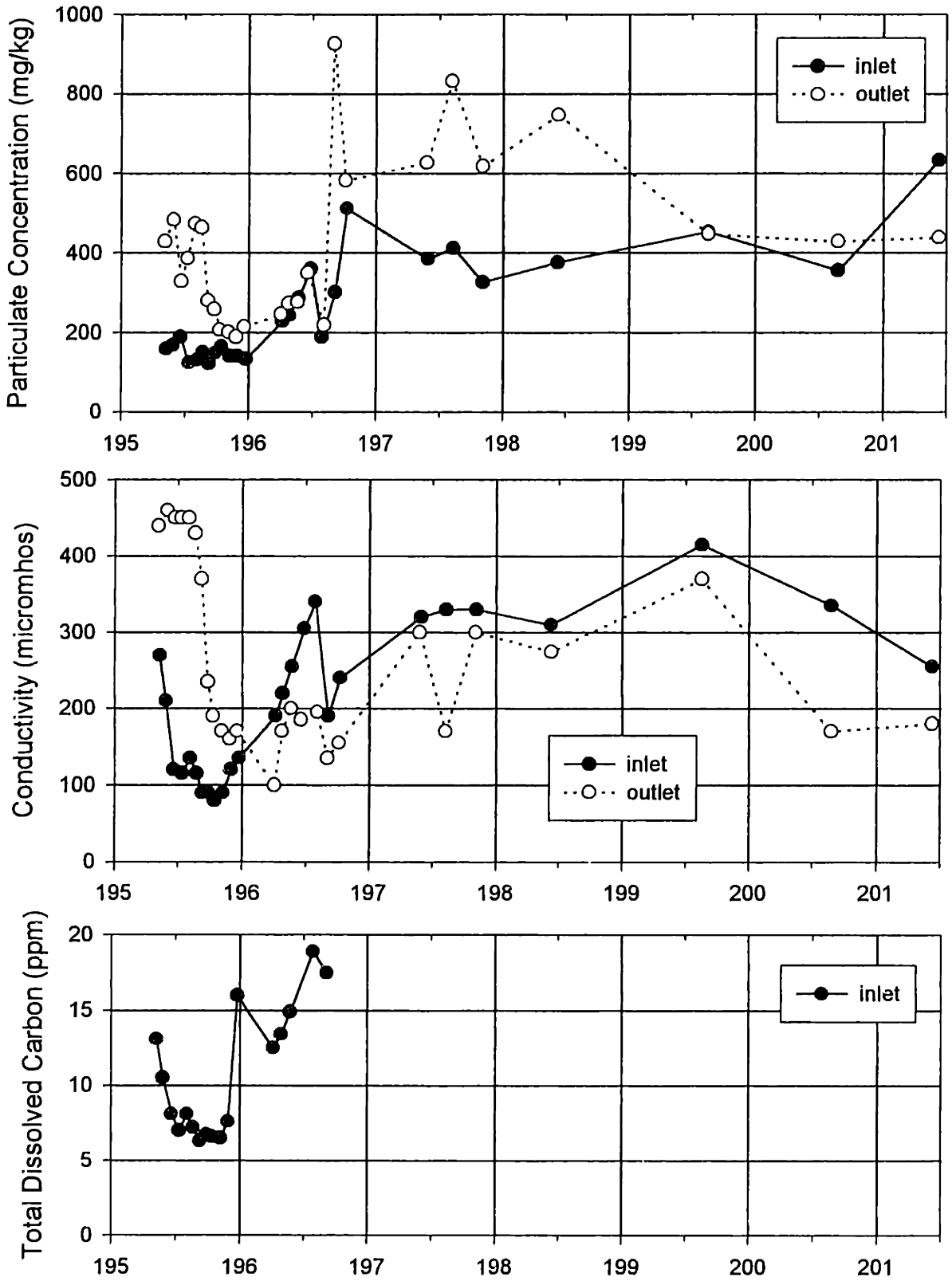

Figure 2-29: Particulate Concentration, Conductivity, and Total Dissolved Carbon during July Storm

increases can be detected on Julian days 279 and 280, but both dissolved and particulate arsenic had very large increases starting Julian day 281, two days after the peak concentrations at the inlet. Particulate arsenic remained elevated until Julian day 287, while dissolved arsenic leveled off by Julian day 285.

Particulate arsenic at the inlet during October storm II showed a double peak pattern similar to October storm I, with the first coming during the quick-storm response and the second coming during the slow-storm response (Figure 2-22). Particulate concentrations dropped down to 200 mg/kg during the peak discharge before returning to ~ 500 mg/kg (Figure 2-25). Dissolved arsenic at the outlet increased on the day after the peak at the inlet, but it is difficult to detect any clear association between particulate arsenic at the outlet and the two pulses at the inlet.

Double peaks in particulate arsenic (nM) were again observed during the January storm, each arriving during the same stage of the hydrograph as the double peaks in the previous two storms (Figure 2-23). Both dissolved and particulate concentrations (mg/kg) were diluted at the inlet during the quick-storm response, followed by a burst of more concentrated water and particles near the middle of the slow-storm response (Figure 2-24). The arrival of both these trends can be clearly seen at the outlet, and beginning Julian day 21 outlet concentrations were slightly higher than inlet concentrations as the tail of the second pulse passed through. Figure 2-26 shows flux curves for dissolved and particulate arsenic at the inlet and outlet obtained by linearly interpolating between the sample points. Figure 2-27 shows the flux curve for total arsenic as well as the load reduction caused by the Upper Forebay over the course of the storm (percent reduction = (load in - load out) / load in).

Double peaks in particulate arsenic at the inlet occurred during the July storm, but dissolved arsenic remained nearly constant even though conductivity showed a strong dilution effect (Figures 2-28 and 2-29). The conductivity curve at the outlet indicates that diluted river water reached the outlet a few hours after entering at the inlet, and there was a small increase in suspended sediment at the end of Julian Day 195 (Figure 2-19), yet particulate arsenic actually decreased at this time. This suggests that

the suspended sediment at the outlet was not associated with the suspended sediment at the inlet. The suspended sediment at the outlet may have been the result of direct surface runoff into the forebay or a flushing of particles already in the forebay. This was the only indication throughout the study that there may be a flushing phenomenon. The second pulse at the inlet had slightly more particulate than dissolved arsenic, and there was a sharp increase in concentrations at the outlet in response to this pulse a few hours after its arrival at the inlet.

Discussion

The observations of arsenic concentration indicate that two distinct pulses can be identified in the river load that enters the forebay during high-flow events. (Samples were probably not taken frequently enough during the September storm to reveal the multiple pulses.) The first pulse arrives during the quick-storm response, has a duration of 6-12 hours, and brings an extremely large particulate arsenic flux, even though particulate (mg/kg) and often dissolved (nM) concentrations are reduced by a dilution effect. The second pulse arrives near the middle of the slow-storm response (½-1 day after the peak flowrate), has a duration of 2-4 days, and is composed of highly concentrated water and particles. This second pulse was just about to begin when Solo-Gabriele (1995) ended sampling, although possible indications of the beginning of a second pulse can be seen in Figure IV.E-31.

The appearance of multiple pulses can likely be attributed to the different travel times of water and sediment coming from different parts of the watershed. The hydrological model developed by Solo-Gabriele (1995) was able to reproduce the storm hydrograph at the USGS station by accounting for the delivery of water from different sub-basins of the watershed. The Winchester sub-basin is located in the southern portion of the watershed and was the primary contributor to the quick-storm response, while the Woburn-central and Woburn-north sub-basins were the primary contributors to the slow-storm response (see Solo-Gabriele, Figure IV.2-2, for a map of the sub-basins). The model used the Muskingum method with constant travel times to route flows through the two channel reaches, with

channel 1 having a travel time of seven hours and channel 2 having a travel time of eight hours. Woburn-central water was routed through channel 2 and lagged behind the Winchester water by eight hours, while Woburn-north water was routed through both channels and lagged behind the Winchester water by 15 hours. This 15 hour lag time is very close to the lag time between the two arsenic pulses observed in the present study, suggesting that the first pulse originates in the Winchester sub-basin and arrives at the forebay inlet relatively quickly while the second pulse originates in the northern part of the watershed and has a delayed arrival.

The first arsenic pulse has a large fraction of surface runoff and re-suspended channel sediment and a much larger particulate flux than dissolved flux. In the second pulse particulate flux and dissolved flux are comparable in size, and this pulse may include arsenic released from Halls Brook Storage Area (HBSA), a nine hectare impoundment (2 ha pond, 7 ha stream/wetland) built for flood control that is located in the Woburn-north sub-basin and receives groundwater directly from Industriplex (Figure 1-1). Concentrations of up to 1100 nM have been measured in surface water samples on the side closest to Industriplex, and concentrations of sediment samples have been measured as high as 9800 mg/kg (Aurilio *et al*, 1994). The pond area is meromictic with a permanently anoxic bottom layer (Lukas Wick, personal communication), and this layer may have highly concentrated water that is entrained into the surface layer during storms and subsequently transported out of HBSA and into the Aberjona River. The highest hypolimnetic concentrations in the Upper Mystic Lake (380 nM) have been observed in the early fall after a period of heightened anoxia, primarily as a result of release of As (III) from the sediments (Spliethoff *et al*, 1995). As (III) is not very particle-reactive and tends to remain highly soluble, and high As (III) concentrations may be a regular feature of the anoxic HBSA monimolimnion.

Further evidence to support the association of the second arsenic pulse with HBSA comes from examining total dissolved carbon (TDC) at the inlet during the July storm (Figure 2-29). The TDC curve shows a dilution effect very similar to the conductivity curve with the exception of the

point at Julian Day 195.98. The concentration of TDC at this time was nearly twice as large as would be expected from extrapolating between the point before and after it, and the water sample had a distinct brownish yellow color that was not observed in any other sample. This may indicate the presence of humic substances that originated in the wetlands near Wells G and H (Figure 1-1). If water from Wells G and H was arriving at the Upper Forebay during the early hours of Julian Day 196, then it is reasonable that water from HBSA (~2 km upstream of Wells G and H) arrived mid-day when the second arsenic pulse was observed.

One of the consequences of this multiple pulse phenomenon is that there are not simple rating curve relationships between concentration and flowrate. Concentrations of dissolved species (nM) and particulate concentrations (mg/kg) are often indirectly proportional to flowrate due to a dilution effect at high flows (Johnson, 1979; Bradley, 1984; Klarer and Millie, 1989), but in the Aberjona watershed it appears that not only the magnitude of the flowrate but the position within the hydrograph are important factors. Figure 2-30 shows the rating curves for all the measurements taken during this study for which flowrate data is available (i.e., excluding the July storm), and while the trend of $C \sim 1/Q$ is the dominant feature there are outliers that correspond to the second arsenic pulse.

Along with showing how variable travel times from different reaches in a watershed can affect downstream concentration time-series during storms, this study shows some of the consequences of this phenomenon for contaminant transport at a river/lake interface. The multiple arsenic pulses observed on the Aberjona River have different constituencies, and this results in their having different fates in the Upper Forebay. Table 2-3 shows that while the majority of the arsenic load in the first pulse during the January storm was in the particulate form and was subject to considerable settling in the forebay, the second pulse had more dissolved arsenic (and particulate arsenic associated with smaller particles having slower settling rates) and passed through to the Upper Mystic Lake with little reduction. For the July storm the second pulse also had a pronounced arrival at the outlet while the first pulse was largely retained. Consequently there is a difference in timing between the highest total

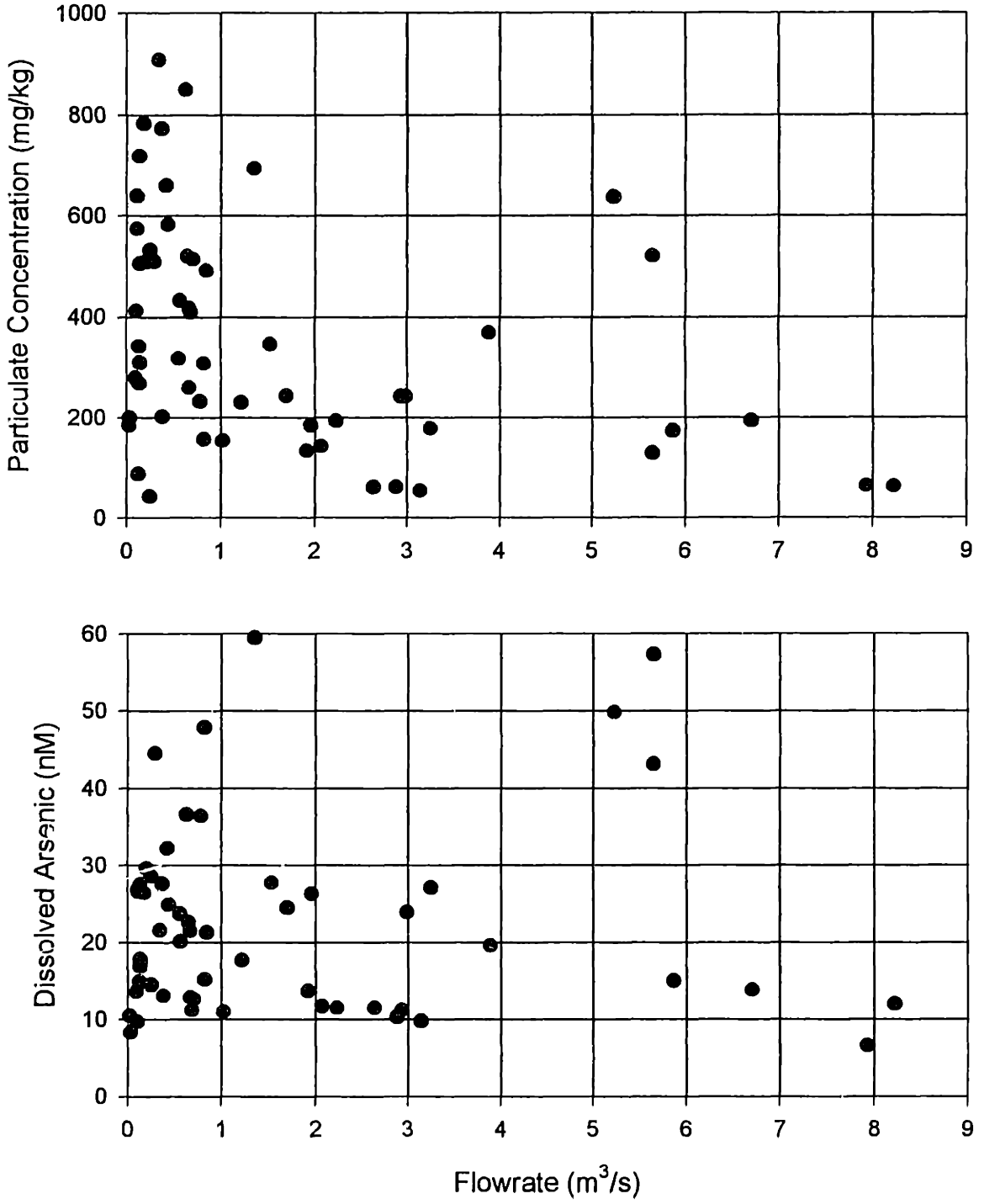

Figure 2-30: Rating Curves at Inlet for Particulate Concentration and Dissolved Arsenic

arsenic concentrations seen in the river and the lake, with the highest concentrations in the river occurring during the first pulse and the highest concentrations in the lake occurring during the second pulse (Table 2-4), and this has implications for exposure risks. For the July storm there was rain almost constantly on Julian Day 195 but the two following days were sunny and hot with heavy beach use, coinciding with the times when the highest concentrations were being delivered to the lake.

Table 2-3: Arsenic Loads and Reduction Percentages during January Storm

Pulse	Total (kg)			Dissolved (kg)			Particulate (kg)			% Dissolved	
	In	Out	% Red.	In	Out	% Red.	In	Out	% Red.	In	Out
1	2.61	1.03	61	0.34	0.35	-3	2.27	0.68	70	13	34
2	3.39	2.98	12	1.95	1.71	12	1.44	1.27	12	58	57

Note: pulse 1 = Julian day 19.67-20.33
pulse 2 = Julian day 20.33-23.35

Table 2-4: Peak Arsenic Concentrations at Inlet/Outlet during High-flow Events

Storm	Time of Highest Concentration (Julian Day)		Total Arsenic (nM)		% Reduction
	Inlet	Outlet	Inlet	Outlet	
September storm	260.79	261.83	222.2	54.4	76
October storm I	279.29	281.54	131.9	94.2	29
October storm II	294.96	295.40	91.1	39.6	57
January storm	19.85	20.85	134.2	66.0	51
July storm	195.78	196.76	201.2	97.0	52
		197.40		93.3	54

A comparison of all five storms indicates that retention of arsenic in the forebay depends both on the momentum of the river flow and the drag/blockage provided by plants. Estimates for the arsenic loads transported in and out of the forebay during the first four storms were made by integrating the flux curves (Table 2-5). The loads transported during the summer are also shown, as well as the

number of days in each period and the amount of reduction that occurred. For the September storm there was a rapid decrease in flowrate following the quick-storm response, a large plant presence in the forebay, and a very low water level (which prevented the inflow from bypassing the plants by flowing over them). As a result the advective zone appears to have become very small by the time it reached the outlet and much of the inflow water was mixed with the ambient forebay water. While there was a small but noticeable increase in dissolved arsenic at the outlet there was never an increase in particulate arsenic (Figure 2-20). For October storm I flowrates were slightly higher than the September storm and there was less drag/blockage due to a higher water level (and probably less plants). While much of the first pulse was retained, there was a definite arrival of both the dissolved and particulate components of the second pulse at the outlet (Figure 2-21) and less reduction than the September storm. October storm II had a low net reduction compared to the first two storms, due in part to the smaller contribution of particulate arsenic to the total load. For the January storm flows were high and remained elevated for days, the water level was high, and there were little or no plants, resulting in a well-defined advective zone that allowed almost half of the first pulse and nearly all of the second pulse to be carried into the Upper Mystic Lake. Flowrate data from the July storm was not yet available for calculating fluxes, but the flows were observed to be quite strong and were probably similar in magnitude to the January storm. Measurements of conductivity indicate that river water was reaching the outlet soon after arriving at the inlet and thus that the advective zone was continuous across the forebay. The large retention of the first (primarily particulate) arsenic pulse during this storm, despite the rapid communication between the inlet and the outlet, points to vegetation as being the determining factor in regulating the fate of this pulse in the forebay.

Table 2-5: Reduction of Arsenic Loads by Upper Forebay										
	# days	Total			Dissolved			Particulate		
		Inlet (kg)	Outlet (kg)	Red. (%)	Inlet (kg)	Outlet (kg)	Red. (%)	Inlet (kg)	Outlet (kg)	Red. (%)
7/19 - 9/17	60	1.40	1.62	-16						
Sept. Storm	6	3.91	1.23	69	1.26	0.62	51	2.66	0.61	77
Oct. Storm I	10.5	4.37	2.01	54	1.43	0.98	32	2.94	1.04	65
Oct. Storm II	6	1.60	1.05	35	0.75	0.60	19	0.86	0.44	48
Jan. Storm	3.5	6.00	4.01	33	2.29	2.06	10	3.71	1.95	47
total	86	17.28	9.92	43						

2.4 Sediment Cores

Sediment cores were taken along the direct line-of-travel between the inlet and outlet, in the dead-zone area on the northwest side of the Upper Forebay, and in the northern part of the main basin (Figure 1-2). The main basin core (Figure 2-31) only extended to a depth of 30 cm but is consistent with the deeper cores taken by Spliethoff and Hemond (1996) down to this point (see also Knox, 1991). Concentrations increased from ~100 mg/kg at the surface to a peak of ~400 mg/kg at 30 cm, and this peak is believed to be related to land-moving activities in the late 1960's that mobilized large amounts of contaminated soil. The cores taken in the forebay (Figures 2-32 through 2-34) do not appear to provide much of a historical record of arsenic delivery from the watershed, probably due to factors such as variable plant growth from year to year, benthic re-working, and human disruption (e.g., dragging the bottom with rakes during the spring and summer to do plant surveys before spraying). All the cores show strong correlations between water content and arsenic (mg/kg), which agrees with the findings of Knox (1991), who also found water content to be correlated with organic content and percentage of fine-grained particles. Fine-grained particles have higher adsorption potentials due to their relatively large surface area/volume ratios. The cores in the advective zone have lower concentrations (100-200 mg/kg) and lower water content (85-92.5%) compared to the dead zone

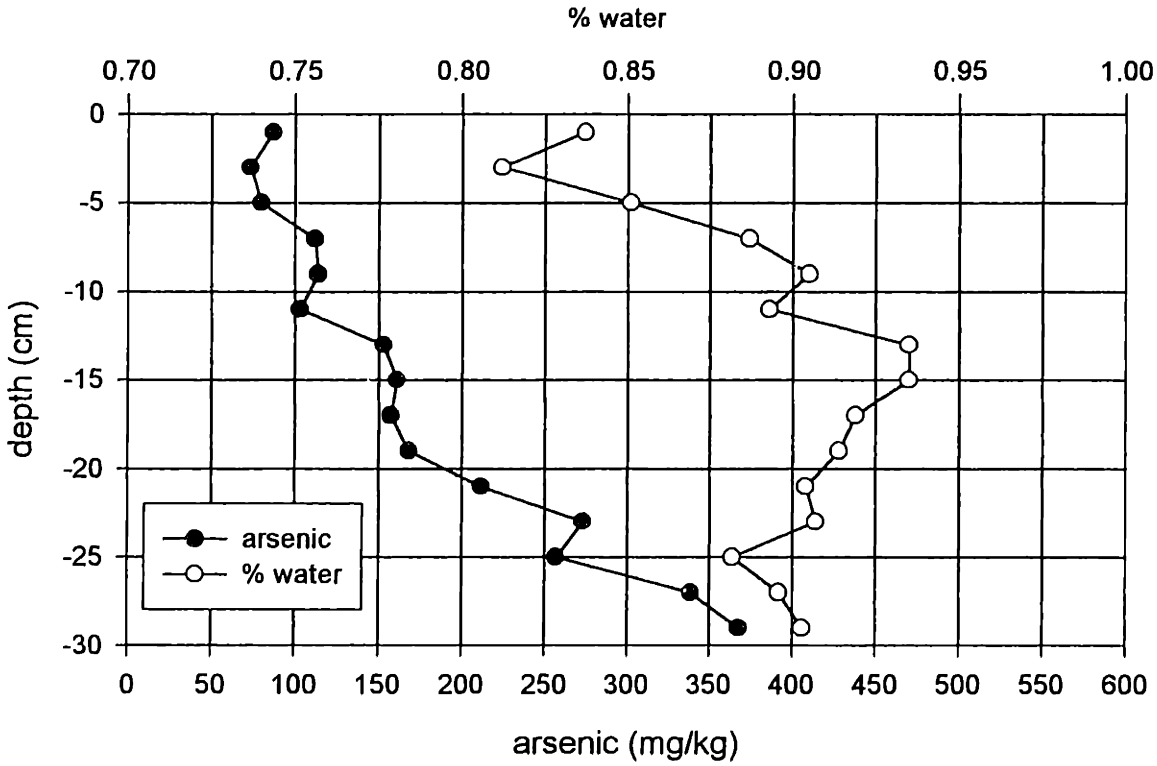

Figure 2-31: Main Basin Sediment Core

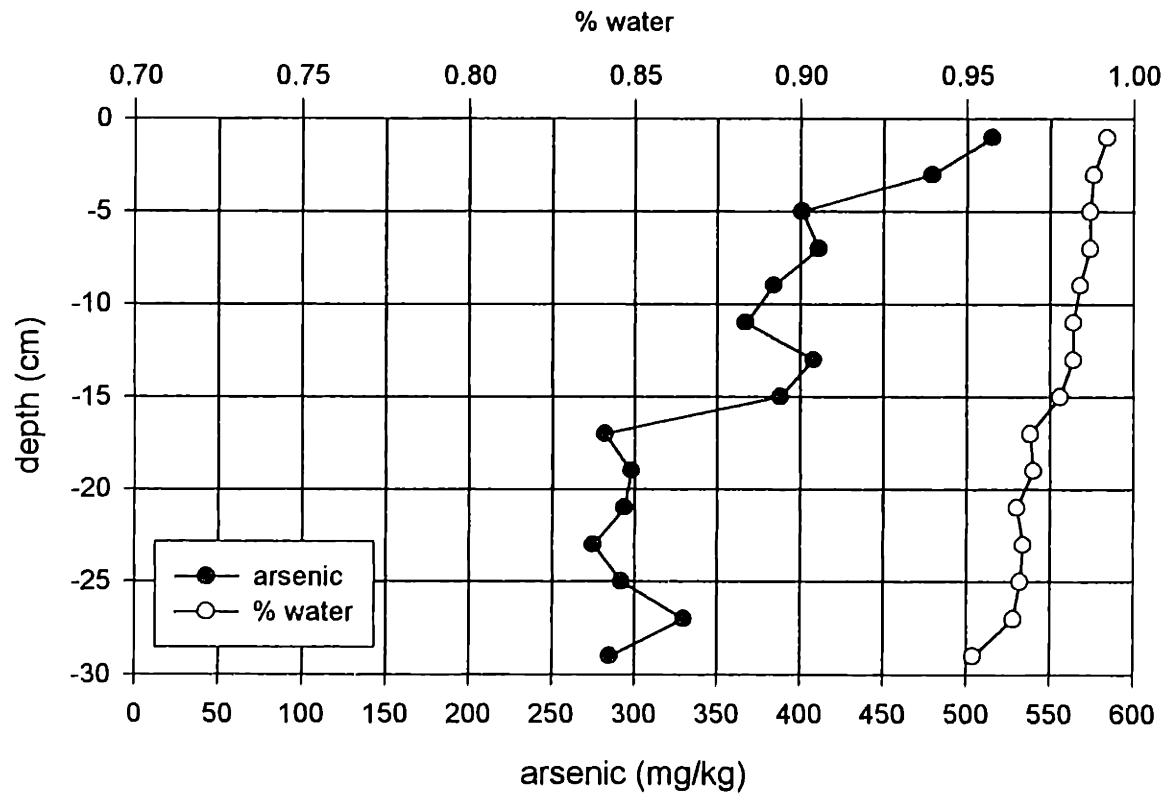

Figure 2-32: Upper Forebay Dead Zone Sediment Core

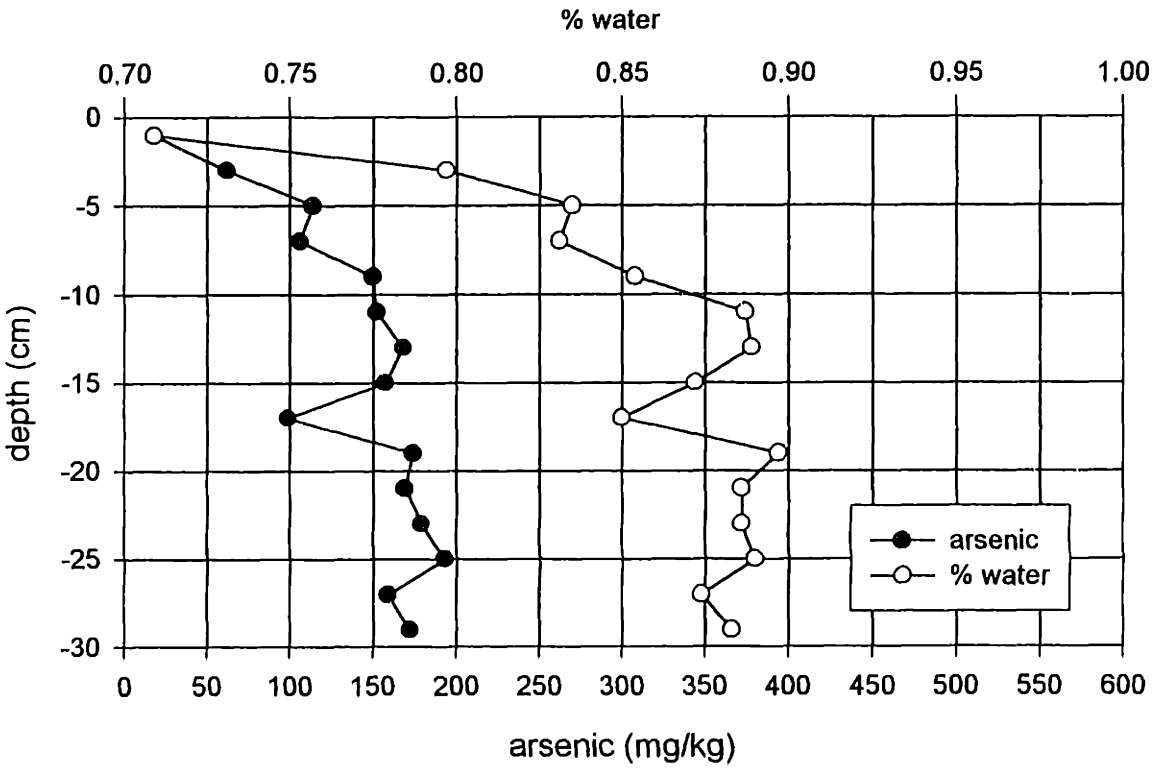

Figure 2-33: Upper Forebay Inlet Sediment Core

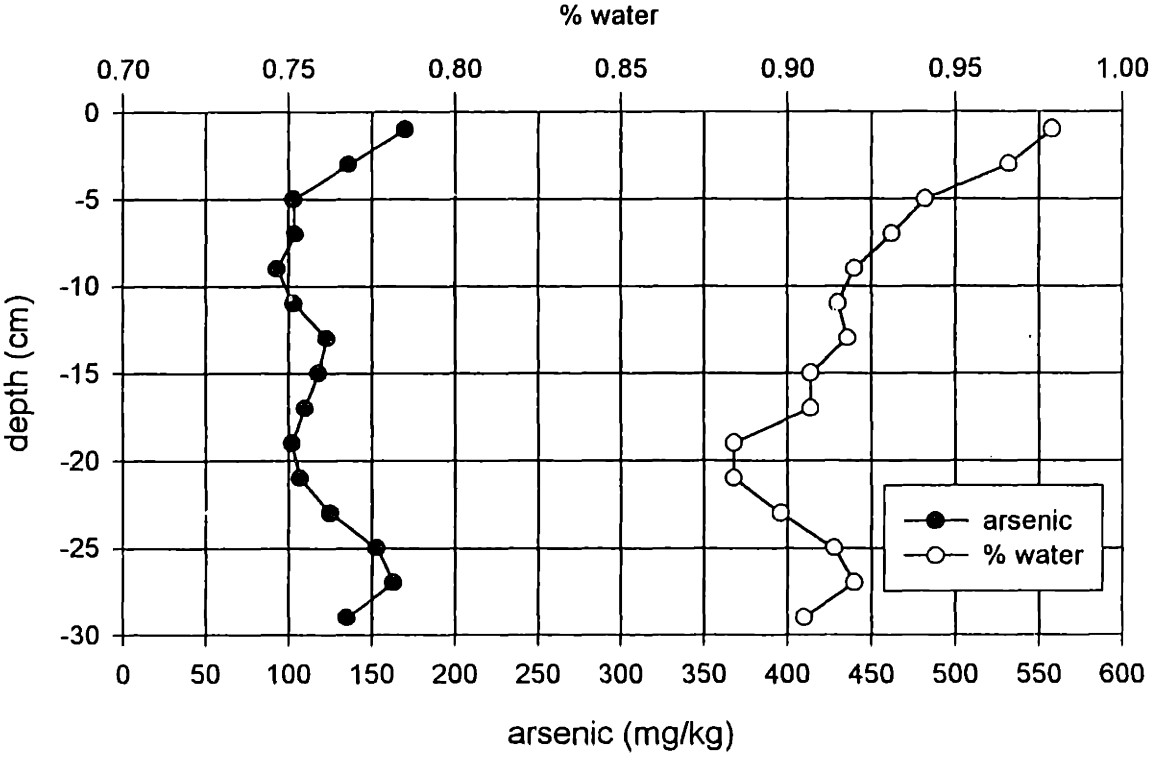

Figure 2-34: Upper Forebay Outlet Sediment Core

core (300-400 mg/kg, >95% water), indicating that the sediments in the advective zone may have a higher percentage of the coarse material from the input suspended sediment load that is deposited in the forebay.

The cores were used to estimate the total arsenic load in the sediments. For this analysis the forebay was simply divided into an advective zone and a dead zone, and based on forebay geometry the advective zone was taken to have an area of 25,000 m^2 while the dead zone was taken to have an area of 75,000 m^2. The concentration in the advective zone was taken to be 140 mg/kg and the concentration in the dead zone was taken to be 350 mg/kg. Total accumulation is the product of accumulation rate (g/m^2-yr) and area (m^2), where

accumulation rate =
concentration ($g/10^6$ g) * bulk density ($10^6 g/m^3$) * accretion rate (10^{-2} m/yr)

bulk density = S * (F * 1.3 g/cm^3 + (1 - F) * 2.6 g/cm^3)
S = solid fraction
F = organic fraction

(The values of 1.3 and 2.6 g/cm^3 are typical densities of organic and mineral particles, respectively.) The ranges of accretion rates and water contents that were considered are expected to bracket the actual values of these parameters (Table 2-6). A comparison with the average yearly arsenic flux at the USGS station of 150 kg/yr found by Solo-Gabriele (1995) indicates that 10-30% of the yearly river input load is retained in the forebay. The observed reduction during typical non-storm conditions of 19% (Section 2.2.2) is exactly in the middle of this range, while the reduction during the January storm (Table 2-5) is at the high end of this range. The fall storms (and probably the July storm) had reductions significantly larger than this range, which may simply reflect the fact that the months during which vegetation is prominent (July through October) are the months with the lowest average flowrates over the last 54 years (Solo-Gabriele, 1995), and thus the summer and fall storms sampled during this study may not be representative of the storms that have the largest net effect on arsenic transport in this system. The flowrates during these storms were small relative to the largest stormflows that have

occurred in the river (and thus had less inertia to counter the drag by plants), and larger flows tend to occur during months when there is little vegetation present in the forebay.

Table 2-6: Retention of Arsenic in Upper Forebay Based on Sediment Cores

Accretion Rate (cm/yr)	Advective Zone			Dead Zone			% of Yearly River Input
	% Water	Bulk Density (g/cm^3)	Accumulation (kg/yr)	% Water	Bulk Density (g/cm^3)	Accumulation (kg/yr)	
0.5	0.90	0.21	3.7	0.97	0.06	7.9	0.08
	0.80	0.43	7.5	0.90	0.21	27.6	0.24
0.6	0.90	0.21	4.4	0.97	0.06	9.5	0.09
	0.80	0.43	9.0	0.90	0.21	33.1	0.28

2.5 Conclusion

The Mystic Lake Upper Forebay has been found to be a transient system that can act as an arsenic source under extremely low-flow conditions and as a sink during storms and typical non-storm conditions. Under extremely low-flow conditions the internal source in the forebay causes concentrations to be higher in the water that is delivered to the lake than the water coming in from the river. These conditions were observed during the summer (1995) when the forebay was also a source of particulate organic matter due to algae and detritus from aquatic macrophytes, and these particulates appear to have provided sites for sorption of arsenic and facilitated arsenic transport out of the forebay. This internal arsenic source may be a common forebay feature (e.g., groundwater-driven) that is normally overshadowed by the larger arsenic fluxes from the river. Thus even if the loading of arsenic from the river where completely terminated in the future there may continue to be a delivery of arsenic to the main basin from the forebay sediments.

During high-flow events, suspended sediment concentrations in the Aberjona river drop down to baseline values a few hours after the peak flowrate but arsenic concentrations can remain elevated

for days due to a multiple pulse phenomenon. The timing of these pulses during the hydrograph as well as measurements of total dissolved carbon suggest that the first pulse is primarily composed of runoff and channel re-suspension and the second pulse includes water from Halls Brook Storage Area in the northern part of the watershed. The forebay is able to retain at least half of the first pulse due to deposition but can allow much of the second pulse through to the main lake basin, depending on the momentum of the flow and the amount of filtering provided by vegetation. Vegetation was also observed to play a role in the retention of the first pulse. The forebay thus affects the degree to which lake concentrations are event-driven and the timing of peak concentrations in the lake. During high-flow events the peak concentration in the lake may be reduced 25-50% from the peak river concentration, and the peak lake concentration may occur 1-2 days after the rainfall has ended.

Appendix A.1

Table A.1: Hydrological Data during Field Study, 1995-1996							
	Flowrate				Precipitation		
	1995-1996			1939-1993	1995-1996	1957-1992	
	Average	Hourly Minimum	Hourly Maximum	Average		Average	Minimum
	m^3/s	m^3/s	m^3/s	m^3/s	inches	inches	inches
June	0.34	0.12	1.47	0.62	2.96	3.44	0.36
July	0.15	0.062	1.53	0.28	0.51	3.30	0.47
August	0.082	0.024	1.02	0.28	0.91	3.47	0.91
September	0.20	0.024	5.65	0.27	3.23	3.60	0.57
October	0.56	0.068	5.87	0.35	6.41	3.83	1.14
November	1.28	0.35	6.79	0.65	6.05	4.78	0.81
December	0.59	0.35	3.15	0.88	3.14	4.47	1.13
January	1.81	0.26	8.74	1.03	6.49	3.90	0.60
February	1.38	0.22	3.77	1.16	2.76	3.65	0.33
March	-	-	-	1.84	3.74	4.07	0.82

Note: 1 m^3/s = 35.3 cfs
historical flowrate and precipitation data from Solo-Gabriele (1995)

Flood Routing

Kinematic wave celerity is the speed at which variations in flow propagate along a channel, assuming negligible acceleration and pressure terms in the equation of momentum, and is given by

$$C_k = \frac{dQ}{dA} = \frac{5}{3}\frac{1.49 S_o^{1/2} y^{2/3}}{n}$$

where S_o = surface slope
n = bottom roughness
y = depth (ft)

For S_o = 0.0015 (Solo-Gabriele, 1995), n = 0.03, and y = 3 ft, C_k is 6.67 ft/s and the travel time from the USGS station to the Upper Forebay inlet is L/C_k = 7 minutes.

Appendix A.2

Table A.2: Meteorological Data during Field Study, 1995-1996					
	Average Temperature	Average Windspeed	Average Direction	Maximum Hourly Windspeed	Comments
	°F	m/s		m/s	
June	66.0	1.49	S	6.60	
July	73.8	1.74	S	6.61	
August	70.1	2.00	N	7.37	
September	59.7	2.12	N	7.84	
October	54.7	1.84	NW	7.12	
November	37.7	2.42	NW	12.36	
December	26.7	2.70	NW	8.61	anemometer not deployed after Dec. 8

Table A.3: Wind Data during Summer, 1995			
Date	Julian Day	Windspeed (m/s)	Direction
July 19	200	3.0	NW
July 27	208	1.5	NW
August 7	219	2.1	NE
August 9	221	1.1	N
August 17	229	1.6	NE
August 25	237	6.4	N
September 1	244	2.8	NE
September 8	251	3.0	NE
September 11	254	4.1	NW
September 14	257	2.5	S
September 17	260	1.9	N

Note: The average windspeed and direction two hours prior to sampling time are listed.

Appendix A.3

Two estimates of evaporation were made using different forms of Dalton's Law. Studies of Lake Mead resulted in a model that accounts for water temperature as well as windspeed and vapor pressure differences (Chow, 1964). Evaporation in inches per day is given by:

$$E = 0.001813\ w\ (e_w - e_a)\ [1 - 0.03(T_a - T_w)]\ t \qquad \text{Equation A.1}$$

where

w = windspeed (knots)
T_w = water surface temperature (°C)
T_a = air temperature + 1.9 °C
e_a = vapor pressure at dew point temperature (millibars)
e_w = vapor pressure at water surface temperature (millibars)
t = time period (days)

Another common evaporation model (Chow *et al*, 1988) is given by

$$E_a = B\ (e_{as} - e_a) \qquad \text{Equation A.2}$$

with

$$B = \frac{0.622k^2\rho_a u_{10}}{P\rho_w[\ln(z_{10}/z_o)]^2}$$

where

k = von Karman's constant (0.4)
ρ_a = density of air (assumed constant 1.2 kg/m^3)
u_{10} = windspeed (m/s)
P = pressure (Pa)
ρ_w = density of water (assumed constant 1000 kg/m^3)
z_{10} = height of wind measurement (m)
z_o = roughness height (m)
e_{as} = saturation vapor pressure (Pa)
e_a = ambient vapor pressure (Pa)

Average daily dew point, relative humidity, and pressure were measured at Logan Airport. Temperatures were taken with the CTD profiler or a YSI temperature probe, except for August 25, September 1, and September 11 for which estimates were made. Windspeeds at 2 meters were calculated based on a logarithmic profile assuming a roughness height z_o of 0.0001 m. The equivalent flowrate was calculated assuming a constant surface area of 103,000 m^2, although this was most likely smaller due to the low water conditions during the summer. Transpiration was not taken into account.

Table A.4: Evaporation During Summer, 1995							
Date	T_a (°C)	Windspeed (m/s)	T_w (°C)	Dew Point (°C)	Evaporation (cm/day)		% Flowrate Reduction, Equation 1
					Equation 1	Equation 2	
July 19	23.1	2.20	25	15.1	0.25	0.21	0.03
July 27	27.2	1.26	29	21.5	0.14	0.10	0.02
August 7	16.7	2.79	23	13.2	0.32	0.11	0.01
August 9	21.9	0.95	26	14.8	0.13	0.08	0.01
August 17	25.3	1.35	29	18.3	0.21	0.10	0.05
August 25	17.8	4.73	24	7.1	0.81	0.39	0.37
September 1	25.0	2.17	28	15.4	0.35	0.22	0.13
September 8	17.5	1.86	22	11.4	0.20	0.07	0.09
September 11	12.5	1.94	21	3.1	0.31	0.12	0.12
September 14	21.7	2.67	22	17.1	0.14	0.13	0.02

The Lake Mead model consistently produced the highest estimates of evaporation rate. Table A.4 shows that evaporation was significant on August 25 due to the high windspeed and low humidity, moderately significant on September 1 and September 11, and insignificant on the other seven days. The three days in which evaporation was apparently significant are also the days in which water temperature was not directly measured but estimated based on correlations between air temperature and water temperature data, which could imply that water temperatures for these three days were over-estimated.

Evaporation was considered in order to test the hypothesis that during the summer the fluxes at the inlet were greater than or equal to the outlet fluxes even though the outlet concentrations were higher. The above estimates indicate that evaporation did not affect the water balance enough to support this hypothesis (i.e., arsenic fluxes at the outlet were still consistently higher when taking evaporation into account).

Appendix A.4

For deep water waves (h/L > 0.5), significant wave height and period are related to fetch and wind velocity by the following empirical equations (U.S. Army Coastal Engineering Research Center, 1973):

$$\frac{gH_s}{U_{10}^2} = 0.283\tanh\{0.0125(\frac{gF}{U_{10}^2})^{.42}\}$$

$$\frac{gT_s}{2\pi U_{10}} = 1.2\tanh\{0.077(\frac{gF}{U_{10}^2})^{.25}\}$$

where

H_s = significant wave height (m)
T_s = significant wave period (s)
U_{10} = windspeed at height of 10 m (m/s)
F = fetch (m)
g = gravitational constant (9.81 m/s^2)
h = water depth (m)
L = wavelength (m)

The wave parameters predicted by these equations were compared with measured wave parameters on November 4 when relatively strong winds were blowing from the northwest. Three-dimensional velocity measurements (U,V,W) were taken for five minutes at 15 Hz in front of the inlet to the Upper Forebay, which also happened to be the lee side for the given wind conditions. These measurements were rotated into a stream-wise coordinate system in which there was no mean velocity in the y- or z-direction by using the following transformations:

$$\alpha = \tanh^{-1}(\frac{\overline{V}}{\overline{U}})$$

$$\beta = \tanh^{-1}(\frac{\overline{W}}{\overline{U_h}})$$

$$\overline{U_h} = \overline{U}\cos(\alpha) + \overline{V}\sin(\alpha)$$

$$U_r = U\cos(\alpha)\cos(\beta) + V\sin(\alpha)\cos(\beta) + W\sin(\beta)$$

$$V_r = -U\sin(\alpha) + V\cos(\alpha)$$

$$W_r = -U\cos(\alpha)\sin(\beta) - V\sin(\alpha)\sin(\beta) + W\cos(\beta)$$

Figure A-1 shows the directional distribution of horizontal velocity variance (U^2+V^2), where θ is the direction relative to the x-axis. Variance was calculated for each U,V pair and the sum of U^2+V^2 was found in 1° bins for θ. This figure shows that the waves were travelling almost exactly upstream relative to the river current. The period of the equivalent periodic wave, T, was found by the following relationship (Madsen *et al*, 1993):

$$T = \frac{\int Su_{(f)} df}{\int f Su_{(f)} df}$$

where

$Su_{(f)}$ = power spectrum (cm^2/s^2-Hz)
f = frequency (Hz)

The rms velocity associated with the wave motion was found by

$$\frac{1}{2} U_{rms}^2 = \int Su_{(f)} df$$

The rms waveheight was calculated using linear theory, which holds that

$$\frac{H_{rms}}{2} = \frac{U_{rms}}{\omega e^{kz}}$$

Significant wave height H_s was then evaluated as $\sqrt{2}$ H_{rms}. Table A.5 shows that the wave height from the empirical equation is 7% smaller than the actual waveheight while the wave period is over-predicted by nearly 15%. This is probably due in part to the fact that the empirical equations were generated assuming no accompanying current, and waves travelling on an opposing current become shorter and taller relative to waves under no-current conditions.

Table A.5: Comparison of wave parameters

Fetch (m)	Windspeed (m/s)	predicted		measured	
		T (s)	H_{rms} (cm)	T (s)	H_{rms} (cm)
300	4.4	0.89	4.06	0.75	4.37

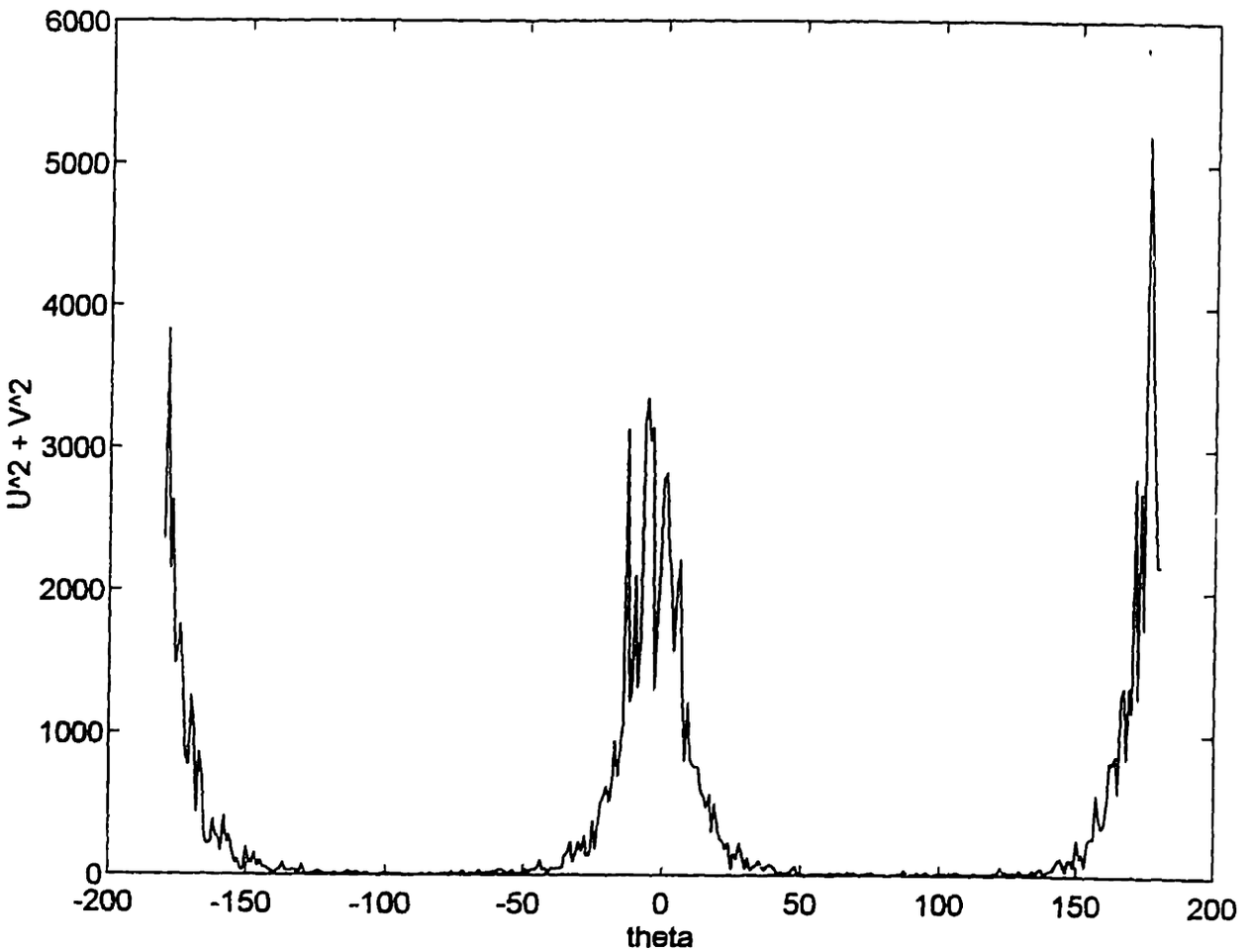

Figure A-1: Directional Distribution of Waves

Having established that empirical wave equations are applicable to a small-fetch system, the equations were then used to predict the windspeed necessary for re-suspension. The wavelength (L, in meters) of a deepwater wave is related to its period by the equation

$$L = \frac{gT^2}{2\pi}$$

The water depth must be less than one-half the wavelength of a deepwater wave for the wave to start to "feel" the bottom, at which point the horizontal motion of the water directly above the sediment may generate stresses that can initate motion of sediment grains and cause sediment transport. The empirical equations given above indicate that for a fetch of 300 m, winds of 10 m/s would generate 1.4 second waves with a significant wave height of 15 cm. The wavelength for these conditions would be 2.9 m, which is approximately the value that is required for deepwater waves to feel the bottom for an average depth is 1.5 m. Table A.2 shows that only one month out of the six that were monitored during the summer and fall of 1995 had winds above 10 m/s, and this occurred during only one night for roughly 5 hours. These estimates, along with the observation that the organic material added to the sediments by autochthonous plant growth most likely increases their cohesiveness and raises the critical shear stress needed for initiation of motion, indicate that wind waves are not expected to be a regular cause of sediment re-suspension in the Upper Forebay. It should be noted that wave motion could generate stirring of rooted macrophytes without penetrating to the bottom of the water column.

APPENDIX B.1

Table B.1: Concentrations and Fluxes at Inlet during Summer, 1995								
Date	Flowrate (m^3/s)	Suspended Sediment		Particulate Arsenic			Dissolved Arsenic	
		mg/L	kg/hr	mg/kg	nM	g/hr	nM	g/hr
July 19	0.102	2.6	0.96	384	13.2	0.36	9.7	0.27
July 27	0.094	3.8	1.3	277	14.2	0.36	13.6	0.34
August 7	0.282	3.6	3.7	509	24.5	1.86	44.5	3.39
August 9	0.112	3.1	1.2	687	25.6	0.77	26.6	0.80
August 17	0.051	-	-	-	5.7	0.08	12.4	0.17
August 25	0.026	-	-	-	6.3	0.04	9.0	0.06
September 1	0.032	-	-	-	7.8	0.07	6.9	0.06
September 8	0.027	2.0	0.20	184	4.9	0.04	10.5	0.08
September 11	0.030	-	-	-	7.2	0.06	7.9	0.06
September 14	0.085	6.4	2.0	200	17.1	0.39	8.3	0.19
September 17	0.039	-	-	215	6.6	0.07	12.0	0.12

Table B.2: Concentrations and Fluxes at Outlet during Summer, 1995								
Date	Flowrate (m^3/s)	Suspended Sediment		Particulate Arsenic			Dissolved Arsenic	
		mg/L	kg/hr	mg/kg	nM	g/hr	nM	g/hr
July 19	0.102	7.1	2.6	247	23.4	0.64	23.6	0.65
July 27	0.094	8.0	2.7	209	22.4	0.57	30.2	0.77
August 7	0.282	7.9	8.0	237	25.0	1.90	30.0	2.28
August 9	0.112	7.7	3.1	189	19.3	0.58	23.9	0.72
August 17	0.051	-	-	-	14.3	0.20	24.8	0.34
August 25	0.026	-	-	-	20.5	0.14	30.3	0.21
September 1	0.032	-	-	-	18.5	0.16	24.2	0.21
September 8	0.027	12.8	1.2	166	28.4	0.21	26.8	0.20
September 11	0.030	-	-	-	18.0	0.15	21.4	0.17
September 14	0.085	7.6	2.3	230	23.3	0.53	17.7	0.41
September 17	0.039	8.3	1.2	176	19.5	0.21	19.0	0.20

Table B.3: Size Fractions at Inlet, Top of Water Column						
	Diameter > 8 μm			Diameter < 8 μm		
	Arsenic	Suspended Sediment	Particulate Concentration	Arsenic	Suspended Sediment	Particulate Concentration
	nM	mg/L	mg As / kg sediment	nM	mg/L	mg As / kg sediment
July 19	8.7	2.2	294	2.2	0.7	329
July 27	8.2	2.8	219	6.0	1.4	321
August 7	22.5	3.0	562	4.6	0.6	574
August 9	15.2	1.8	633	11.4	1.1	776

Table B.4: Size Fractions at Inlet, Bottom of Water Column						
		Diameter > 8 µm			Diameter < 8 µm	
	Arsenic	Suspended Sediment	Particulate Concentration	Arsenic	Suspended Sediment	Particulate Concentration
	nM	mg/L	mg As / kg sediment	nM	mg/L	mg As / kg sediment
July 19	3.6	2.1	125	1.6	0.7	176
July 27	10.0	2.4	360	4.0	1.3	777
August 7	15.6	4.5	260	3.5	0.3	874
August 9	20.0	1.5	999	7.9	0.9	658

Table B.5: Size Fractions at Outlet, Top of Water Column						
		Diameter > 8 µm			Diameter < 8 µm	
	Arsenic	Suspended Sediment	Particulate Concentration	Arsenic	Suspended Sediment	Particulate Concentration
	nM	mg/L	mg As / kg sediment	nM	mg/L	mg As / kg sediment
July 19	21.2	4.9	323	2.2	1.2	134
July 27	17.7	6.9	191	4.7	0.9	497
August 7	26.2	6.5	302	1.8	1.5	90
August 9	18.3	6.6	209	4.1	1.5	200

Table B.6: Size Fractions at Outlet, Bottom of Water Column						
		Diameter > 8 µm			Diameter < 8 µm	
	Arsenic	Suspended Sediment	Particulate Concentration	Arsenic	Suspended Sediment	Particulate Concentration
	nM	mg/L	mg As / kg sediment	nM	mg/L	mg As / kg sediment
July 19	19.9	7.0	213	8.7	0.9	724
July 27	30.5	8.5	271	7.9	1.0	694
August 7	26.0	7.6	258	3.5	0.9	301
August 9	28.6	10.4	207	4.2	0.8	371

Table B.7: Suspended Sediment during Fall and Winter, 1995-1996									
Date	Julian Day	Inlet			Outlet			Wind	Comments
		m^3/s	mg/L	kg/hr	m^3/s	mg/L	kg/hr	m/s, dir.	
9/17	260.38	0.039	-	-	0.039	8.3	1.2	1.9, N	sample lost in As analysis
	260.54	0.384	2.3	3.2	0.384	6.7	9.3	0.3, SE	
	260.79	5.651	95.5	1942.9	5.651	8.4	170.9	7.8, N	
9/18	261.83	0.825	11.3	33.6	0.825	8.7	25.8	0.3, SE	
9/19	262.43	0.425	4.8	7.3	0.425	6.4	9.8	2.7, N	
9/20	263.33	0.204	4.3	3.2	0.204	5.4	4.0	3.9, N	
9/21	264.42	0.136	4.7	2.3	0.136	6.8	3.3	0.3, S	
9/22	265.33	0.110	2.1	0.8	0.110	3.5	1.4	2.7, S	
9/23	266.42	0.345	3.6	4.5	0.345	4.0	5.0	3.8, NW	
10/4	277.79	0.253	10.7	9.8	0.253	4.9	4.5	1.0, S	0.36" rain 9a.m.-4p.m.
10/5	278.46	0.123	4.6	2.0	0.123	3.6	1.6	1.1, NE	
	278.83	0.825	8.0	23.8	0.643	5.2	12.0	0.7, NE	
10/6	279.29	5.868	50.5	1066.8	5.505	7.2	142.7	2.8, NE	
	279.75	2.989	9.8	105.5	3.050	5.6	61.5	5.1, N	
10/7	280.54	1.357	7.5	36.6	1.462	4.0	21.1	1.3, NE	
10/8	281.54	0.631	5.4	12.3	0.737	6.1	16.2	1.6, NW	
10/9	282.46	0.370	3.5	4.7	0.395	3.8	5.4	3.9, N	
10/10	283.46	0.253	3.4	3.1	0.284	3.3	3.4	1.1, NE	
10/12	285.33	0.179	2.9	1.9	0.193	4.0	2.8	0.8, SW	
10/14	287.40	0.143	5.2	2.7	0.143	5.1	2.6	2.3, S	
10/15	288.40	0.784	9.9	28.0	0.784	6.3	17.8	1.4, S	0.60" rain a.m.
10/19	292.75	0.136	4.6	2.3	0.136	5.6	2.7	0.8, SE	
10/20	293.73	0.136	1.9	0.9	0.136	9.9	4.8	2.3, NE	
10/21	294.40	0.139	4.0	2.0	0.139	4.0	2.0	1.8, SE	
	294.7?	0.558	5.6	11.3	0.558	3.0	6.0	4.4, SE	

Table B.7: Suspended Sediment during Fall and Winter, 1995-1996									
	294.96	3.254	26.9	315.1	2.860	2.7	27.8	5.5, SE	
10/22	295.40	1.958	5.2	36.7	1.793	4.0	25.8	0.8, SW	
	295.59	1.702	3.7	22.7	1.702	3.7	22.7	2.0, SW	
	295.71	1.533	3.7	20.4	1.562	3.6	20.2	1.6, W	
10/23	296.71	0.846	3.7	11.3	0.846	2.7	8.2	1.2, W	
10/24	297.73	0.563	3.2	6.5	0.610	3.9	8.6	2.8, S	
10/25	298.72	0.439	3.7	5.8	0.439	3.1	4.9	3.4, NW	
11/4	308.52	0.706	-	-	0.706	2.7	6.9	4.7, NW	
	308.58	0.668	-	-	0.668	2.7	6.5	4.2, NW	
	308.60	0.668	2.3	5.5	-	-	-	4.2, NW	
	308.66	0.650	1.8	4.2	-	-	-	5.6, NW	
	308.68	0.650	-	-	0.650	2.3	5.4	5.6, NW	
11/29	333.69	0.706	2.2	5.6	0.706	2.5	6.4	3.8, NE	
11/30	334.71	0.668	3.2	7.7	0.668	1.6	3.8	0.4, W	
12/2	336.58	0.687	2.8	6.9	0.687	1.8	4.5	8.3, NW	
1/18	18.51	1.023	3.9	14.4	-	-	-	-	iced over at outlet
1/19	19.38	1.920	14.8	102.3	1.920	7.3	50.5	-	
	19.67	3.146	25.4	287.7	3.017	5.1	55.4	-	
	19.85	7.934	149.0	4256.0	6.918	10.7	266.5	-	
1/20	20.00	8.229	73.3	2171.4	8.156	43.8	1286.0	-	
	20.33	6.708	7.3	176.3	6.708	5.6	135.2	-	
	20.66	5.651	4.5	91.5	5.724	4.6	94.8	-	
	20.85	5.232	4.2	79.1	5.305	3.4	64.9	-	
1/21	21.65	3.890	2.7	37.8	4.017	2.5	36.2	-	
1/22	22.44	2.938	2.6	27.5	3.024	2.6	28.3	-	
1/23	23.35	2.237	2.1	16.9	2.278	1.6	13.1	-	
2/1	32.73	2.075	3.2	23.9	2.075	2.5	18.7	-	
2/10	41.65	1.222	2.9	12.8	1.222	2.8	12.3	-	

Table B.7: Suspended Sediment during Fall and Winter, 1995-1996									
2/18	49.48	0.765	1.9	5.2	0.765	1.1	3.0	-	no As analysis
2/24	55.54t	-	-	-	3.093	3.4	37.9	-	0.51" rain a.m.
	55.54b	-	-	-		3.6	40.1	-	
	55.58t	2.887	8.7	90.4	-	-	-	-	
	55.58b		12.2	126.8	-	-	-	-	
	55.63t	2.643	8.7	82.8	-	-	-	-	
	55.63b		15.2	144.6	-	-	-	-	
	55.67t	-	-	-	2.549	4.6	42.2	-	
	55.67b	-	-	-		6.1	56.0	-	

Table B.8: Arsenic Concentrations and Fluxes at Inlet during Fall and Winter, 1995-1996							
Date	Julian Day	Flowrate (m^3/s)	Particulate Arsenic			Dissolved Arsenic	
			mg/kg	nM	g/hr	nM	g/hr
September 17	260.38	0.039	-	7.0	0.07	11.1	0.12
	260.54	0.384	202	6.2	0.64	13.1	1.36
	260.79	5.651	129	164.9	251.29	57.3	87.32
September 18	261.83	0.825	308	46.4	10.32	47.8	10.63
September 19	262.43	0.425	660	42.3	4.84	32.2	3.69
September 20	263.33	0.204	509	29.2	1.61	29.6	1.63
September 21	264.42	0.136	268	16.8	0.62	27.5	1.01
September 22	265.33	0.110	574	16.1	0.48	26.9	0.80
September 23	266.42	0.345	909	43.7	4.07	21.6	2.01
October 4	277.79	0.253	43	6.1	0.42	14.5	0.99
October 5	278.46	0.123	88	5.4	0.18	14.9	0.49
	278.83	0.825	157	16.8	3.74	15.2	3.38
October 6	279.29	5.868	173	116.9	184.98	15.0	23.74
	279.75	2.989	242	31.6	25.47	23.9	19.27
October 7	280.54	1.357	694	69.5	25.43	59.5	21.77
October 8	281.54	0.631	850	61.3	10.44	36.6	6.23

Table B.8: Arsenic Concentrations and Fluxes at Inlet during Fall and Winter, 1995-1996							
Date	Julian Day	Flowrate (m^3/s)	Particulate Arsenic			Dissolved Arsenic	
			mg/kg	nM	g/hr	nM	g/hr
October 9	282.46	0.370	773	36.1	3.60	27.6	2.76
October 10	283.46	0.253	533	24.2	1.65	28.6	1.95
October 12	285.33	0.179	783	30.3	1.47	26.4	1.28
October 14	287.40	0.143	310	21.3	0.83	17.6	0.68
October 15	288.40	0.784	232	30.6	6.47	36.4	7.70
October 19	292.75	0.136	342	21.0	0.77	16.9	0.62
October 20	293.73	0.136	718	18.2	0.67	17.9	0.66
October 21	294.40	0.139	506	27.0	1.02	17.8	0.67
	294.73	0.558	318	23.8	3.58	23.7	3.57
	294.96	3.254	178	64.0	56.16	27.1	23.78
October 22	295.40	1.958	184	12.8	6.76	26.3	13.89
	295.59	1.702	243	12.0	5.51	24.5	11.24
	295.71	1.533	346	17.1	7.07	27.7	11.45
October 23	296.71	0.846	492	24.3	5.54	21.3	4.86
October 24	297.73	0.563	433	18.5	2.81	20.1	3.05
October 25	298.72	0.439	583	28.8	3.41	24.9	2.95
November 4	308.60	0.668	417	12.8	2.31	21.5	3.87
	308.66	0.650	520	12.5	2.19	22.6	3.96
November 29	333.69	0.706	514	15.1	2.87	12.6	2.40
November 30	334.71	0.668	260	11.1	2.00	12.9	2.32
December 2	336.58	0.687	409	15.3	2.83	11.2	2.07
January 18	18.51	1.023	154	8.0	2.21	11.0	3.03
January 19	19.38	1.920	134	26.4	13.67	13.7	7.09
	19.67	3.146	54	18.2	15.44	9.8	8.31
	19.85	7.934	64	127.6	273.02	6.6	14.12
January 20	20.00	8.229	63	61.4	136.25	12.0	26.63

Table B.8: Arsenic Concentrations and Fluxes at Inlet during Fall and Winter, 1995-1996							
Date	Julian Day	Flowrate (m^3/s)	Particulate Arsenic			Dissolved Arsenic	
			mg/kg	nM	g/hr	nM	g/hr
	20.33	6.708	193	18.8	34.01	13.8	24.96
	20.66	5.651	521	31.3	47.70	43.1	65.68
	20.85	5.232	637	35.7	50.37	49.8	70.26
January 21	21.65	3.890	369	13.3	13.95	19.6	20.56
January 22	22.44	2.938	242	8.4	6.65	11.2	8.87
January 23	23.35	2.237	193	5.4	3.26	11.5	6.94
February 1	32.73	2.075	143	6.1	3.41	11.7	6.55
February 10	41.65	1.222	230	8.9	2.93	17.7	5.83
February 24	55.58t	2.887	61	7.1	5.53	10.3	8.02
	55.58b		31	5.0	3.89	10.7	8.33
	55.63t	2.643	61	7.1	5.06	11.5	8.20
	55.63b		20	4.0	2.85	9.3	6.63
March 5	65.63t	-	-	8.9	-	19.2	-
	65.63b	-	-	5.6	-	19.8	-
March 6	66.35t	-	-	13.0	-	14.3	-
	66.35b	-	-	6.5	-	17.0	-
March 7	67.39	-	-	8.8	-	17.4	-
March 31	91.59	-	-	12.0	-	19.6	-
April 6	97.49	-	-	5.0	-	12.1	-

Table B.9: Arsenic Concentrations at Outlet during Fall and Winter, 1995-1996							
Date	Julian Day	Flowrate (m^3/s)	Particulate Arsenic			Dissolved Arsenic	
			mg/kg	nM	g/hr	nM	g/hr
September 17	260.38	0.039	176	19.5	0.20	19.0	0.20
	260.54	0.384	273	24.4	2.52	16.8	1.74
	260.79	5.651	206	23.1	35.20	16.4	24.99
September 18	261.83	0.825	208	24.2	5.38	30.2	6.72
September 19	262.43	0.425	233	19.9	2.28	28.3	3.24
September 20	263.33	0.204	183	13.2	0.73	33.2	1.83
September 21	264.42	0.136	217	19.7	0.72	29.7	1.09
September 22	265.33	0.110	370	17.3	0.46	24.0	0.63
September 23	266.42	0.345	316	16.9	1.57	28.3	2.63
October 4	277.79	0.253	95	6.2	0.42	16.3	1.11
October 5	278.46	0.123	173	8.3	0.28	14.0	0.46
	278.83	0.643	128	8.9	1.54	14.5	2.51
October 6	279.29	5.505	151	14.5	21.53	12.8	19.00
	279.75	3.050	165	12.3	10.12	17.4	14.31
October 7	280.54	1.462	262	14.0	5.52	19.9	7.85
October 8	281.54	0.737	673	54.8	10.89	39.4	7.83
October 9	282.46	0.395	771	39.1	4.16	25.3	2.69
October 10	283.46	0.284	785	34.6	2.65	23.3	1.78
October 12	285.33	0.193	607	32.4	1.69	18.7	0.97
October 14	287.40	0.143	316	21.5	0.83	19.5	0.75
October 15	288.40	0.784	257	21.6	4.57	19.5	4.12
October 19	292.75	0.136	152	11.4	0.42	20.4	0.75
October 20	293.73	0.136	135	17.9	0.66	13.8	0.51
October 21	294.40	0.139	236	12.6	0.47	14.7	0.55
	294.73	0.558	502	20.1	3.03	16.3	2.45
	294.96	2.860	266	9.6	7.40	17.5	13.50

Table B.9: Arsenic Concentrations at Outlet during Fall and Winter, 1995-1996							
Date	Julian Day	Flowrate (m^3/s)	Particulate Arsenic			Dissolved Arsenic	
			mg/kg	nM	g/hr	nM	g/hr
October 22	295.40	1.793	399	21.3	10.30	18.3	8.85
	295.59	1.702	346	17.1	7.85	18.4	8.44
	295.71	1.562	204	9.8	4.13	23.2	9.77
October 23	296.71	0.846	269	9.7	2.21	26.3	6.00
October 24	297.73	0.610	415	21.6	3.55	15.0	2.47
October 25	298.72	0.439	435	18.0	2.13	16.2	1.92
November 4	308.52	0.706	350	12.6	2.40	15.3	2.91
	308.58	0.668	241	8.7	1.57	18.1	3.26
	308.68	0.650	300	9.2	1.61	19.8	3.47
November 29	333.69	0.706	282	9.4	1.79	11.5	2.19
November 30	334.71	0.668	243	5.2	0.94	10.9	1.96
December 2	336.58	0.687	175	4.2	0.78	13.6	2.52
January 18	18.51	1.023	-	-	-	-	-
January 19	19.38	1.920	101	9.8	5.07	11.6	6.01
	19.67	3.017	131	8.9	7.24	11.6	9.44
	19.85	6.918	49	7.0	13.06	11.3	21.08
January 20	20.00	8.156	29	17.0	37.39	14.7	32.33
	20.33	6.708	159	11.9	21.53	9.2	16.64
	20.66	5.724	285	17.5	27.01	18.6	28.71
	20.85	5.305	626	28.4	40.63	37.6	53.79
January 21	21.65	4.017	515	17.2	18.63	26.0	28.16
January 22	22.44	3.024	277	9.6	7.83	14.0	11.42
January 23	23.35	2.278	281	6.0	3.69	12.7	7.80
February 1	32.73	2.075	135	4.5	2.52	9.8	5.48
February 10	41.65	1.222	80	3.0	0.99	15.4	5.07
February 24	55.54t	3.093	108	4.9	4.09	10.1	8.42

Table B.9: Arsenic Concentrations at Outlet during Fall and Winter, 1995-1996							
Date	Julian Day	Flowrate (m^3/s)	Particulate Arsenic			Dissolved Arsenic	
			mg/kg	nM	g/hr	nM	g/hr
	55.54b		69	3.3	2.75	12.9	10.76
	55.67t	2.549	67	4.1	2.82	10.8	7.42
	55.67b		65	5.3	3.64	10.4	7.15
March 5	65.58t	-	-	6.2	-	17.8	-
	65.58b	-	-	7.2	-	16.4	-
March 6	66.33t	-	-	7.4	-	15.3	-
	66.33b	-	-	8.2	-	13.0	-
March 7	67.38	-	-	7.7	-	14.8	-
March 31	91.58	-	-	10.4	-	18.2	-
April 6	97.48	-	-	3.6	-	13.4	-

Table B.10: Concentrations at Inlet during July Storm							
Date	Julian Day	Suspended Sediment (mg/L)	Dissolved Arsenic (nM)	Particulate Arsenic		Conductivity (μmhos)	Total Dissolved Carbon (ppm)
				nM	mg/kg		
7/13	195.35	45.2	29.4	96.4	160	270	13.1
	195.40	57.0	28.6	128.4	169	210	10.5
	195.47	38.4	27.6	97.2	190	120	8.1
	195.53	50.9	29.9	84.8	125	115	7.0
	195.59	58.5	27.7	102.9	132	135	8.1
	195.64	59.9	28.6	121.7	152	115	7.2
	195.69	84.7	27.9	138.9	123	90	6.3
	195.74	75.3	29.6	149.8	149	90	6.7
	195.78	76.1	32.1	169.1	166	80	6.6
	195.85	47.9	30.8	90.9	142	90	6.5
	195.91	30.4	30.5	57.7	142	120	7.6
	195.98	30.4	39.8	54.4	134	135	16.0
7/14	196.26	17.5	33.8	53.5	229	190	12.5

Table B.10: Concentrations at Inlet during July Storm							
	196.32	20.1	37.8	65.4	244	220	13.4
	196.39	17.3	47.4	66.5	288	255	14.9
	196.49	17.1	56.4	82.2	360	305	-
	196.57	26.4	84.2	66.9	190	340	18.9
	196.68	20.8	72.9	83.9	302	190	17.5
	196.77	12.4	67.0	84.8	512	240	-
7/15	197.41	6.2	46.2	31.9	385	320	-
	197.61	4.8	42.7	26.4	412	330	-
	197.84	6.4	34.2	27.9	327	330	-
7/16	198.44	5.2	37.7	26.1	376	310	-
7/17	199.63	4.5	54.1	27.3	454	415	-
7/18	200.65	5.4	46.5	25.7	356	335	-
7/19	201.44	3.1	51.9	26.2	633	255	-
7/22	204.67	5.6	36.7	31.4	420	-	-

Table B.11: Concentrations at Outlet during July Storm						
Date	Julian Day	Suspended Sediment (mg/L)	Dissolved Arsenic (nM)	Particulate Arsenic		Conductivity (μmhos)
				nM	mg/kg	
7/13	195.34	5.9	26.5	33.8	429	440
	195.41	5.0	25.3	32.3	484	460
	195.47	6.9	31.6	30.4	330	450
	195.52	6.1	25.9	31.4	386	450
	195.58	5.6	20.9	35.4	474	450
	195.63	6.3	21.7	39.0	464	430
	195.68	8.6	24.0	32.3	281	370
	195.73	8.2	21.7	28.4	259	235
	195.77	8.5	25.0	23.6	208	190
	195.84	8.8	24.4	23.7	202	170
	195.90	7.7	27.5	19.5	190	160

Table B.11: Concentrations at Outlet during July Storm						
	195.96	9.7	27.2	27.8	215	170
7/14	196.25	7.3	30.0	24.1	247	100
	196.31	5.8	29.4	21.2	274	170
	196.38	5.7	31.6	21.1	277	200
	196.46	4.9	27.2	22.9	350	185
	196.59	6.4	25.9	18.7	219	195
	196.67	4.6	39.1	56.8	925	135
	196.76	7.1	41.8	55.2	582	155
7/15	197.40	6.1	42.2	51.1	627	300
	197.60	4.9	38.6	54.4	832	170
	197.84	5.5	37.4	45.4	618	300
7/16	198.44	4.2	33.7	41.9	747	275
7/17	199.63	4.8	45.7	28.7	448	370
7/18	200.65	4.7	41.6	26.9	429	170
7/19	201.44	4.3	44.2	25.2	439	180
7/22	204.67	5.4	36.2	27.5	381	-

Table B.12: Preliminary Water Samples							
Date	Flowrate (m^3/s)	Location	Arsenic (nM)			Suspended Sediment (mg/L)	
			Total	Dissolved	Particulate	Top	Bottom
June 20	0.192	30 m upstream of UFB bridge	93.4	-	-	-	-
		10 m in front of bridge	75.9	-	-	-	-
		UFB middle	64.5	-	-	-	-
		UFB outlet	66.0	-	-	-	-
		LFB sidearm	44.1	-	-	-	-
June 21	0.173	UFB inlet	86.3	-	-	-	-
		UFB outlet	64.3	-	-	-	-
		LFB sidearm	47.9	-	-	-	-
July 7	0.098	UFB inlet	44.3	28.7	18.8	2.0	2.9
		UFB outlet	> 74.1	46.9	> 27.2	4.3	6.3

Note: For July 7 the sample at the outlet was not diluted enough and total arsenic was higher than the upper limit of the instrument. The sample was used up before further dilution could be performed.

Table B.13: Various Spatial Samples for Arsenic in Upper Forebay				
Date	Location	Arsenic (nM)		
		Total	Dissolved	Particulate
August 17	UFB dead-zone	39.3	24.9	14.3
August 25	UFB dead-zone	50.4	-	-
	UFB middle	49.9	34.2	15.7
September 8	UFB middle	30.7	18.4	12.3
November 4	UFB dead-zone	32.3	19.7	12.6
	UFB middle	29.2	17.0	12.2

APPENDIX B.2

Table B.14: Distribution of Dissolved Oxygen

Date	Location	Time	Temperature (°C)		Dissolved Oxygen (mg/L)	
			Top	Bottom	Top	Bottom
September 8	outlet	9:30 am	19.0	19.0	7.0	6.0
	inlet	10:00 am	17.5	17.0	4.5	4.5
	vegetated area, middle of forebay	10:30 am	19.0	17.0	8.4	7.6
	outlet	11:15 am	20.5	18.0	7.6	7.5
September 14	outlet	9:15 am	19.5	19.0	7.9	7.6
	inlet	9:30 am	18.0	-	5.3	-
	vegetated area, near inlet	10:00 am	21.0	21.0	8.6	8.0
	vegetated area, near outlet	10:30 am	21.0	-	8.1	-
	outlet	11:00 am	21.0	21.0	8.4	8.0

Table B.15: Conductivity and Temperature during Winter, 1996

Date	Time	Inlet		Outlet		Comments
		Conductivity (µmhos)	Temperature (°C)	Conductivity (µmhos)	Temperature (°C)	
February 24	1 pm	-	-	353	5.5	
	2 pm	322	6.25	-	-	
	3 pm	312	6.5	-	-	
	4 pm	-	-	351	7.0	
March 5		338	2.0	359	2.5	increase of conductivity likely due to road salting
March 6		800	2.0	333	2.0	
March 7		520	1.75	413	1.5	

Bibliography

Aquatic Control Technologies, Inc. (1994). Year-end Report for Upper Mystic Lake Chemical Treatment Program. 6 Maple Street, Northborough, MA, 01532.

Aquatic Control Technologies, Inc. (1995).Year-end Report for Upper Mystic Lake Chemical Treatment Program. 6 Maple Street, Northborough, MA, 01532.

Aurilio, A.C., Mason, R.P, and H.F. Hemond (1994). Speciation and fate of arsenic in three lakes of the Aberjona Watershed. Environmental Science and Technology, 28, 577.

Aurilio, A.C., Durant, J.L., Hemond, H.F., and M.L. Knox (1994). Sources and distribution of arsenic in the Aberjona Watershed, Eastern Massachusetts. Water, Air, and Soil Pollution, 78, 1-18.

Baker, L.A. (1992). Introduction to nonpoint source pollution in the United States and prospects for wetland use. Ecological Engineering, 1, 1-26.

Barko, J.W. and R.M. Smart (1980). Mobilization of sediment phosphorus by submersed freshwater macrophytes. Freshwater Biology, 10, 229-238.

Bradley, S.B. (1984). Flood effects on the transport of heavy metals. International Journal of Environmental Studies, 22, 225-230.

Chow, V.T. (1964). Handbook of Applied Hydrology. McGraw-Hill, New York.

Chow, V.T., Maidment, D.R., and L.W. Mays (1988). Applied Hydrology. McGraw-Hill, New York.

DiPietro, Paul. Metropolitan District Commission environmental engineer. 20 Somerset Street, Boston, MA 02108.

Durant, J.L., Zemach, J.J., and H.F. Hemond (1990). The history of leather industry waste contamination in the Aberjona River Watershed: a mass balance approach. Civil Engineering Practice: Journal of the Boston Society of Engineers, 5, 41-66.

Gallagher, J.L. and H.V. Kibby (1980). Marsh plants as vectors in trace metal transport in Oregon tidal marshes. American Journal of Botany, 67(7), 1069-1074.

Johnson, A.H. (1979) Estimating solute transport in streams from grab samples. Water Resources Research, 15, 10, 1224-1228.

Jones, A. and G.F. Lee (1980). An approach for the evaluation of efficacy of wetlands-based phosphorus control programs for eutrophication-related water quality improvement in downstream waterbodies. Water, Air and Soil Pollution, 14, 359-378.

Kadlec, R.H. and D.L. Tilton (1979). The use of freshwater wetlands as a tertiary wastewater treatment alternative. C.R.C. Critical Reviews in Environmental Control, 9, 185-212.

Klarer, D.M. and D.F. Millie (1989). Amelioration of storm-water quality by a freshwater estuary. Arch. Hydrobiol., 116, 375-389.

Klopatek, J.M. (1978). Nutrient dynamics of freshwater riverine marshes and the role of emergent macrophytes. *In* Freshwater Wetlands (Eds. R.E. Good, D.F. Whigham and R.L. Simpson), pp. 195-216. Academic Press, New York.

Knox, M.L. (1991). The distribution and depositional history of metals in surface sediments of the Aberjona Watershed. M.S. Thesis, Massachusetts Institute of Technology.

Lee, G.F., Bentley, E., and R. Amundson (1975). Effects of marshes on water quality. *In* Coupling of Land and Water Systems (Ed. A.C. Hasler), pp. 107-127. Springer, Berlin.

Leonard, L.A. and M.E. Luther (1995). Flow hydrodynamics in tidal marsh canopies, Limnology and Oceanography, 40(8), 1474-1484.

Loucks, O.L. (1990). Restoration of the pulse control function of wetlands and its relationship to water quality objectives. *In* Wetland Creation and Restoration: The Status of the Science (Eds. Kusler and Kentula), pp. 467-477.

Madsen, O.S., Wright, L.D., Boon, J.D., and T.A. Chisholm (1993). Wind stress, bed roughness and sediment suspension on the inner shelf during an extreme storm event. Continental Shelf Research, 13, 11, 1303-1324.

Mitsch, W.J. and B.C. Reeder (1991). Modelling nutrient retention of a freshwater coastal wetland: estimating the roles of primary productivity, sedimentation, resuspension and hydrology. Ecological Modelling, 54, 151-187.

Mitsch, W.J. and J.G. Gosselink (1993). Wetlands. Van Nostrand Reinhold, New York.

Mitsch, W.J. (1992). Landscape design and the role of created, restored, and natural riparian wetlands in controlling nonpoint source pollution. Ecological Engineering, 1, 27-47.

Mitsch, W.J. (1995). Restoration of our lakes and rivers with wetlands. Water Science and Technology, 31, 167-177.

Orson, R.A., Simpson, R.L., and R.E. Good (1992). A mechanism for the accumulation and retention of heavy metals in tidal freshwater marshes of the Upper Delaware River estuary. Estuarine, Coastal, and Shelf Science, 34, 171-186.

Otte, M.L. and W.O. Ernst (1994). Arsenic in vegetation of wetlands. *In* Arsenic in the Environment, Part I: Cycling and Characterization (Ed. J.O. Nriagu), pp. 365-379.

Peverly, J.H. (1982). Stream transport of nutrients through a wetland. Journal of Environmental Quality, 11, 38-43.

Simpson, R.L., Good, R.E., Walker, R., and B.R. Frasco (1983). The role of Delaware River freshwater tidal wetlands in the retention of nutrients and heavy metals. Journal of Environmental Quality, 12, 41-48.

Sloey, W.E., Spangler, F.L., and C.W. Fetter (1978). Management of freshwater wetlands for nutrient assimilation. *In* Freshwater Wetlands (Eds. R.E. Good, D.F. Whigham and R.L. Simpson), pp. 321-340. Academic Press, New York.

Solo-Gabriele, H. (1995). Metal transport in the Aberjona River system: monitoring, modeling, and mechanisms. PhD. Thesis, Massachusetts Institute of Technology.

Spliethoff, H.M. (1995). Biotic and abiotic transformations of arsenic in the Upper Mystic Lake. M.S. Thesis, Massachusetts Institute of Technology.

Spliethoff, H.M, Mason, R.P, and H.F. Hemond (1995). Interannual variability in the speciation and mobility of arsenic in a dimictic lake. Environmental Science and Technology, 29, 2157-2166.

Spliethoff, H.M. and H.F. Hemond (1996). History of toxic metal discharge to surface waters of the Aberjona Watershed. Environmental Science and Technology, 30, 121-128.

Thackston, E.L., Shields, F.D., and P.R. Schroeder (1987). Residence time distributions of shallow basins. Journal of Environmental Engineering, 113, 1319-1332.

Trowbridge, P.R. (1995). Evidence for rapid redox cycling of arsenic and characterization of the internal seiches in the Upper Mystic Lake, Medford, Massachusetts. M.S. Thesis, Massachusetts Institute of Technology.

U.S. Army Coastal Engineering Research Center (1973). Shore Protection Manual. Vol. I.

Wetzel, R.G. (1983). Limnology. W.B. Saunders College Publishing, Philadelphia.